ANNUAL REPORT

2015

Scripps Institution of Oceanography

Earth Section

University of California, San Diego
La Jolla, California

24 November 2015

Scripps Institution of Oceanography
Earth Section
Annual Report 2015

The Earth Section of the Scripps Institution of Oceanography includes researchers whose primary area of study is the solid Earth. Many of them have provided reports, included here in alphabetical order, summarizing their research over the last year; the aim has been to present this at a level that should be accessible to a broad scientific audience. We hope that you will find this booklet a useful description of our work.

The research done by the members of the Earth Section spans topics in geology, geophysics, chemistry, biogeosciences, and climate science. This research includes observations, measurements, and collection of samples and data on global, regional, and local scales, using shipboard operations, ground-based methods, and satellite remote sensing. Extensive laboratory work often follows these sampling programs, while theory and modeling guide data interpretation and the design and implementation of experiments and observations.

Awards and Honors

Adrian Borsa is one of the 2015-2016 EarthScope distinguished speakers.

Steve Constable was selected to give the Bullard Lecture for the Geomagnetism and Paleomagnetism Section of the American Geophysical Union.

Dave Hilton received a President's International Fellowship from the Chinese Academy of Sciences.

Miriam Kastner received the V. M. Goldschmidt award for major achievements in geochemistry or cosmochemistry from the Geochemical Society.

Lisa Tauxe was elected to the National Academy of Science.

Duncan Agnew, Head, Earth Section

Earth Section Academic Personnel

Duncan Carr Agnew, *Professor*
Lihini Aluwihare, *Associate Professor*†
Andreas Andersson, *Assistant Professor*
Laurence Armi, *Professor*†
Gustaf Arrhenius, *Research Professor*∗
George Backus, *Professor Emeritus*†
Jeffrey Bada, *Research Professor*∗
Katherine Barbeau, *Professor*
Jon Berger, *Research Scientist*∗
Wolf Berger, *Research Professor*∗†
Donna Blackman, *Research Scientist*
Yehuda Bock, *Distinguished Research Scientist*
Adrian Borsa, *Assistant Research Scientist*
Kevin Brown, *Professor*†
James Brune, *Professor Emeritus*†
Steven C. Cande, *Research Professor*∗†
Paterno Castillo, *Professor*
C. David Chadwell, *Research Scientist*
Christopher Charles, *Professor*†
Catherine Constable, *Professor*
Steven Constable, *Professor*
Geoffrey Cook, *Associate Lecturer*†
Joseph Curray, *Professor Emeritus*†
J. Peter Davis, *Specialist*
James Day, *Associate Professor*
Catherine Degroot-Hedlin, *Research Scientist*
Leroy Dorman, *Professor Emeritus*
Neal Driscoll, *Professor*
Matthew Dzieciuch, *Project Scientist*
Peng Fang, *Specialist* ∗†
Yuri Fialko, *Professor*
Robert P. Fisher, *Emeritus Research Scientist*†
Helen Amanda Fricker, *Professor*
Jeffrey Gee, *Professor*†
Jennifer Haase, *Associate Research Scientist*†
Alistair Harding, *Research Scientist*
Richard Haubrich, *Professor Emeritus*†
James Hawkins, *Professor Emeritus*
Michael Hedlin, *Research Scientist*
David Hilton, *Professor*
Glenn Ierley, *Professor Emeritus*†
Miriam Kastner, *Distinguished Professor*
Kerry Key, *Associate Professor*
Deborah Lyman Kilb, *Project Scientist*
Gabi Laske, *Professor-in-Residence*
Peter Lonsdale, *Professor*†
Gunter Lugmair, *Research Scientist*∗†
Douglas J. Macdougall, *Professor Emeritus*†
Todd Martz, *Assistant Professor*†
Guy Masters, *Distinguished Professor*†
Bernard Minster, *Distinguished Professor*
Walter Munk, *Research Professor*∗
Richard Norris, *Professor*
John Orcutt, *Distinguished Professor*†
Robert L. Parker, *Professor Emeritus*†
Anne Pommier, *Assistant Professor*
William Riedel, *Emeritus Research Scientist*†
David Sandwell, *Distinguished Professor*
Annika Sanfilippo, *Specialist* ∗
John G. Sclater, *Distinguished Professor*†
Peter Shearer, *Distinguished Professor*
Alex Shukolyukov, *Project Scientist*∗†
Len Srnka, *Professor of Practice*
Hubert Staudigel, *Research Scientist*∗†
David Stegman, *Associate Professor*
Lisa Tauxe, *Distinguished Professor*
Frank Vernon, *Research Scientist*†
Martin Wahlen, *Professor Emeritus*†
Edward L. Winterer, *Professor Emeritus*†
Peter Worcester, *Research Scientist*∗
Mark Zumberge, *Research Scientist*

∗ RTAD (Return to Active Duty): retired, but with active research program
† no report received

Duncan Carr Agnew, Professor
dagnew@ucsd.edu
Phone: 534-2590

Frank K. Wyatt, Prin. Dev. Engin., RTAD
fwyatt@ucsd.edu
Phone: 534-2411

Research Interests: Crustal deformation measurement and interpretation, Earth tides, Southern California seismicity.

We have long used long-base laser strainmeters to collect continuous deformation data at locations close to the two most active faults in Southern California. Pinyon Flat Observatory (PFO, operating since 1974) is 14 km from the Anza section of the San Jacinto fault (2-3 m accumulated slip since the last large earthquake) and Salton City (SCS, since 2006) within 15 km of the same fault further SE. Two other sites (Cholame, or CHL, since 2008, and Durmid Hill, or DHL, since 1994) are within three km of the San Andreas fault (SAF): CHL, at the N end of the segment that ruptured in 1857, and DHL at the S end of the Coachella segment (4-6 m accumulated slip). Surface-mounted laser strainmeters (LSM's), 400 to 700 m long and anchored 25 m deep, provide long-term high-quality measurements of strain unmatched anywhere else: though in geological settings ranging from weathered granite to clay sediments, the LSM's record secular strain accumulation consistent with continuous GPS, something not otherwise possible. The LSM's record signals from 1 Hz to secular; at periods less than several months, they have a noise level far below that of fault-scale GPS networks.

The high installation and operating costs of these LSM's has created a need for a cheaper, if lower-quality sensor. With Dr. Mark Zumberge, we continue to develop long-base laser strainmeters that use optical fiber, rather than a vacuum pipe, for the optical path, to provide a robust, widely deployable, inexpensive, and sensitive instrument. Since optical fibers have long-term drift and are temperature sensitive they cannot provide the same data quality over as wide a range of frequencies, but can still be useful for studying seismic waves, Earth tides, and slow slip events.

At PFO we have installed a 250-m-long borehole optical fiber vertical strainmeter, and two horizontal optical fiber strainmeters installed in trenches (about 1 m deep). The first, a 180 m instrument, is parallel to the NWSE vacuum laser strainmeter. It consists of optical fiber stretched between two points anchored to the Earth; length changes in this are measured using an interferometer, in which light from a laser is split by an optical fiber coupler into two fibers, one the Earth strain sensing fiber, the other a fixed reference length. Light travels the lengths of the two arms and recombines coherently: in a Michelson interferometer Faraday mirrors at the far end of each fiber reflect the light back, so the light recombines in the original coupler. By making the two arms of equal optical length the laser used can have relatively poor frequency stability. The reference arm is coiled around a quartz mandrel next to the laser and coupler, so that its temperature can be kept constant.

The extended fiber, though buffered from very rapid temperature changes by the overlying soil, still shows the effect of temperature at periods longer than a few hours. To reduce this effect, we have built (and installed at PFO) an instrument in which two optical fibers are both part of the strain sensing cable, with one being a normal fiber and the other using a different type of glass with a different temperature coefficient of the index of refraction. The two fibers undergo identical strain and temperature changes, but their different temperature coefficients allow the strain and temperature effects to be separated by forming appropriately scaled differences between the two fiber outputs. Extensive lab testing showed that an alternatively-doped fiber had a 14% difference in temperature coefficient.

We have installed a two-fiber system at PFO, extending over 230 m, and parallel to the EW vacuum strainmeter. The figure shows the data from the two fibers, along with the estimated strain and

temperature. The temperature changes agree well with a point measurement made at one location along the fiber, and the estimated strain shows much less variability after the temperature correction.

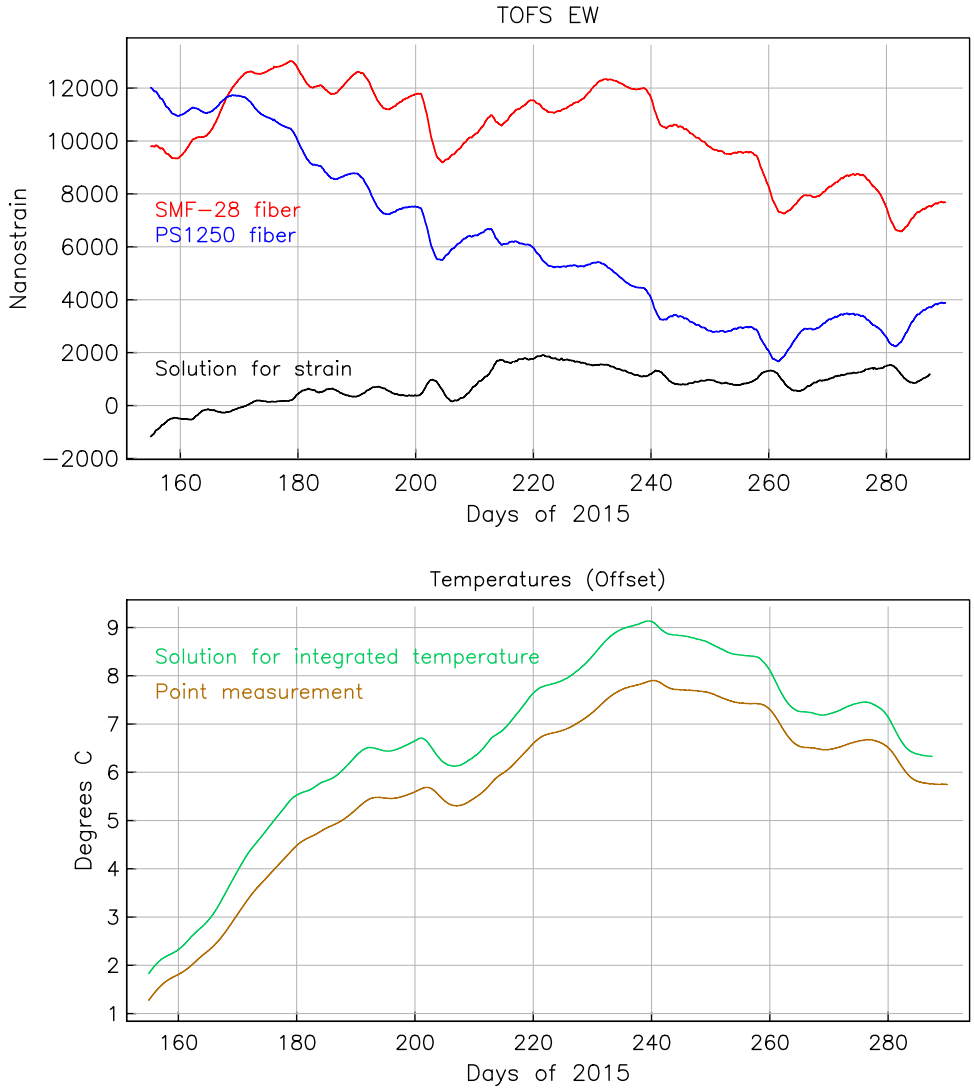

Figure 1: Data from the EW TOFS (Trench Optical-Fiber Strainmeter) installed at PFO. The upper panel shows the apparent strains observed on the two fibers, and the estimated strain from the temperature-neutral combination (black). The lower panel shows the estimated temperature and that measured at one point.

Recent Publications

D. C. Agnew (2015). Equalized plot scales for exploring seismicity data, *Seismol. Res. Lett.* **86**, 1412-1423 `http://dx.doi.org/10.1785/0220150054`

A. J. Barbour, D. C. Agnew, and F. K. Wyatt (2015). Coseismic strains on Plate Boundary Observatory borehole strainmeters in southern California, *Bull. Seismol. Soc. Am.*, **105**, 431-444, `http://dx.doi.org/10.1785/0120140199`

Andreas J. Andersson

Associate Professor of Oceanography

Email: aandersson@ucsd.edu

Phone: (858) 822-2486

Research Interests: Global environmental change owing to both natural and anthropogenic processes, mainly ocean acidification and its effects on biogeochemical processes in coastal and coral reef ecosystems, but also the effect on the overall function, role, and cycling of carbon in marine environments. Find out more at: www.anderssonoceanresearch.com

My group's research mainly focuses on the effects of ocean acidification on coral reefs and the cycling of carbon in these ecosystems (**Fig. 1**). To address this problem we need to understand how seawater CO_2 chemistry on coral reefs will change as a result of increasing atmospheric CO_2 concentrations, and how marine organisms and biogeochemical processes will be affected by these changes. Perhaps this would have been straightforward if it wasn't for the fact that the net reef metabolism, i.e., the sum of primary production, respiration, calcification and $CaCO_3$ dissolution, has a significant influence on the overlying seawater CO_2 chemistry. The extent to which reef metabolism modify seawater CO_2 chemistry is a function of a wide range of parameters including, for example, light, temperature, nutrients, flow regime, and community composition. The aim of our research attempts to address the relative importance and control of these parameters on reef biogeochemistry as well as the interactions between physics, chemistry, and biology. We utilize chemical measurements of seawater at different spatial and temporal scales to "take the pulse" of a given reef system in order to monitor its biogeochemical function and performance in the cycling of carbon. We complement this with controlled experiments in aquaria and mesocosms as well as numerical model simulations. We also study $CaCO_3$ dissolution, and especially the susceptibility and rates of dissolution of Mg-calcite mineral phases to changing seawater CO_2 chemistry.

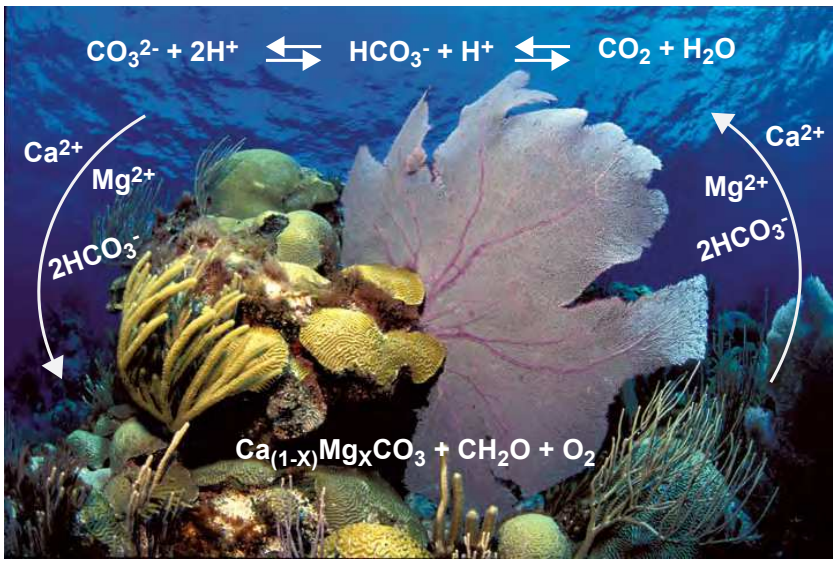

Figure 1. Illustration of the coupled organic and inorganic carbon cycles on coral reefs via photosynthesis, calcification, respiration and calcium carbonate dissolution.

In 2015, we have carried out fieldwork at Heron Island, Australia, Bermuda, and Bocas del Toro Panama (for pictures see: https://www.facebook.com/anderssonoceanresearch). Some of the objectives of these expeditions were: 1) to investigate rates of carbonate sediment dissolution under different seawater pH and for environments with different sediment grain size and mineralogy, 2) investigate the threshold in sediment pore water at which calcareous substrates start to dissolve and how this change as a function of the bulk sediment mineral composition, 3) investigate how different benthic communities modify the overlying seawater carbonate chemistry and how this differ as function of depth, currents, and light conditions, and 4) investigate the coupling between reef biogeochemical processes and larger scale atmospheric and oceanographic processes. In addition, we have been conducting numerous $CaCO_3$ dissolution experiments in the laboratory and also worked on numerical models capturing coral reef biogeochemical processes. This year, we also conducted a very exciting outreach project with Ocean Discovery Institute (ODI) and their ocean leaders. Briefly, we investigated to what extent seagrasses can modify their surrounding seawater carbonate chemistry and whether seagrass ecosystems locally can counteract ocean acidification. The project involved a 24-hour study in Mission Bay, San Diego.

Some of our collaborators in 2015 included Drs. Rod Johnson, Nick Bates and Tim Noyes at the Bermuda Institute of Ocean Sciences (BIOS) investigating coral reef biogeochemistry in Bermuda; NOAA PMEL monitoring seawater CO_2 on the Bermuda coral reef; Drs. Eric Tambutté and Alex Venn, Centre Scientifique de Monaco (CSM), investigating how chemical and environmental parameters affect cellular, physiological, and mineralogical properties in corals; Dr. Bradley Eyre Southern Cross University, Australia, studying the effect of ocean acidification on $CaCO_3$ sediment dissolution.

Recent Publications

Eyre, B., Andersson, A. J., Cyronak, T., 2014. Benthic coral reef calcium carbonate dissolution under ocean acidification. *Nature Climate Change*, DOI:10.1038/NCLIMATE2380.

Pickett, M. and Andersson A. J., 2015. Dissolution rates of biogenic carbonates in natural seawater at different pCO_2 conditions: A laboratory study. *Aquatic Geochemistry*, DOI: 10.1007/s10498-015-9261-3.

Andersson, A.J., Kline, D.I., Edmunds, P.J., Archer, S.D., Bednaršek, N., Carpenter, R. C., Chadsey, M., Goldstein, P., Grottoli, A. G., Hurst, T.P., King, A.L., Kübler, J.E., Kuffner, I.B., Mackey, K.R.M, Paytan, A., Menge, B., Riebesell, U., Schnetzer, A., Warner, M.E., and Zimmerman, R.C., 2015. Understanding ocean acidification impacts on organismal to ecological scales. *Oceanography magazine,* 28, 10-21.

Andersson, A. J., 2015. A fundamental paradigm for coral reef carbonate sediment dissolution. *Frontiers in Marine Science*, 2:52, doi: 10.3389/fmars.2015.00052.

Yeakel, K., Andersson, A. J., Bates, N. R., Noyes, T., Collins, A., and Garley, R., 2015. Shifts in coral reef biogeochemistry and resulting acidification linked to offshore productivity. *PNAS, in press*.

Gustaf Arrhenius Research Professor
arrhenius@ucsd.edu
Phone: 534-2255 or 731-6680

Research Interests*:* biogeochemistry. cosmochemistry, materials science

Our investigations during the last few years have focused on potential life indicators in the oldest preserved sediments on Earth (at 3.8 billion years) from Isua in southern West Greenland. In these rocks time, temperature and pressure have led to the complete obliteration of any microfossil shapes by crystallization to graphite.

Graphite also occurs in forms of inorganic origin, which may be confused with the graphite produced by decomposition of organic matter unless physical criteria can be found that distinguish between the genetically different types.

Graphite crystallizes in two modifications – one metastable with rhombohedral layer stacking, the other, the stable hexagonal end member. Our previous work led to the discovery that the graphite in these oldest rocks, thought likely to be of biogenic origin, have a high proportion of rhombohedral graphite. We also know that the highly disordered graphite nanocrystals in younger rocks, growing from organic matter, initially inherit hydrogen and heteroatoms like nitrogen, oxygen and sulfur from the source organics and we postulate that these impurity atoms, until they are gradually expelled, stabilize the rhombohedral structure that largely survives into old age, slowly converting to the stable hexagonal form and bearing witness to the live origin of this carbon.

Seeking support for this hypothesis we have, this year, continued separation and analysis of the biogenic carbon from rocks, at 3.4 Byr. geologically "slightly" younger and consisting of remaining recognizable organic matter. The results, illustrated in Figure 1, confirm that all samples of biogenic proto-graphite show proportionally higher diffracted energy from the rhombohedral- than from the hexagonal structure, confirming the preponderance of the rhombohedral form in incompletely crystallized biogenic carbon. The exceptionally high content of rhombohedral graphite in the Isua carbonaceous shale is interpreted as the result of incomplete conversion of originally rhombohedral carbon to hexagonal form under the prevailing altering pressure and temperature conditions. From the interpretation of the Isua carbon as a biogenic disequilibrium residue follows also the indication of the presence of life 3.8 billion years ago.
A caveat for a generalized interpretation of rhombohedral graphite as an indicator of organic matter and therefore of life comes from the observation that hexagonal graphite may convert to the rhombohedral form when exposed to extreme tectonic deformation such as in slip faults. Such conditions are, however, easily recognizable from disruption of the rock fabric. The microscopic texture of the finely laminated Isua carbonaceous shale investigated lacks any indication of such deformation.

Source and contributors
Analyses and observations at the base of the present discussion are given in "Search for traces of life in Earth's oldest rocks" – Final report to NASA on Grant NNG04GJ05, G.Arrhenius PI with contributing scientists S.Perez, A.Misra, C.Daraio, M.van Zuilen, A.Lepland, M.Rosing and M.L.Rudee, For conclusions and claims this original report depends on the present results and awaits their publication.
Support from the Agouron Institute Drilling Project is gratefully acknowledged.

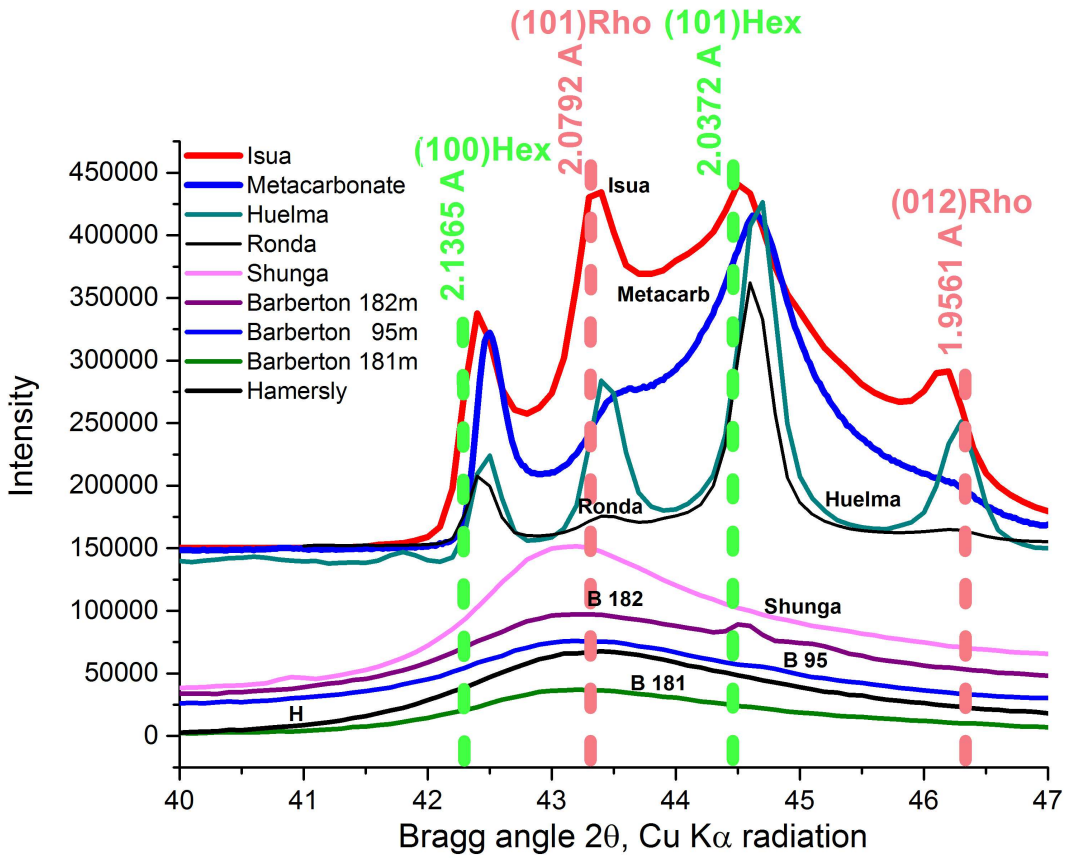

Figure 1. X-ray diffraction structures of two genetically different groups of natural graphites. The upper group of diffractograms comes from carbon of inorganic origin. Superposed on this group is the record (red curve) of graphite at the center of discussion here about its origin. Notable in this material is the high relative content of rhombohedral graphite, suggesting an organic source.

The lower group comes from immature graphitic carbon, growing from organic debris (kerogen) in <3.4 byr old cherts from South Africa and Australia, except the 2 Byr old organogenic bituminous Shunga. Due to the small size of the diffracting domains in these nascent crystals their diffraction lines are broadened into overlapping unresolved bands. Their diffraction maxima closely coincide with the position of the strongest rhombohedral diffraction line (101), confirming that this crystal form dominates and characterizes graphite of organic origin.

The strong enhancement of the reflections from the rhombohedral form of graphite (red vertical lines) suggests that also the Isua carbon is derived from decaying organic matter. In contrast inorganically formed graphite, exemplified by carbon formed by disproportionation of iron carbonate ("metacarb"; black diffraction curve) and by fluid deposited graphite (Ronda and Huelma) is dominated by hexagonal graphite (green vertical Miller index lines).
These observations may be taken as material support for the circumstantial interpretation of the Isua carbon as organogenic and thus indicating the existence of life as early as 3.8 billion years ago.

Your Name: Jeffrey Bada

Title: Professor Distinguished Research Professor and Distinguished Professor Emeritus

Email: jbada@ucsd.edu

Phone: (858) 534-2458

Research Interests*:* My research deals with 3 general topics: How the ingredients for the origin of life where synthesized and preserved on the primitive Earth and elsewhere; the geochemically plausible synthesis of simple polymers on the early Earth; and the use of the annual duration of lake ice cover on high latitude lakes as a proxy for regional climate change.

How the ingredients for the origin of life where synthesized and preserved on the primitive Earth and elsewhere: This has been a long-term effort in my laboratory for several years. We recently published a short paper criticizing the potential use of theoretical *Ab initio* simulations to ascertain the mechanism of synthesis of amino acids in the Miller spark discharge experiment. In addition, during the last year we have focused on completing a project addressing the issue: what happened to the non-protein amino acids likely present in the early oceans once primitive heterotrophic like arose? An experiment dealing with this issue was started by one of my former graduate students, Karen Brinton, in the mid 1990s. In 1994, we collected a seawater sample off the end of the SIO pier as well as a sample of beach sand. We placed these into a small glass covered container. We then added via a sample port a mixture of both biological and non-biological racemic amino acids. We have periodically sampled the mixture over a period 20+years. We found that the biological amino acids, with the exception of D-valine, rapidly disappeared but the non-biological amino acids remained intact. We assumed that this was because of marine bacteria in the seawater and sand. To test if there were still viable organisms present, we spiked the experiment periodically with the biological amino acid glycine. We found that over the entire length of the experiment, the glycine spike was rapidly consumed. We have used this information to suggest that when the first living entities appeared on the Earth, if an early ocean contained both biological and non-biological amino acids, the biological amino acids could have preferentially been consumed by heterotrophic primitive entitles, whereas the non-biological amino acids would have likely persisted for millions of years before they were destroyed by circulation through hydrothermal vents at high temperatures.

The geochemically plausible synthesis of simple polymers on the early Earth: The chemical evolution by which simple monomers (amino acids) were converted in simple polymers (such as peptides) was an important step in the transition from pure abiotic chemistry to biotic chemistry that was characteristic of the first living entities. We showed in 2014 [*Angewandte Chemie* **126**:31 (2014): 8270-8274] that the molecule cyanamide that was likely readily synthesized on the earth Earth and played an important role in inducing amino acid polymerization. We are now extending these experiments to α-hydroxy acids, which like amino acids were likely plentiful on the early Earth. The goal is to determine whether simple mixed amino acid/hydroxyl acid polymers can be synthesized in the presence of cyanamide and whether these molecules could have played an important role in various aspects the abiotic-biotic transition.

Annual duration of lake ice cover on high latitude lakes as a proxy for regional climate change: During the last year I have begun a study on the duration of lake ice to potentially provide a monitor of global warming on a local scale. In high northern latitude regions (generally >40° N) the freezing over of local lakes and the duration of this ice cover

can provide a measure of climate change/warming on a small regional scale. Data on northern latitude lake ice cover is available and in some cases the records cover a century or more. The data suggest that the duration of lake ice cover has started to show a decrease over the last couple of decades. Continued monitoring of northern latitude lake ice duration can be used as a proxy for testing whether downsizing GCM (Global Climate Models) provides accurate predictions of regional climate change and warming. The monitoring of lake ice cover by local residents could increase this database. The involvement of citizens in such an effort gives them an opportunity to directly observe climate change/regional warming and how this impacts their environment. These results also offer a way to further help convince the public of the importance of climate change science.

Recent Publications:

Bada, Jeffrey L., and Henderson James Cleaves. "Ab initio simulations and the Miller prebiotic synthesis experiment." *Proceedings of the National Academy of Sciences* 112.4 (2015): E342-E342.

Bada, Jeffrey L., Reviewed on-line comment posted in *Science* on paper by Hall, Alex. "Projecting regional change." *Science* **34:**.6216 (2014): 1461-1462.

Parker, E.T.; Brinton, K.L.; Burton, A.S.; Glavin, D.P.; Dworkin, J.P.; Bada, J.L. **(2015)** Amino Acid Stability in the Early Oceans. *Astrobiology Science Conference*, Abstract #7019.

Katherine Barbeau Professor, Marine Chemistry

kbarbeau@ucsd.edu

Phone: 858-822-4339

Research Interests: chemistry, biological availability and ecological effects of bioactive trace metals in the marine environment

Research in the Barbeau group focuses on the biogeochemical cycling of trace metals in marine systems. We study the ecological effects of trace elements as limiting or co-limiting micronutrients (or toxins); trace metal bioavailability to and cycling by marine microorganisms; and the chemistry of trace metals in seawater. This year, in collaboration with colleagues in the California Current Ecosystem Long Term Ecological Research (CCE LTER) program, we published a study which explores the effect of iron limitation on carbon export in a coastal upwelling regime (Brzezinski et al. 2015). In this work nutrient dynamics, phytoplankton rate processes, and particle export from the upper ocean were examined in a frontal region 120 km off the coast of southern California. Water masses where diatom growth was inhibited by a lack of iron were characterized by low silicic acid:nitrate ratios (Si:N) and high nitrate to iron ratios. Iron-limited low Si:N waters had low biogenic silica content, intermediate productivity, but high export compared to surrounding waters, indicating increased export efficiency under iron stress. Biogenic silica and particulate organic carbon export were both high beneath low Si:N waters with biogenic silica export being especially enhanced. This suggests that carbon export from low Si:N waters was supported by silica ballasting from iron-limited diatoms. The results imply that iron stress can enhance carbon export, despite lowering productivity, by driving higher export efficiency.

Figure 1. Barbeau group and their trace metal sampling gear on a CCE LTER process cruise in August 2014.

Recent Publications

Semeniuk, D. M. and Bundy, R. M. and Payne, C. D. and Barbeau, K. A. and Maldonado, M. T. 2015. Acquisition of organically complexed copper by marine phytoplankton and bacteria in the northeast subarctic Pacific Ocean. Marine Chemistry. 173:222-233. 10.1016/j.marchem.2015.01.005

Fitzsimmons, J. N. and Bundy, R. M. and Al-Subiai, S. N. and Barbeau, K. A. and Boyle, E. A. 2015. The composition of dissolved iron in the dusty surface ocean: An exploration using size-fractionated iron-binding ligands. Marine Chemistry. 173:125-135. 10.1016/j.marchem.2014.09.002

Brzezinski, M. A. and Krause, J. W. and Bundy, R. M. and Barbeau, K. A. and Franks, P. and Goericke, R. and Landry, M. R. and Stukel, M. R. 2015. Enhanced silica ballasting from iron stress sustains carbon export in a frontal zone within the California Current. Journal of Geophysical Research-Oceans. 120:4654-4669. 10.1002/2015jc010829

Pizeta, I. and Sander, S. G. and Hudson, R. J. M. and Omanovic, D. and Baars, O. and Barbeau, K. A. and Buck, K. N. and Bundy, R. M. and Carrasco, G. and Croot, P. L. and Garnier, C. and Gerringa, L. J. A. and Gledhill, M. and Hirose, K. and Kondo, Y. and Laglera, L. M. and Nuester, J. and Rijkenberg, M. J. A. and Takeda, S. and Twining, B. S. and Wells, M. 2015. Interpretation of complexometric titration data: An intercomparison of methods for estimating models of trace metal complexation by natural organic ligands. Marine Chemistry. 173:3-24. 10.1016/j.marchem.2015.03.006

Bundy, R. M. and Abdulla, H. A. N. and Hatcher, P. G. and Biller, D. V. and Buck, K. N. and Barbeau, K. A. 2015. Iron-binding ligands and humic substances in the San Francisco Bay estuary and estuarine-influenced shelf regions of coastal California. Marine Chemistry. 173:183-194. 10.1016/j.marchem.2014.11.005

Dupont, Chris L. and McCrow, John P. and Valas, Ruben and Moustafa, Ahmed and Walworth, Nathan and Goodenough, Ursula and Roth, Robyn and Hogle, Shane L and Bai, Jing and Johnson, Zackary I. and Mann, Elizabeth and Palenik, Brian and Barbeau, Katherine A. and Craig Venter, J. and Allen, Andrew E. 2015. Genomes and gene expression across light and productivity gradients in eastern subtropical Pacific microbial communities. ISME J. 9:1076-1092. : International Society for Microbial Ecology 10.1038/ismej.2014.198

Jonathan Berger Emeritus Researcher RTAD

jberger@ucsd.edu

Phone: 534-2889

Research Interests: Global seismological observations, marine seismoacoustics, geophysical instrumentation, deep ocean observing platforms, ocean robotics, global communications systems.

With my collaborators John Orcutt, Gabi Laske, and Jeff Babcock we continued testing of the Autonomous Deployable Deep Ocean Seismic System. With a new tow cable and acoustic modem power system, we deployed the ADDOSS in August in 4000 m of water 300 km west of Point Loma within a few km of the site of the DSDP Hole 469, drilled in 1978. We are now third month of successful operation with sensor data being telemetered to IGPP in near real-time.

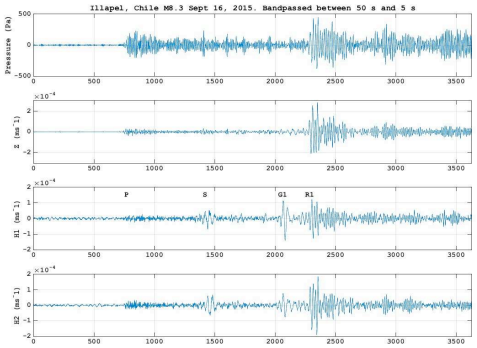

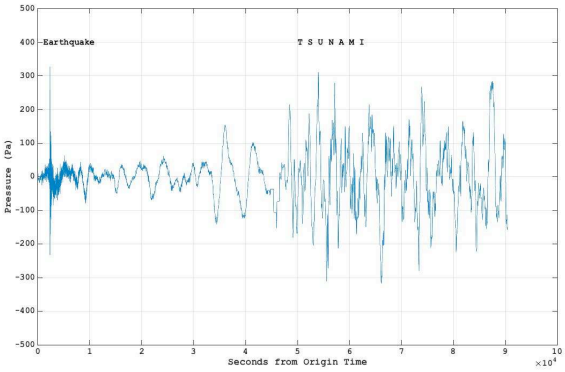

The figure to the left shows the telemetered sensor data recorded from the Illapel, Chile earthquake of Sept. 16 and on the right the seafloor pressure showing the arrival of the tsunami at the site.

I continued my research with Bill Farrell, Walter Munk, and Peter Worcester on trying to understand the relationship between the wind and wave environment, and bottom acoustics. We analyzed data collected from an experiment in the deep ocean of the northeastern subtropical Pacific. The figure to the left shows spectra on the bottom (purple, blue) and at +1,000 m (red) at OBSANP location. Wind recorded on R/V Melville (up to 100 km away from the study area) is shown in black dashes. The comparison between the bottom pressure at 4 Hz (purple, shifted by 30 dB) and 400 Hz (blue) is extraordinary and as far as we know, never before been reported. Of particular interest is the a quick (1 hr, 1 < f < 400 Hz) increse in pressure and vertical velocity on the deep seafloor observed during day 182 on seven instruments comprising a 20 km array. We associate the jump with the passage of a cold front. The changes in the power spectra through the jump, at 4 and 400 Hz, were characterized by a half-way time and the time derivative of the spectra at the half-way time. At every station the half-way time of the

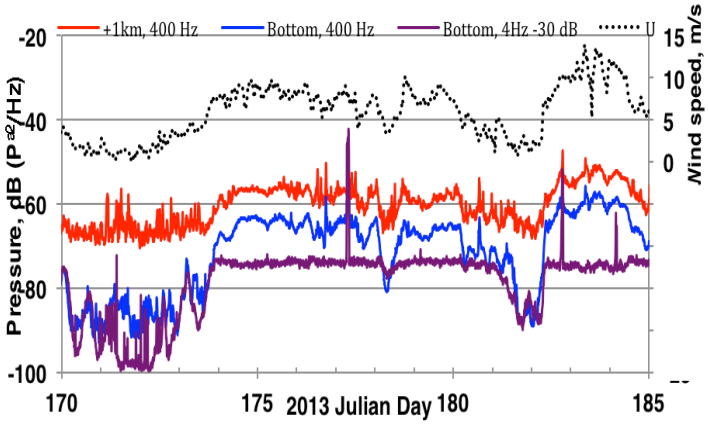

jump is consistent with the front coming out of the northwest. The apparent rate of progress, 10-20 kmhr−1 (2.8-5.6 ms−1), agrees with meteorological observations. The deep signature of the front is modeled as radiation from a moving half-plane of uncorrelated acoustic dipoles. The half-plane is preceded by a 10 km transition zone over which the radiator strength increases linearly from zero. With this model and the measurements of the time derivative of the jump in pressure at the time of passage, a second and independent estimate of the front's speed, 8.5 kmhr−1 (2.4 ms−1), is obtained. For the 4 Hz spectra, we take the source physics to be Longuet-Higgins radiation. Its strength depends on the wave amplitude spectrum and the overlap integral. Thus, the one-hour time constant observed in the bottom data implies a similar time constant for the growth of the wave field quantity as the front crosses a patch of ocean overhead. The spectra at 400 Hz have a similar jump and a similar time constant, but the half-way times are about 25 minutes later than those for 4 Hz. We are now trying to understand the implications of this difference for the source physics behind the high frequency acoustics at depth.

Recent Publications

Jonathan Berger, John Orcutt, Gabi Laske, and Jeffrey Babcock (2015). ADDOSS Annual Report*, NSF, Sept 2015*.

Donna Blackman Research Geophysicist

dblackman@ucsd.edu

Phone: 534-8813

Research Interests*:* Understanding mantle flow, melting, and tectonic evolution along plate boundaries using marine geophysics and numerical modeling.

My work this year was split between program management, for the Marine Geology & Geophysics program at the National Science Foundation, and research conducted upon return to Scripps mid-year. My research focused in two areas– numerical modeling of mantle flow, associated rheologic and seismic anisotropy, and oceanic core complexes.

A collaborative Ridge 2000 project was completed this year, as we wrapped up analysis and publication of the Lau Integrated Studies Site seismic imaging study. Mantle wedge flow and seismic structure varies along the Lau Basin backarc spreading centers. The differences are partly due to kinematics of varying along-basin subduction and spreading rates, but narrowing of the distance between the Tonga trench and the back-arc spreading center from north to south is a stronger control. Observed seismic anisotropy patterns (Menke et al. 2015; Wei et al., 2015) indicate dynamic flow processes that impact mantle melt production and distribution.

Modeling of anisotropic viscosity that develops during mantle flow beneath an oceanic spreading center is the main focus of my ongoing research. In collaboration with colleagues at Cornell and Paris, we are testing feedbacks between mineral alignment and flow pattern, tracking grain scale deformation by dislocation creep and linking that to regional scale flow. We employ a second-order visco-plastic self consistent method, linking viscosity solutions to a FEM calculation of regional flow. Asthenosphere viscosities are calculated throughout the model, based on the response of an mineral aggregate with crystal preferred orientation (CPO) that develops along a flowline tracked from the base of the model to the given finite element. The figures shows results between CPO, viscosity tensors, and updated flow solution, near steady stateafter 15 iterations.

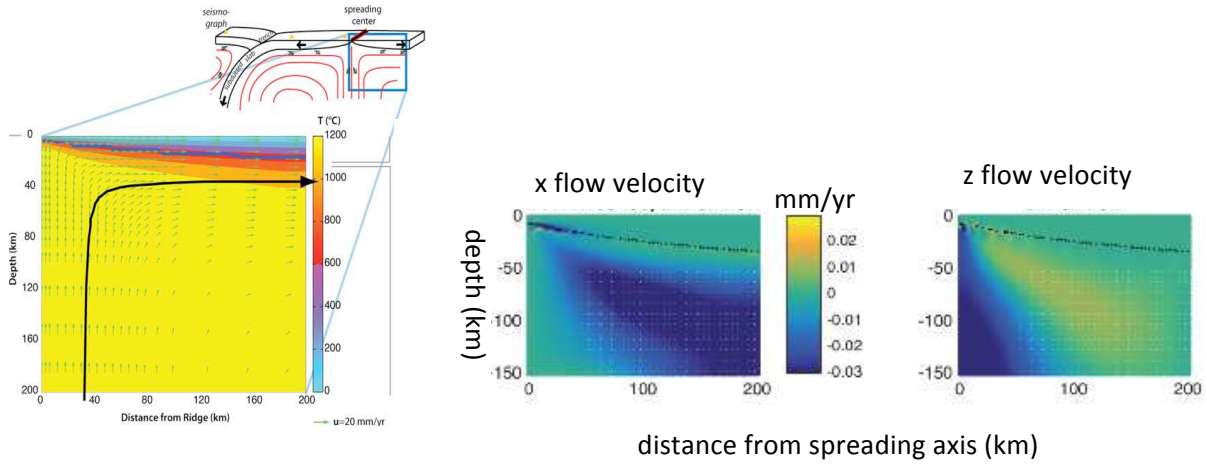

Figure 1a. Model geometry (left) and difference in mantle flow computed for isotropic asthenosphere and self-consistent CPO/rheology case. Black line shows base of rigid lithosphere. Horizontal (x) flow rates are up to 10% slower than an isotropic rheology model; vertical (z) flow rates are up to 10% slower in the upwelling zone beneath the spreading axis and ~5% faster through the corner in the flow field.

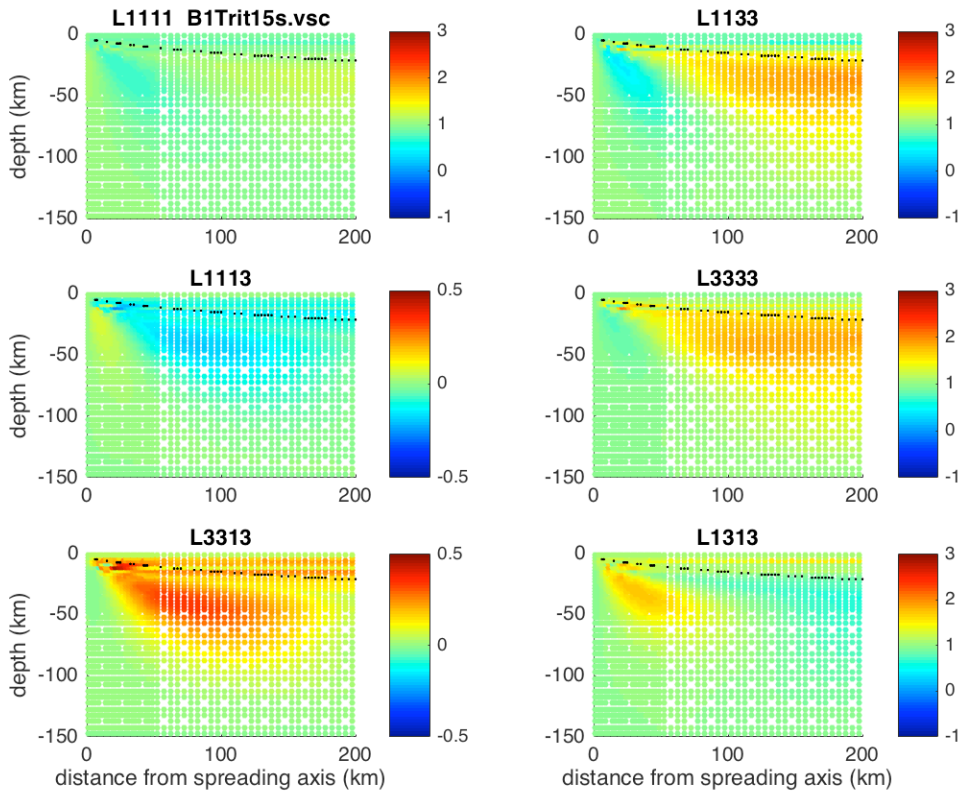

Figure 1b. Independent components of the 6x6 viscosity tensor based on asthenosphere CPO. Green indicates value near isotropic viscosity. Greatest rheologic anisotropy is predicted in the tight flow corner near the spreading axis (L3313 & L1313) and below the base of aging lithosphere (L1133 & L3333).

Oceanic core complex work included documentation of the seafloor character at Atlantis Massif and preparation for an International Ocean Discovery Program coring/logging expedition at Atlantis Bank, on the Southwest Indian Ridge. Undergraduate John Greene was co-mentored by Masako Tominaga (Michigan State) and I for the Mid-Atlantic Ridge work at Atlantis Massif. Complete photo-mosaicking of seafloor imagery showed that there is no systematic pattern in the occurrence of lithified carbonate cap on the detachment-fault-exposed domal core. The scale of the area affected by low level hydrothermal flow was assessed, this process being responsible for rapid lithification of young marine sediments. John applied this information to estimate the volume of carbon storage associated with carbonate cap lithification at oceanic core complexes in the write up for a special volume of Deep Sea Research honoring Peter Rona.

Recent Publications

Greene, J.A., M. Tominaga, D.K. Blackman, Geologic implications of seafloor character an carbonate lithification imaged on the domal core of Atlantis Massif, Deep Sea Res. II, 2015.

Menke, W., Y. Zha, S.C. Webb, D.K. Blackman, Seismic anisotropy indicates ridge-parallel asthenospheric flow beneath the E Lau Spreading Center, J. Geophys. Res.,doi: 10.1002/2014JB011154, 2015.

Wei, S.S., D.A. Wiens, Y. Zha, T. Plank, S.C. Webb, D.K. Blackman, R.A. Dunn, J.A. Conder, Seismological evidence of effects of water on mantle melt transport beneath the Lau back-arc basin, Nature 518, doi:10.1038/nature14113, 2015.

Yehuda Bock
Distinguished Researcher and Senior Lecturer
Director, Scripps Orbit and Permanent Array Center (SOPAC)
ybock@ucsd.edu; Phone: (858) 534-5292

Research Interests: GPS/GNSS, space geodesy, crustal deformation, early warning systems for natural hazards, seismogeodesy, GPS meteorology, data archiving and information technology, sensors

Our research group is application oriented with an emphasis on mitigating effects of natural hazards on people and critical infrastructure through improved forecasting, early warning and rapid response to events such as earthquakes, tsunamis, volcanoes and severe weather. We approach this in a holistic manner from the design and deployment of geodetic and other sensors, real-time data collection and analysis, physical modeling, for example a kinematic earthquake source model followed by tsunami prediction, to communicating actionable information the "last mile" to emergency responders and decision makers during disasters. We maintain a global archive of GNSS data including a growing database of high-rate measurements of large earthquakes, with accompanying IT infrastructure and database management system. In 2014-2015, the SOPAC group included Peng Fang, Jennifer Haase, Jianghui Geng, graduate students Diego Melgar, Dara Goldberg, Jessie Saunders and Lina Su (visiting from China), and Mindy Squibb, Anne Sullivan, Maria Turingan, Glen Offield and Allen Nance.

Earthquake Early Warning and Rapid Response

Reducing warning time is the key goal in early warning and rapid response to earthquakes of medium magnitude and greater in the near-source where losses are most severe. Rapid earthquake characterization requires real-time near-field displacement data in addition to strong motion data. Accurate broadband displacement and velocity waveforms can be estimated by *seismogeodesy*, the optimal combination of high-rate GNSS displacement observations with collocated very-high-rate accelerometer data. Currently, few collocated GNSS/strong-motion stations exist along the western coast of the U.S. where large earthquakes, including tsunamigenic earthquakes, can occur. For the purposes of affordable monitoring, we developed SIO Geodetic Modules and low-cost MEMS accelerometer packages ("GAPs"), designed as a simple plug-

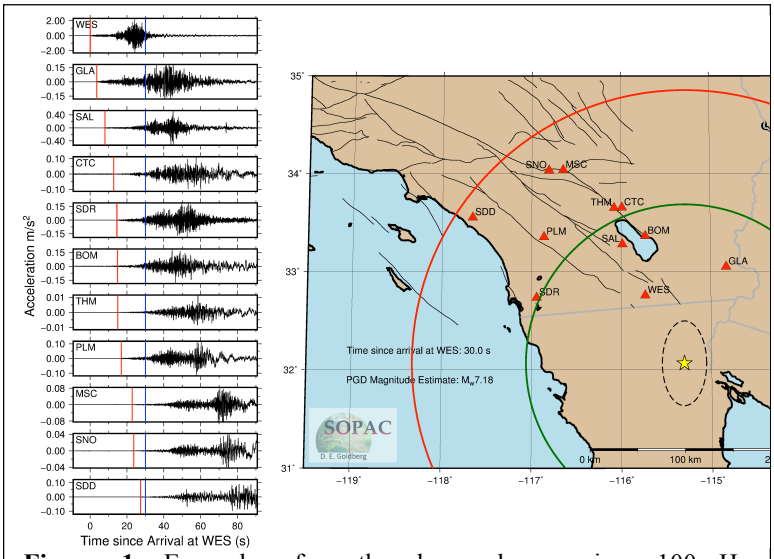

Figure 1. Example of earthquake early warning. 100 Hz seismogeodetic displacement and velocity waveforms were analyzed retrospectively in simulated real-time mode for the 2010 Mw 7.2 El Mayor-Cucapah earthquake in northern Baja California, Mexico. On the left are shown the acceleration waveforms at 11 GPS/seismic stations sorted by order of P-wave detection. The continuous blue vertical line denotes the current epoch. The preceding red lines indicate when the *P* wave was detected at each station. Once 4 stations have triggered, an estimate of the hypocenter can be made, denoted by the yellow star with one-sigma error ellipse on the map. Propagation of *P* and *S* waves can be determined as shown by the partial circles (red and green, respectively), with the *S* wave trailing the *P* wave. In this scenario, it would take the *S* wave front about 80-90 seconds until it arrived in the heavily-populated regions of Riverside and Los Angeles Counties. Shown here is one frame at 30 s after earthquake origin time using peak ground displacement (PGD) magnitude scaling providing an estimate of Mw 7.18, .02 magnitude units smaller than the final magnitude. Prepared by Dara Goldberg. A video showing the complete sequence can be obtained from Dara (degoldberg@ucsd.edu).

in for existing GNSS stations. The Geodetic Module is an instrument that receives, time tags, buffers, analyzes and transmits data from multiple sensors, including a GNSS receiver, accelerometer, and meteorological instruments (pressure and temperature).

Testing of the GAPs against observatory-grade accelerometers was conducted in an experiment on the Large High-Performance Outdoor Shake Table (LHPOST) at UCSD in December 2013 through January 2014, which used large-magnitude earthquake simulations based off of the seismic hazard for Berkeley, CA and Seattle, WA. Jessie Saunders and Dara Goldberg, third year PhD students, helped collect and analyze the data. Direct comparison of SIO MEMS accelerometers with observatory-grade accelerometers indicate that the two types of accelerometers agree within frequency ranges of engineering and seismological interest.

Currently, there are 25 collocated GNSS stations equipped with SIO GAPs in the field, 10 in the San Francisco Bay Area and 15 in southern California. The first assessment of the SIO MEMS packages in the field is underway thanks to four earthquakes of magnitude ~4 that occurred in the past year within this network. These earthquakes are too small to be of interest to earthquake early warning (typically magnitude 5.5 and higher) and have surface displacements well below the uncertainty level of the GNSS data. However, the SIO MEMS were sensitive enough to record the shaking within several tens of kilometers from the epicenters of these events, and the seismogeodetic combinations at these stations produced stable displacement and velocity time series. The seismogeodetic waveforms for these events showed that while an earthquake was occurring, the event was not developing into large ruptures with significant displacement, an important datum for whether or not to issue a warning for an earthquake of consequence. The combination of the analyses in the field and at the LHPOST demonstrate that GAPs are sufficient for early warning and that there is little benefit to investing in higher-cost upgrades to GNSS stations for the purposes of earthquake early warning.

We are implementing an automated detection algorithm that recognizes *P* waves on an individual station basis. This is followed by an automatic hypocenter estimation and earthquake magnitude scaling according to peak ground displacements (PGD), which will comprise a preliminary warning (Figure 1). The seismogeodetic dataset is uniquely fit for determining earthquake magnitude as the inclusion of GNSS data avoids underprediction (saturation) associated with acceleration data alone. Finally, a CMT solution, finite fault slip model, and tsunami model are estimated to provide a more detailed description of rupture parameters and potential hazard.

Using a combination of GNSS and inexpensive pressure and temperature sensors, we can also estimate the variations of water vapor in the lower atmosphere (troposphere), a critical driver of extreme weather such as the southern California summer monsoons. NOAA's weather forecasting offices in San Diego and Los Angeles Counties successfully used our data to forecast and track a monsoon in the summer of 2013 and issue an accurate flash flood warning for the region (*Moore et al*., 2014).

Publications (2014-2015)

Bock, Y. and D. Melgar (2015), Physical Applications of GPS Geodesy: A Review, Reports on Progress in Physics, in press.

Galetzka, J., et al. (2015), Slip pulse and resonance of Kathmandu basin during the 2015 Mw 7.8 Gorkha earthquake, Nepal imaged with space geodesy, *Science*, *349*, 1091. doi: 10.1126/science.aac6383

Melgar, D. and Y. Bock (2015), Kinematic earthquake source inversion and tsunami inundation prediction with regional geophysical data, *J. Geophys. Res*., doi: 10.1002/2014JB011832.

Melgar, D., J. Geng, B. W. Crowell, J. S. Haase, Y. Bock, W. C. Hammond, and R. M. Allen (2015), Seismogeodesy of the 2014 Mw6.1 Napa earthquake, California: Rapid response and modeling of fast rupture on a dipping strike-slip fault, *J. Geophys. Res. Solid Earth*, *120*, doi:10.1002/2015JB011921.

Melgar, D., et al. (2015), Earthquake Magnitude Calculation without Saturation from the Scaling of Peak Ground Displacement, *Geophys. Res. Lett. 42* (13), 5197-5205. doi: 10.1002/2015GL064278

Moore, A., I. Small, S. Gutman, Y. Bock, J. Dumas, J. Haase, M. Jackson, J. Laber (2015), Densified GPS Estimates of Integrated Water Vapor Improve Forecaster Situational Awareness of Variable Moisture Fields in the Southern California Summer Monsoon, *Bull. Amer. Meteorol. Soc*. (BAMS), doi:10.1175/BAMS-D-14-00095.1

Adrian Borsa Assistant Research Scientist and Senior Lecturer
aborsa@ucsd.edu
Phone: 858-534-6845

Research Interests: Remote hydrology from GPS and GRACE. Satellite altimeter calibration/ validation and measurements of topographic change. Differential lidar techniques applied to problems in geomorphology and tectonic geodesy. Kinematic GPS for positioning, mapping, and recording transient deformation due to earthquakes, fault creep and short-period crustal loading. GPS multipath and other noise sources. Dry lake geomorphology.

My recent research involves the characterization of the hydrological cycle using crustal loading observations from GPS, in collaboration with SIO colleagues Duncan Agnew and Dan Cayan. Changes in water storage in lakes, aquifers, soil moisture, and vegetation results in elastic deformation of the crust that yields measureable vertical displacements of the surface. The seasonal signal from water loading has been extensively studied, but loading changes over longer periods are typically smaller and have not been broadly documented. Since 2013, however, drought in the western USA has caused rapid and widespread uplift of mountainous areas of California and the West. The vertical displacements from the drought are unprecedented in magnitude over the past decade of continuous GPS observations.

The drought uplift signal, which exceeds 15 mm at locations in the Sierra Nevada, is large enough to be obvious by inspection of GPS time series. We apply a seasonal filter derived from the econometrics literature (the Seasonal-Trend-Loess estimator) to completely remove the annual signal due to water loading and pumping, and we invert the filtered GPS position data to recover the spatiotemporal loading required to account for observed uplift. In the case of the current drought, our estimate of the accrued water deficit ranges up to 50 cm and totals 240 gigatons, equivalent to a 10 cm uniform layer of water over the land area east of the Rocky Mountains. Currently, we are extending our analysis to look at short-term changes in loading from individual storms, and we are investigating drought-induced Coulomb stress changes on all faults in the UCERF3 fault model.

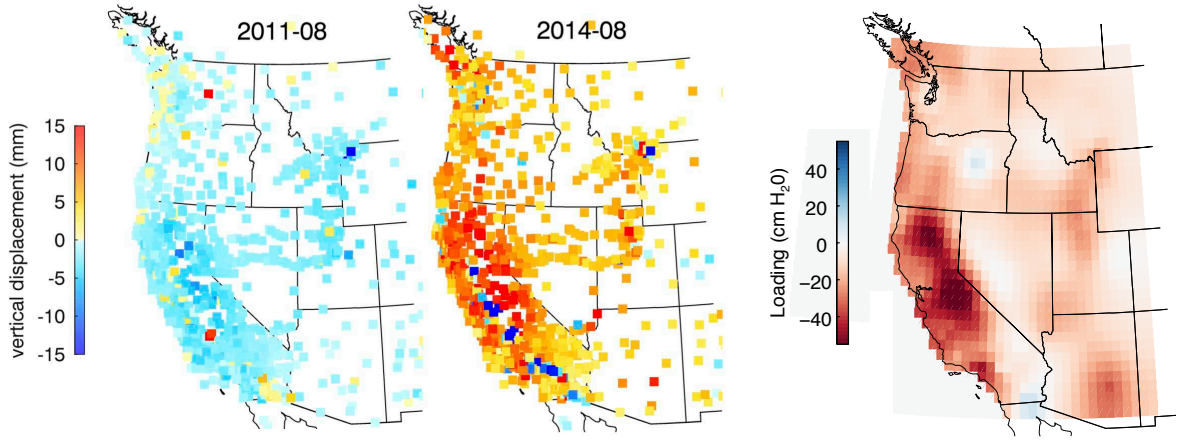

Figure 1: **Left**: Spatial distribution of vertical displacements from Plate Boundary Observatory continuous GPS stations in the western USA in March of 2013 and 2014. Color indicates deviations of seasonally-adjusted elevations from decadal mean, with blues related to subsidence and yellow-reds related to uplift. **Right**: Mass load in mm of water equivalent derived from inversion of March 2014 vertical displacements, assuming elastic strains on a spherical Earth.

My other primary area of research has been the calibration and validation of satellite altimeter measurements using a reference surface at the salar de Uyuni, Bolivia. In collaboration with SIO colleague Helen Fricker, I have led three expeditions to the salar de Uyuni (in 2002, 2009 and 2012) to survey the surface with kinematic GPS. We have established that the surface is both exceptionally flat (80 cm total relief over 50 km) and stable (< 3 cm RMS elevation change over a decade), while maintaining coherent geoid-referenced topography at wavelengths of tens of kilometers. In 2013, using our salar digital elevation model (DEM), I found and was able to identify the source of an inadvertent error in ICESat-1 processing that was the source of large shot-to-shot errors late in the mission period and that significantly changed ICESat-derived elevation change trends for the stable portions of the Greenland and Antarctic ice sheets.

Recently we have began to explore surface change at the salar using ALOS InSAR observations, with the goal of linking absolute GPS measurements with relative motions provided by InSAR to provide a continuous time series of surface displacement for calibration purposes. We have also expanded our cal/val activity to the CryoSat mission and are currently evaluating improvements between Baseline B and Baseline C datasets. Our ongoing interaction with the CryoSat mission team has led ESA to switch CryoSat from SARIN to LRM mode for all passes over the salar de Uyuni from 2015 onward, allowing us to provide a cross-calibration of elevations from these different operational modes.

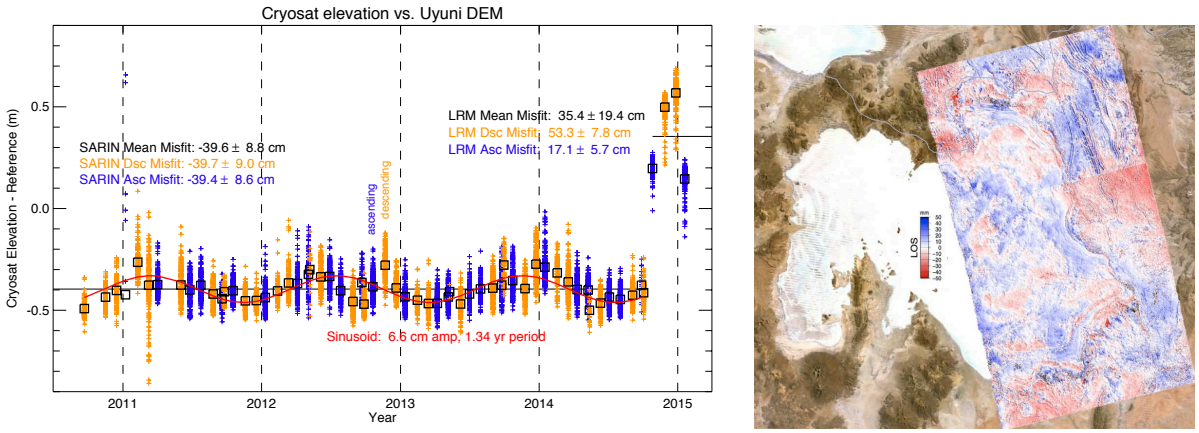

Figure 2: **Left**: Cryosat elevation validation relative to the salar de Uyuni DEM, with residuals showing a.) a uniform range bias of -40 cm for SARIN mode and +35 cm for LRM mode, b.) an 7 cm amplitude sinusoidal anomaly of 1.34 yr period that is still unexplained, and c.) higher range resolution than reported elsewhere, even with the sinusoidal anomaly. **Right:** ALOS InSAR results over the salar de Uyuni for the period 8/27/2010 ~ 1/12/2011, indicating that seasonal elevation change is <1 cm averaged over the salar surface.

Publications since October 2014

Becker, T.W., A.R. Lowry, C. Faccenna, B. Schmandt, A. Borsa, C. Yu (2015). "Western U.S. intermountain seismicity caused by changes in upper mantle flow." Nature, **524**, 458–461

Trugman, D.T., A.A. Borsa, D.T. Sandwell, (2014). "Did Stresses From the Cerro Prieto Geothermal Field Influence the El Mayor-Cucapah Rupture Sequence?" Geophysical Research Letters, **41**(24)

Pat Castillo Professor of Gology

pcastillo@ucsd.edu

Phone: 534-o383

Research Interests: geochemistry and petrogenesis of magmas produced within and along divergent and convergent margins of tectonic plates; magmatic and tectonic evolution of continental margins; mantle geodynamics

Last year, my student and I started a NSF-funded project on subduction zone magmatism. The bulk of subduction zone or arc magmas are produced by partial melting of the mantle wedge metasomatized by the so-called 'slab component'. This component is enriched in volatiles and other fluid-mobile elements and mainly comes from subducted sediment and underlying altered oceanic crust (AOC). Many studies have shown a strong link between subduction component (input) and arc magmas (output), particularly in sedimented arc-trench systems. The Izu-Bonin system is basically sediment-poor and, thus, the observed latitudinal compositional variation of its arc magmas, particularly that of Pb isotopes, must be coming from AOC. Indeed, AOC is estimated to supply up to ~50% or more of the Pb in arc magmas. However, whereas the Izu-Bonin arc magma chemistry requires influx of Pb from a subducted Indian-type AOC, the spot sample of incoming AOC at Ocean Drilling Program (ODP) Site 1149 near the center of the Pacific Plate subducting beneath Izu-Bonin arc is Pacific-type. The apparent discrepancy of Pb input and output in the Izu-Bonin system thus puts into question the concept of AOC being an important source of Pb in arc magmas and our understanding of subduction component in general. To resolve these issues, we went on an expedition aboard R/V Revelle in October-November 2014 (RR1412 Cruise) to systematically sample the AOC in the Pacific Plate subducting beneath the Izu-Bonin arc by dredging. The expedition marks the start of a combined field and laboratory investigation to test whether AOC samples from the northern, younger (<125 Ma) segment of the Pacific Plate subducting beneath Izu-Bonin arc have an Indian-type signature, similar to the composition of Izu-Bonin arc magmas. We dredged AOC from active, vertical fault scarps along a ~700 km long section of the Pacific Plate from 26.5 oN to 34.5 oN. Our sampling transect encompassed a significant range of crustal ages that includes the purported compositional change from Pacific-type to Indian-type of the subducting Pacific crust at ~125 Ma. Our preliminary analytical results after the cruise indicate that the major element composition of AOC from the older, southern side of ODP Site 1149 (127 Ma) is normal, Pacific-type tholeiitic basalt. However, AOC composition becomes more alkalic in the younger, northern side of ODP Site 1149. This compositional trend is supported by an increase in incompatible trace element concentrations and their ratios with less incompatible trace elements. Thus, preliminary data indicate that there is at least a compositional change in the subducting Pacific AOC at ~125 Ma. However, we need more detailed analytical data, particularly Pb isotopes, in order to verify whether AOC provides the subduction component responsible for the Indian-type composition of Izu-Bonin arc magmas. The project will continue for ~2 more years.

Also last year, I published my hypothesis that recycled marine carbonates are the key ingredient in the so-called 'HIMU' and 'FOZO' components in the mantle source of ocean island basalts (OIB). Many, and perhaps all OIB clearly contain crustal materials that have been shoved into the mantle through subduction or other geologic processes. One of the first recycled materials to be recognized was mid-ocean ridge basalt (MORB), and this was later fine-tuned as having a long time-integrated (b.y.) high U/Pb ratio or high μ (HIMU) and producing OIB with the most radiogenic Pb isotopic ratios ($^{206}Pb/^{204}Pb > 20.0$) and among the least radiogenic $^{87}Sr/^{86}Sr$ (~0.7030). However, it is becoming more evident that the compositional connection between

subducted MORB and HIMU basalts is problematic. My alternative hypothesis is that a small amount (a few %) of recycled Archaean marine carbonates (primarily CaCO3) inherently had low U/Pb and $^{87}Sr/^{86}Sr$ and, thus, is the main source of the distinctly high $^{206}Pb/^{204}Pb$, $^{207}Pb/^{204}Pb$ and low $^{87}Sr/^{86}Sr$ isotopic and some of the major-trace element compositions of classic HIMU whereas post-Archaean marine carbonates are the main source of younger HIMU or FOZO mantle sources. As an extension of the hypothesis, I also proposed a conceptual model showing that FOZO mainly consists of the lithospheric mantle portion of ancient metamorphosed oceanic slabs that have accumulated deep in the mantle, perhaps all the way to the core-mantle boundary. Such an ultramafic source is geochemically depleted due to prior extraction of basaltic melt plus removal of the enriched subduction component from the slabs through dehydration and metamorphic processes. Combined with other proposed models in the literature, the conceptual model can provide reasonable solutions for the $^{208}Pb/^{204}Pb$, $^{143}Nd/^{144}Nd$, $^{176}Hf/^{177}Hf$, and $^{3}He/^{4}He$ isotopic paradoxes or complexities of oceanic lavas. The general model is illustrated in the figure below (from Castillo, 2015).

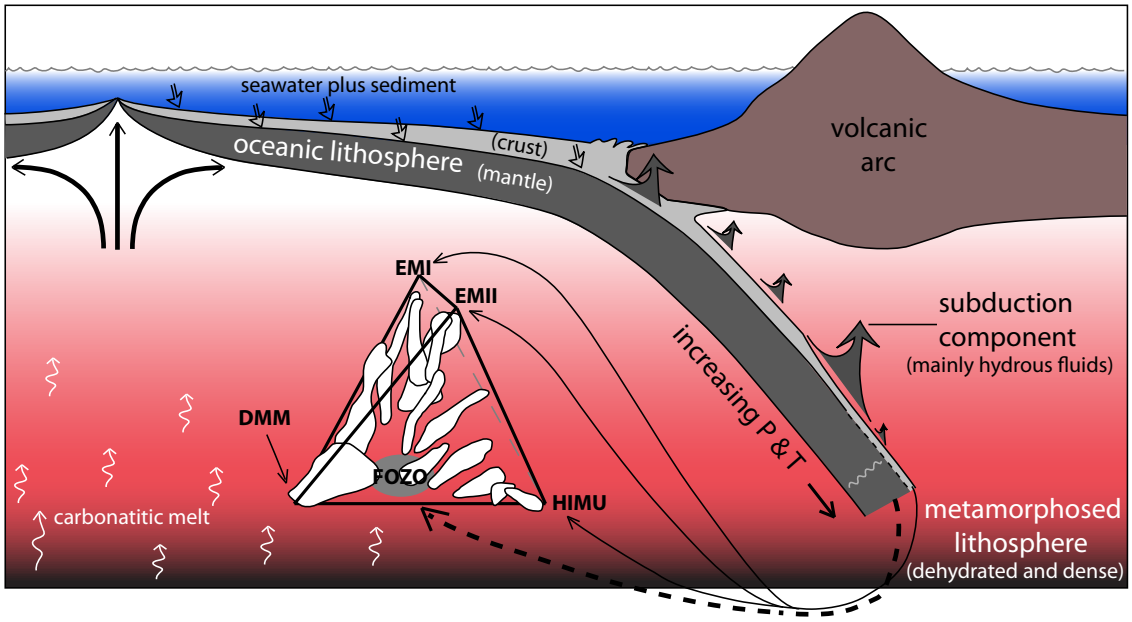

A schematic diagram showing the origin of isotopically defined mantle components. The EMI, EMII and HIMU corners of the tetrahedron, constructed from Sr, Nd and Pb isotopic data for oceanic basalts, represent recycled crustal materials and these generally are mixing with FOZO, which represents the depleted, lithospheric mantle portion of subducted slab. The DMM is the upper mantle that supplies melt to mid-ocean ridges. A small amount of carbonatitic melt is coming from below and mixing with DMM.

Recent Publications

Castillo, P.R. "The recycling of marine carbonates and sources of HIMU and FOZO ocean island basalts" Lithos 216-217, doi:10.1016/j.lithos.2014.12.005, 2015.

Yan, Q., Castillo, P.R., Shi, X., Wang, L., Liao, L., and Ren, J. "Geochemistry and petrogenesis of volcanic rocks from Daimao Seamount (South China Sea) and their tectonic implications" Lithos 218-219, doi:10.1016/j.lithos.2014.12.023, 2015.

C. David Chadwell

Research Geophysicist

cchadwell@ucsd.edu

Research Interests: Seafloor tectonics of subduction, transform motion, and seafloor spreading. Volcanic collapse, slope stability and associated geo-hazards. Seafloor geodetic techniques with acoustics and GPS.

In 2015, we used a new, lower cost approach to collect GPS-Acoustic data for long-term measurements of seafloor deformation. The GPS-Acoustic method combines high-precision kinematic GPS positioning from an ocean surface platform with precision acoustic ranging from the platform to transponders on the seabed. The technique was developed by our group here at SIO. Wider adoption of GPS-A has been restricted by the high-cost of shiptime (~$50k/day) and the finite life of batteries in the seafloor transponders.

We re-measured a site first measured in 2000 and now have a 14 year-long time series, the longest seafloor geodetic time series in existence. Results from this site and two other GPS-A sites on the Juan de Fuca plate are being combined to provide a present-day estimate of the Juan de Fuca plate Euler pole.

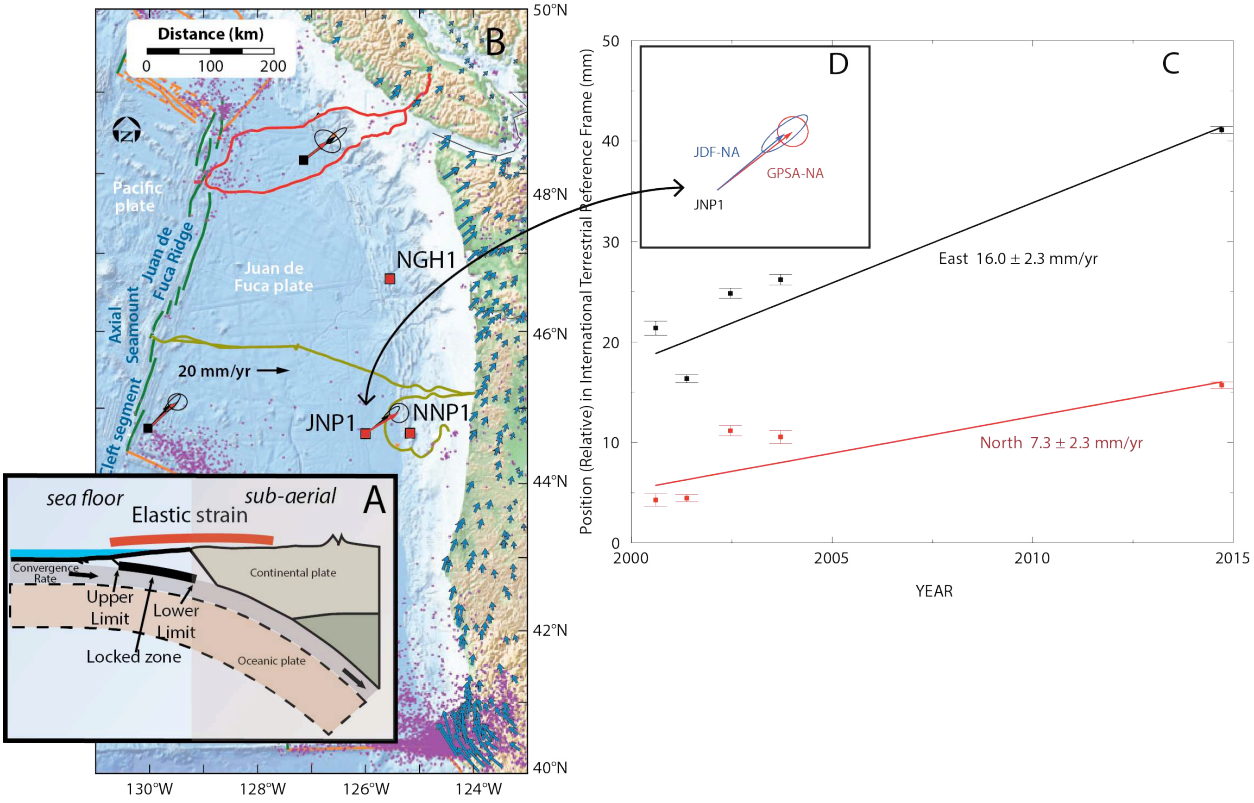

Figure 3: (**A**) Subduction process showing incoming plate in contact along interface with upper plate which accumulates elastic strain as uplift and contraction. Much of the deformation occurs offshore, highlighting the significance of seafloor measurements in a space geodetic frame to bridge the sub-aerial and marine regions. (**B**) In 2014, two sites NNP1 and NGH1 were established, the first sites on the seaward slope of Cascadia subduction zone. Also in 2014, site JNP1 offshore Newport was reestablished and its position re-measured. Two earlier GPS-Acoustic sites (black squares) are also shown. Red and black arrows show the GPS-Acoustic and geomagnetically-derived plate motions relative to North America, respectively. (**C**) East (black) and North (red) positions and velocities in the ITRF frame for **JNP1**. (**D**) The GPSA-NA (red) and the JdF-NA motion from geomagnetics and GPS. There is no significant difference.

Recent Publications:

Burgmann, R. and Chadwell, C. D. Seafloor Geodesy, *Annu. Rev. Earth Planet. Sci. 2014*, 42: 509-534.

Catherine Constable **Professor**
cconstable@ucsd.edu
Phone: 534-3183

Research Interests: Earth's magnetic field and electromagnetic environment; Paleo and geomagnetic secular variation; Linking paleomagnetic observations to geodynamo simulations; Paleomagnetic databases; Electrical conductivity of Earth's mantle; Inverse problems; Statistical techniques.

The natural spectrum of geomagnetic variations at Earth's surface extends across an enormous frequency range, and is controlled by a variety of internal and external physical processes. As indicated in the grand spectrum of field strength variations in Figure 1(a) the spatial origin of the sources can be roughly divided according to the characteristic time scales of their variations, into internal fields produced by the geodynamo in Earth's core, external fields generated in the magnetosphere and ionosphere as result of interactions with the solar wind and sferics (lightning) and anthropogenically generated signals. There are also lithospheric contributions to the field which are essentially static and make no contribution to the frequency spectrum.

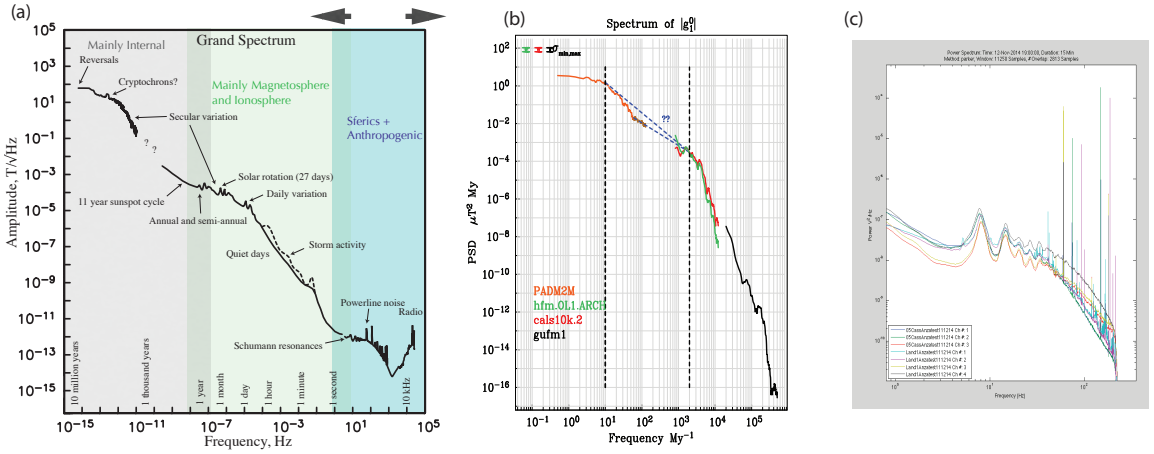

Figure 1: Amplitude spectrum of geomagnetic field variations at Earth's surface: (a) composite extending from 10^{-15} to 10^{5} Hz, based on paleomagnetic and direct surface magnetic field observations; (b) power spectrum of axial dipole moment variations based on models constructed from paleomagnetic (PADM2M, hfm.OL1.ARCH, cals10k.2) and geomagnetic data (gufm1); (c) uncalibrated spectrum from 1-500 Hz in ELF range showing sferics, Schumann resonances, and anthropogenic signals.

The overall shape of the spectrum is red, reflecting the time scale of variations in the predominantly dipolar internal field produced by the geodynamo in Earth's liquid outer core. Fluid flow in the highly electrically conductive ($\sim 10^{6}$ Sm^{-1}), core produces a secular variation in the magnetic field, which propagates upward through the much lower conductivity mantle and lithosphere. The dipole part of the field has the longest term changes, associated with geomagnetic excursions and reversals which require the axial dipole part of the field to vanish as it changes sign. Finite electrical conductivity of the mantle effectively filters variations in the core field on time scales much less than a year. Thus the internal part of the spectrum is greatly diminished in the frequency range dominated by the solar cycle, and magnetospheric processes.

Ongoing research projects (with postdoc Sanja Panovska (IGPP) and Monika Korte of GeoForschungs Zentrum, Helmholtz Center, Potsdam) have been concerned with analysis of behavior

of the geomagnetic field on centennial to 100 kyr timescales helping to fill the gap in Figure 1(a). Figure 1(b) shows new power spectra: the gap between 1 ky and 10 ky periods will be filled when 100 ky field models become available. This work has relied on compilations of published datasets for the MagIC (Magnetics Information Consortium with Lisa Tauxe, Anthony Koppers), and GEOMAGIA50.v3 database projects with Maxwell Brown (GeoForschungs Zentrum, Helmholtz Center, Potsdam). The 100 ky model being finalized now also allows a study of field structure during the Laschamp excursion which occurred around 40 ka. Work is continuing with PhD student Margaret Avery, postdoctoral researcher Christopher Davies (Leeds University, U.K.) and research associate David Gubbins on compatibility of numerical geodynamo simulations with paleomagnetic results.

Very long geomagnetic observatory records are being used to isolate external magnetic variations for deep mantle induction studies using geomagnetic depth sounding. Above the insulating atmosphere is the relatively electrically conductive ionosphere, which supports *Sq* currents as a result of dayside solar heating. Outside the solid Earth the magnetosphere, the manifestation of the core dynamo, is deformed and modulated by the solar wind, compressed on the sun side and elongated on the nightside. Inside the magnetosphere are the Van Allen Radiation belts, which are layers of energetic charged particles: usually there are two main belts typically ranging in altitude from about 1000 to 60 000 km. The outer belt, at about 3 Earth radii, contains the magnetospheric ring current which acts to oppose the main field is also modulated by solar activity. Magnetic fields generated in the magnetosphere and ionosphere propagate by induction into the conductive Earth, providing information on electrical conductivity variations in the crust and mantle.

At frequencies >1 Hz, the spectrum is dominated by sferics and anthropogenic noise, as in the local Californian data in Figure 1(c) This frequency range is useful for near-surface audiomagnetotelluric and global lightning studies. At frequencies higher than 10^4 Hz the global EM spectrum becomes blue, rising in response to man-made signals. In the spectrum of Figure 1(a) one can clearly see a frequency separation in the various natural sources, with signal from magnetic storms, and daily variation in the ionosphere dying away around 1 Hz, and the sferics losing energy around 1-3 kHz. These are well known as "dead bands" with very low signal in the MT source field.

Recent Publications

Ziegler, L.B., & C.G. Constable (2015). Testing the geocentric axial dipole hypothesis using regional paleomagnetic intensity records from 0-300 ka,*Earth Planet. Sci Lett.*,**423**, 48–56, 10.1016/ j.epsl.2015.04.022

Panovska, S., M. Korte, C.C. Finlay, and C.G. Constable (2015). Limitations in paleomagnetic data and modeling techniques and their impact on Holocene geomagnetic field models, *Geophysical Journal International*, **202**, 402–418, 10.1093/gji/ggv137

Brown, M.C., F. Donadini, M. Korte, A. Nilsson, K. Korhonen, A. Lodge, S.N. Lengyel and C.G. Constable (2015). GEOMAGIA50.v3: 1. General structure and modifications to the archeological and volcanic database, *Earth Planets Space*, **67**, 1–31, 10.1186/s40623-015-0232-0

Brown, M.C., F. Donadini, A. Nilsson, S. Panovska, U.Frank, K. Korhonen, M. Schuberth, M. Korte, C.G. Constable (2015). GEOMAGIA50.v3: 2. A new paleomagnetic database for lake and marine sediments, *Earth Planets Space*, **67**, 1-19, 10.1186/s40623-015-0232-0

Constable, C.G. & M. Korte (2015). Centennial to millennial-scale geomagnetic field variations , *Treatise on Geophysics (Second Edition), Volume 5, Geomagnetism*, Editor, M. Kono, Ed in Chief: G. Schubert, Elsevier, Amsterdam, Chapter 9, pp 309-341, ISBN: 978-0-444-53803-1, 10.1016/B978-0-444-53802-4.00103-2

Constable, C.G. (2015). Earth's Electromagnetic Environment, *Surveys in Geophysics*, submitted.

Steven Constable **Professor**
sconstable@ucsd.edu
Phone: 534-2409

Research Interests: Marine EM methods, electrical conductivity of rocks

Steven Constable runs the SIO Marine Electromagnetic (EM) Laboratory at IGPP, and along with Kerry Key oversees the Seafloor Electromagnetic Methods Consortium, an industry funding umbrella which helps support PhD students and postdocs working in the group. The two main field techniques we use are controlled-source EM (CSEM), in which a deep-towed EM transmitter broadcasts energy to seafloor EM recorders, and magnetotelluric (MT) sounding, in which these same receivers record natural variations in Earth's magnetic field. Both methods can be used to probe the geology of the seafloor, from the near surface to hundreds of kilometers deep, using electrical conductivity as a proxy for rock type.

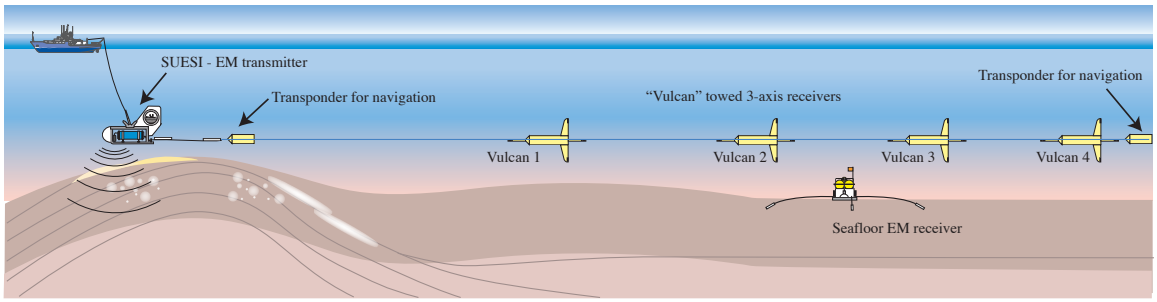

Figure 1: "Vulcan" array of towed, 3-axis electric field recorders.

The lab had another busy year, with an offshore geothermal study in Mexico, a second field season in the Arctic, and a second year of gas hydrate mapping offshore Japan. Kerry took the gear out on NSF-funded projects to the Aleutians and east coast USA.

Gas hydrate, a frozen mixture of water and gas (usually methane), is important as a seafloor hazard, a potential energy resource, and a source of a potent greenhouse gas. Our gas hydrate mapping work uses an array of electric field recorders that are towed behind our EM transmitter close to the seafloor (Figure 1). These "Vulcan" instruments (Figure 2) have been in development for a long time, but we made several significant upgrades this year which we tested on a short 2-day cruise in the San Diego Trough in March. We chose to tow over a known methane vent and cold seep near the north end of the Trough, just to see what we might see (Figure 3).

The instrument upgrades resulted in very high quality data. Graduate student Peter Kannberg inverted the data and Figure 3 shows the result of one tow across the methane vent. Beneath the seep there is a tabular resistor about 1 km across extending from a depth of about 50 m below the sea floor to a depth of around 150 m. At the location of the methane vent we see the high resistivities coming up to the sea floor. The high electrical resistivity of this body (nearly 100 Ωm) and its location within the gas hydrate stability field implies that the resistor is massive hydrate. The methane vent is associated with the San Diego Trough Fault, which presumably provides a path for methane migration from depth.

During the summers of 2015 and 2016 we helped carry out large surveys of offshore gas hydrate for the Japanese geological survey. Although this work is proprietary, it is very exciting to be playing an important part in Japan's alternative energy program.

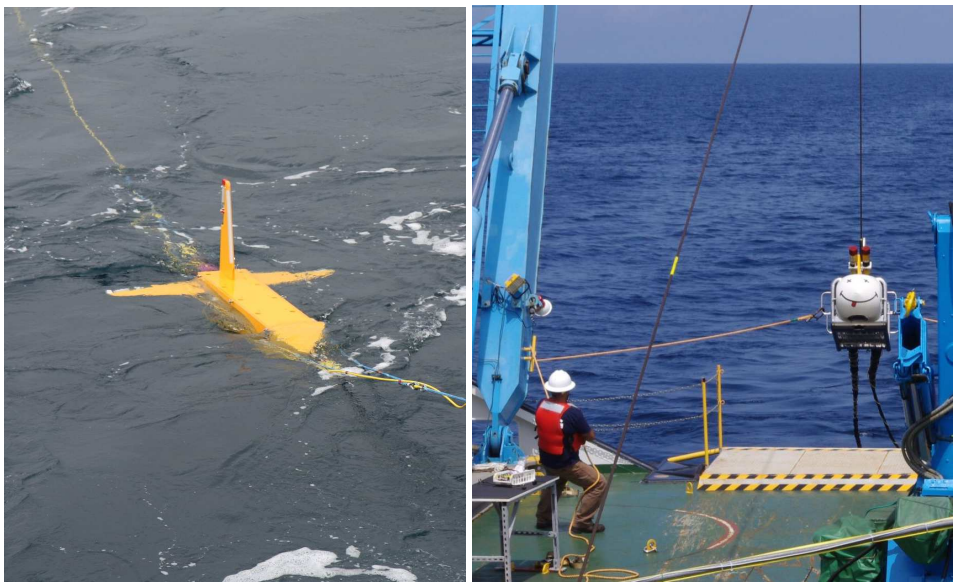

Figure 2: Left: A Vulcan instrument being deployed. Right: Our EM transmitter being recovered during a gas hydrate survey for the Japanese government (photo courtesy Ocean Floor Geophysics).

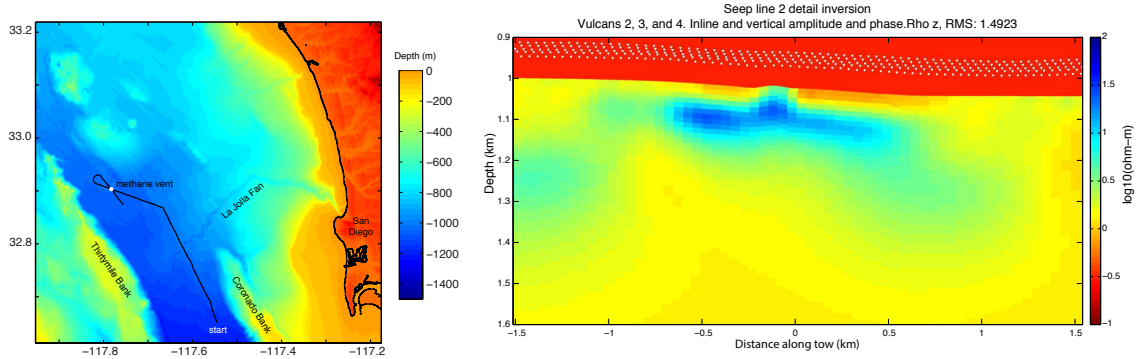

Figure 3: Left: Map of our test tow. Right: Electrical conductivity image of methane seep in the San Diego Trough.

Recent Publications

Du Frane, W., L.A. Stern, S. Constable, K.A. Weitemeyer, M.M. Smith, and J.J. Roberts (2015) Electrical properties of methane hydrate + sediment mixtures, *Journal of Geophysical Research,* **120,** 4773–4783, 10.1002/2015JB011940

Constable S. (2015) Geomagnetic Induction Studies, *in: Treatise on Geophysics, 2nd edition.* Gerald Schubert, editor. Oxford: Elsevier 219-254. 10.1016/B978-0-444-53802-4.00101-9

Wheelock, B., S. Constable, and K. Key (2015) The advantages of logarithmically scaled data for electromagnetic inversion, *Geophysical Journal International,* **201,** 1765–1780, 10.1093/gji/ggv107

Myer, D., K. Key, and S. Constable (2015) Marine CSEM of the Scarborough gas field, Part 2: 2D inversion, *Geophysics,* **80,** E187–E196, 10.1190/GEO2014-0438.1

Constable, S., A. Orange, and K. Key (2015) And the geophysicist replied: "Which model do you want?", *Geophysics,* **80,** E197–E212, 10.1190/GEO2014-0381.1

Further information can be found at the lab's website, http://marineemlab.ucsd.edu/

J. Peter Davis

Specialist

Email: pdavis@ucsd.edu

Phone: 4-2839

Research Interests: seismology, time series analysis, geophysical data acquisition

My research responsibilities at IGPP center upon managing the scientific performance of Project IDA's portion of the Global Seismographic Network (GSN), a collection of 40 seismographic and geophysical data collection stations distributed among 26 countries worldwide. IDA recently concluded upgrading the core data acquisition and power system equipment at all stations using funding provided by NSF via the IRIS Consortium.

During the next phase of network operation, IDA's staff will fine-tune each station's instruments to enable scientists to extract the most accurate information possible from the data collected. One method for accomplishing this task is by examining key phenomena such as Earth tides and normal modes that should register the same on these important geophysical sensors. To the extent that measurements made with multiple instruments that have been calibrated in very different fashions match, we may have greater confidence that the instrument response information IDA distributes with GSN waveform data is accurate. Investigators use this information to compensate for the frequency-dependent sensitivity of sensors so that they may study true ground motion and its underlying physical causes. One test of these methods is illustrated below.

Figure 1 shows very long period normal modes excited by a large earthquake that occurred recently in Chile and recorded on the vertical components of three seismometers installed at IGPP's Seismic Test Facility at the Pinyon Flat Observatory. The upper portion of the figure shows prominent spectral peaks whose frequencies tell us much about the internal structure of the Earth. To the extent that the peaks observed on the three separate instruments overly one another indicates that the responses of each instrument are well determined. Where the spectra do not agree may be attributed to instrument noise.

The consistency of the spectral measurements is clarified in the lower portion of the figure. Here are plotted the ratio of the peak amplitude observed on each of the two instruments (XPFO.*) under test compared to the standard instrument (PFO.*). Any deviation of the mean of these distributions away from unity or linear trend would indicate a problem with the instrument response. That is not observed here. The scatter in the points, which is a measure of instrument noise, begins to increase substantially below 1.5 mHz.

IDA is playing a leading role in a program to evaluate new models of seismometers that may be deployed within the GSN in the future. The two instruments under test here are part of that effort. With new instrumentation and continued data collection from the present instruments of the GSN, we can expect steady scientific progress in understanding Earth structure and earthquakes.

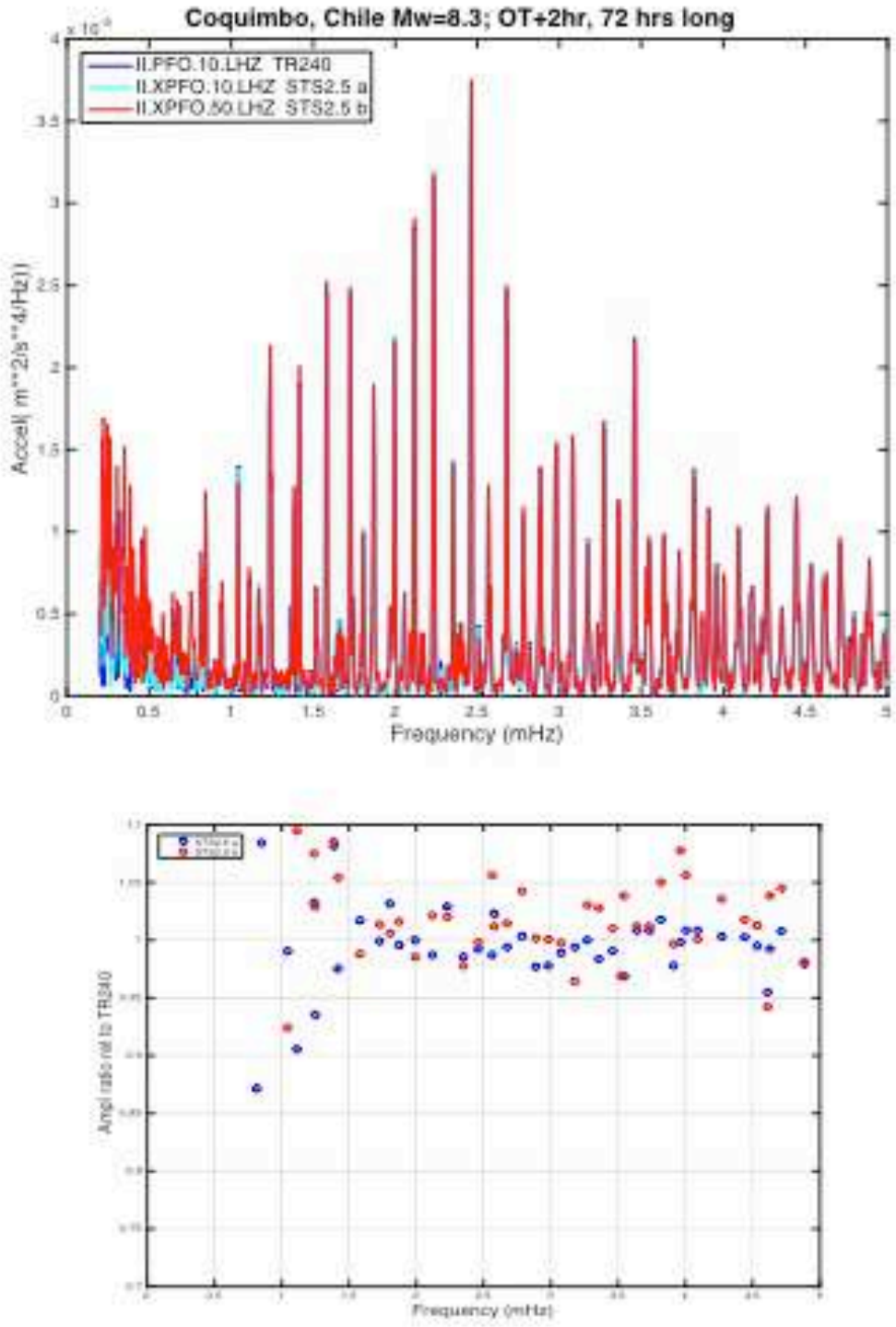

Figure 1. (top) Long period spectra computed from 72-hr long time series beginning 2 hours after the origin time of the 2015 Mw=8.3 Coquimbo, Chile earthquake. The spectra largely overly one another above 1.5mHz indicating the instrument responses are well known. Instrument noise contributes to disagreement below that frequency. (*bottom*) Amplitude ratio of the test instruments' (XPFO*) peaks to the known standard (PFO.10.LHZ). Ideally all points should be unity. That they average to unity indicates the instrument responses are well known; the scatter is a measure of noise.

James Day Associate Professor

jmdday@ucsd.edu

Phone extension: 45431

Web: http://scrippsscholars.ucsd.edu/jmdday

Research Interests: Planetary accretion and differentiation processes; cosmochemistry; mantle geochemistry; igneous and metamorphic petrology; volcanology; ore genesis; analytical methods

Research Focus - Helium isotopes in Earth's mantle:

Helium isotope ratios ($^3He/^4He$) are sensitive tracers of mantle heterogeneity, indicating preservation of relatively undegassed reservoirs in Earth's mantle since planetary accretion. Two important but poorly characterized reservoirs for He are subducted oceanic crust and lithosphere and cratonic continental lithosphere. These reservoirs may play a direct role in the genesis of some intraplate lavas (e.g., Hawaii, Canary Islands) and in He isotope mantle evolution.

Our recent work has shown that He isotope compositions for both cratonic and non-cratonic peridotite xenoliths can be explained through pervasive open-system behaviour of He in cratonic, mobile belt and tectonically-active regions (Barry et al., 2015, *Lithos*; Day et al., 2015, *GCA*). Using He isotope data for cratonic peridotites, and assuming that (a) significant portions (>50 %) of the Archaean and Proterozoic continental lithospheric mantle (CLM) are stable and unaffected by melt or fluid infiltration on geological timescales (>0.1 Ga), and (b) U and Th contents vary between cratonic lithosphere and non-cratonic lithosphere, a ^3He flux of 0.25-2.2 atoms/s/cm^2 is derived for the CLM (Day et al., 2015, *GCA*). These estimates differ by a factor of ten from non-cratonic lithospheric mantle and are closer to the observed ^3He flux from the continents (<1 atoms/s/cm^2).

Pyroxenite and eclogite materials from the continental regions are widely interpreted to be the metamorphic/metasomatic equivalents of recycled oceanic crustal protoliths, and all are characterized by relatively low-$^3He/^4He$ (0.03-5.6 RA) (Day et al., 2015, *GCA*). Together with oceanic peridotites, and the CLM, these materials represent mantle reservoirs with low time-integrated $^3He/(U+Th)$. Pyroxenite and eclogite are also typically characterized by higher Fe/Mg, more radiogenic Os-Pb isotope compositions, and more variable $\delta^{18}O$ values (~3 to 7 ‰), compared with peridotitic mantle. The low-$^3He/^4He$ values of these reservoirs and their distinctive compositions make them probable end-members to explain the compositions of some low-$^3He/^4He$ OIB, and provide an explanation for the low-$^3He/^4He$ measured in most HIMU lavas.

A basic tenet of partial melting models is that concentrations of elements in different protoliths involved in melting are fundamental to generating the resulting composition of magmas. For example, a He-rich source (e.g., DMM, high-$^3He/^4He$ mantle) can 'overprint' pre-existing mantle He-isotope heterogeneity, if He contents are sufficiently low in the host protoliths (e.g., recycled oceanic crust and lithosphere). Alternatively, at high temperatures, diffusion of He will lead to isotopic equilibration of He such that only completely isolated, or volumetrically large mantle reservoirs will preserve unique $^3He/^4He$ signatures. Transformation of recycled oceanic crustal protoliths to pyroxenite and eclogite at high-temperatures will therefore inevitably result in them inheriting the $^3He/^4He$ signature of their ambient surrounding mantle. Thus, at locations where a strong recycled crust or lithospheric component is implicated in OIB mantle sources (HIMU; EM), the helium isotope ratio will be dominantly controlled by He derived from DMM, and possibly from a high-$^3He/^4He$ component. Conversely, where OIB are associated with a high plume flux, or high degrees of partial melting and tholeiitic magmatism (e.g., Hawai'i,

Iceland, Reunion, Galapagos, Siberian LIP), there may be greater interaction between DMM and a high-$^{3}He/^{4}He$ mantle reservoir as enriched flavours (EM, HIMU) become more diluted as a consequence of higher degrees of partial melting.

CLM and recycled oceanic crust and lithosphere protoliths are not reservoirs for high-$^{3}He/^{4}He$ and so alternative, volumetrically significant, He-rich reservoirs, such as less-degassed (lower?) mantle, are required to explain high-$^{3}He/^{4}He$ signatures measured in some intraplate lavas.

Recent Publications:

Barry, P.H., Hilton, D.R., Day, J.M.D., Pernet-Fisher, J.F., Howarth, G.H., Magna, T., Agashev, A.M., Pokhilenko, N.P. Pokhilenko, L.N., Taylor, L.A. (2015). Helium isotopic evidence for modification of the cratonic lithosphere during the Permo-Triassic Siberian flood basalt event. *Lithos*, 216, 73-80. doi:10.1016/j.lithos.2014.12.001

Day, J.M.D. (2015). Planet formation processes revealed by meteorites. *Geology Today*, 31, 12-20. doi:10.1111/gto.12082

Day, J.M.D., Walker, R.J. (2015). Highly siderophile element depletion in the Moon. *Earth and Planetary Science Letters*, 423, 114-124. doi:10.1016/j.epsl.2015.05.001

Day, J.M.D., Corder, C.A., Rumble, D., Assayag, N., Cartigny, P., Taylor, L. A. (2015). Differentiation processes in FeO-rich asteroids revealed by the achondrite Lewis Cliff 88763. *Meteoritics & Planetary Science,* 50, 1750-1766. doi:10.1111/maps.12509

Day, J.M.D., Waters, C.L., Schaefer, B.F., Walker, R.J., Turner, S. (2015). Use of Hydrofluoric Acid Desilicification in the Determination of Highly Siderophile Element Abundances and Re-Pt-Os Isotope Systematics in Mafic-Ultramafic Rocks. *Geostandards and Geoanalytical Research*. doi:10.1111/j.1751-908X.2015.00367.x

Day, J.M.D, Barry, P.H., Hilton, D.R., Burgess, R., Pearson, D.G., Taylor, L.A. (2015). The helium flux from the continents and ubiquity of low-$^{3}He/^{4}He$ recycled crust and lithosphere. *Geochimica Cosmochimica Acta*, 153, 116-133. doi:10.1016/j.gca.2015.01.008

Kato, C., Moynier, F., Valdes, M., Dhaliwal, J.K., Day, J.M.D. (2015) Extensive volatile loss during formation and differentiation of the Moon. *Nature Communications*, 6:7617. doi: 10.1038/ncomms8617

Magna, T., Day, J. M., Mezger, K., Fehr, M. A., Dohmen, R., Aoudjehane, H. C., & Agee, C. B. (2015). Lithium isotope constraints on crust–mantle interactions and surface processes on Mars. *Geochimica et Cosmochimica Acta*, 162, 46-65. doi:10.1016/j.gca.2015.04.029

O'Driscoll, B, Walker, R.J., Day, J.M.D., Ash, R.D. (2015) Generations of Melt Extraction, Melt–Rock Interaction and High-Temperature Metasomatism Preserved in Peridotites of the ~497 Ma Leka Ophiolite Complex, Norway. *Journal of Petrology,* 56, 1797-1828.

Catherine de Groot-Hedlin

Research Scientist

chedlin@ucsd.edu

Phone: 534-2313

Research Interests*:* Acoustic propagation modeling with application to infrasound; application of infrasound to nuclear test-ban verification and hazard monitoring; use of dense seismic and infrasound networks to analyze infrasound signals and also very long wavelength gravity waves.

My main research area is in the physics of infrasound – sound at frequencies lower than human hearing – as well as its applications to investigating large scale atmospheric processes, as well as explosive processes such as bolides and large explosions. Two of the projects that I have been involved in for the past several years are outlined below.

An automated event detector and locator*:* In the past year, I have worked on the development of a new, automated, method to detect and locate events in two-dimensional space and time using large volumes of data. The method is used to create a catalog of infrasound sources in the eastern United States and southeastern Canada using infrasonic and seismic data recorded by the USArray Transportable Array (TA). The purpose of developing this catalog is twofold. First, the catalog provides a list of sources that can be used for basic infrasound research, either for remote study of the events themselves or to study of properties of the atmosphere. Second, we need to understand and document the noise field or other sources that may hamper the performance of International Monitoring System infrasound arrays in monitoring the Comprehensive Nuclear Test Ban Treaty. The method has been successfully applied to TA data – over 1000 events were found in the Midwest and on the east coast in 2013 as shown in the figure below. The method is currently being tested on seismic data to improve current methods of finding small seismic events.

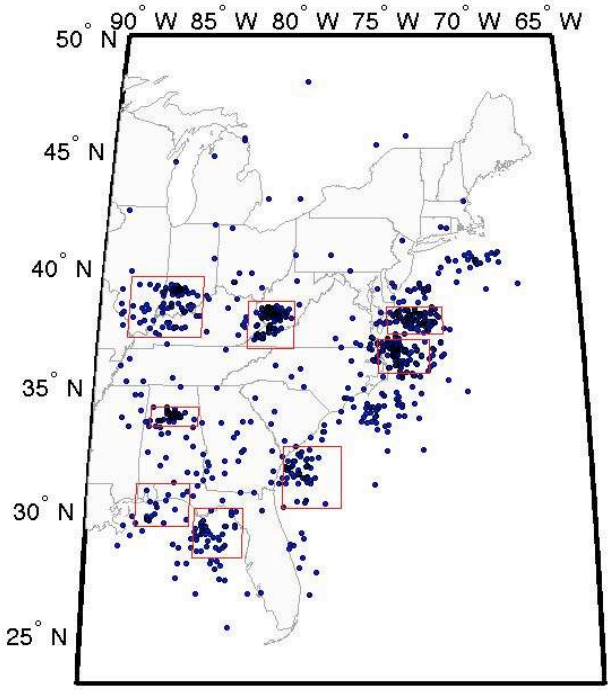

Figure. Infrasound events locations for 2013. The tightly clustered events outlined by the red rectangles occur mostly from 08:00 to 18:00 local time, so we associate them with anthropogenic activity. Several clusters are associated with known mining regions. Very few events are detected between 00:00 and 04:00 local time despite particularly low noise levels at this time that would improve detection rates. These events are randomly distributed across the study area. Several of these isolated events are associated with the terminal burst of meteors entering Earth's atmosphere.

Numerical modeling: A basic research goal in infrasound is to understand the transmission of infrasound through variable atmospheric conditions. To this end I have developed a computationally efficient numerical method to synthesize the propagation of nonlinear acoustic waves through the atmosphere – this nonlinearity arises when pressure perturbations associated with acoustic waves are a significant fraction of the ambient atmospheric pressure. Such situations can arise from meteoroid explosions in the upper atmosphere, volcanic eruptions, or nuclear and chemical explosions. With support from the Air Force Research Laboratory (AFRL), work on this code has progressed to allow for the incorporation of realistic atmospheric effects, such as spatially varying sound speeds and wind speeds, topography, and atmospheric attenuation. The use of this code allows one to determine to what extent nonlinearity affects the estimated source yields for anthropogenic explosions.

Recent Publications

de Groot-Hedlin, C.D., Hedlin, M.A.H. 2015, A method for detecting and locations geophysical events using groups of arrays, *Geop. J. Int.,* doi: 10.1093/gji/ggv345

Edwards, W.E., C. de Groot-Hedlin & M. Hedlin, 2014 Forensic investigation of a probable meteor sighting using USArray acoustic data, Seis. Res. Lett.,

de Groot-Hedlin, C.D., Hedlin, M.A.H. 2014, Infrasound detection of the Chelyabinsk meteor at the USArray., *Earth Planet. Sci Lett*, http:/dx.doi.org/10.1016/j.epsl.2014.01.031

Walker, K.T., A. Le Pichon, T. S. Kim, C. de Groot-Hedlin, I.-Y. Che, M. Garces, 2013, An analysis of ground shaking and transmission loss from infrasound generated by the 2011 Tohoku earthquake, J. Geophys. Res., doi:10.1029/2013JD020187

Brown, P.G., J. D. Assink, L. Astiz, R. Blaauw, M. B. Boslough, J. Borovicka, N. Brachet, D. Brown, M. Campbell-Brown, L. Ceranna, W. Cooke, C. de Groot-Hedlin, & 21 others, 2013, A 500-kiloton airburst over Chelyabinsk and an enhanced hazard from small impactors, Nature Letter, doi:10.1038/nature12741

de Groot-Hedlin, C, Hedlin, M. & Walker, K., 2013, Detection of gravity waves across the USArray: A case study, *Earth Planet. Sci Lett*, http://dx.doi.org/10.1016/j.epsl.2013.06.042

LeRoy Dorman **Emeritus Professor, Recalled to Active Duty**
ldorman@ucsd.edu
Phone: 534-2406

Research Interests: My current work is centered on determining seafloor structure, especially using Ocean-Bottom Seismometers.

I am analyze the dispersion of short-range interface waves (Scholte waves) which are controlled by the shear velocity of the upper 100 meters or so. In particular, data from three arrays of OBSs at sediment depths of, nominally, 10, 100, and 1000 meters. Each of these arrays had 5 or 6 seismometers and recorded 5 or six seafloor explosions, yielding 25 to 30 raypaths to OBSs, each of which used 3 inertial sensors and a hydrophone. Below are two examples of data.

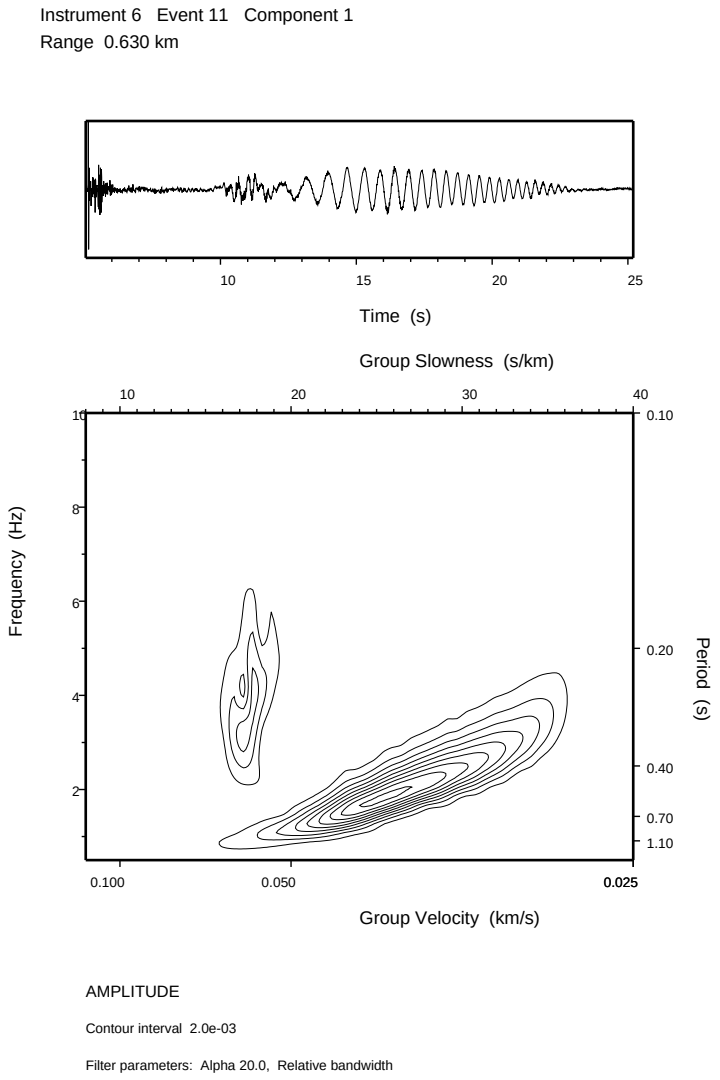

Figure 1: This is an example of a seismogram from an area of simple data. Below is a spectrogram illustrating a fundamental mode and some higher mode structure.

Recent Publications

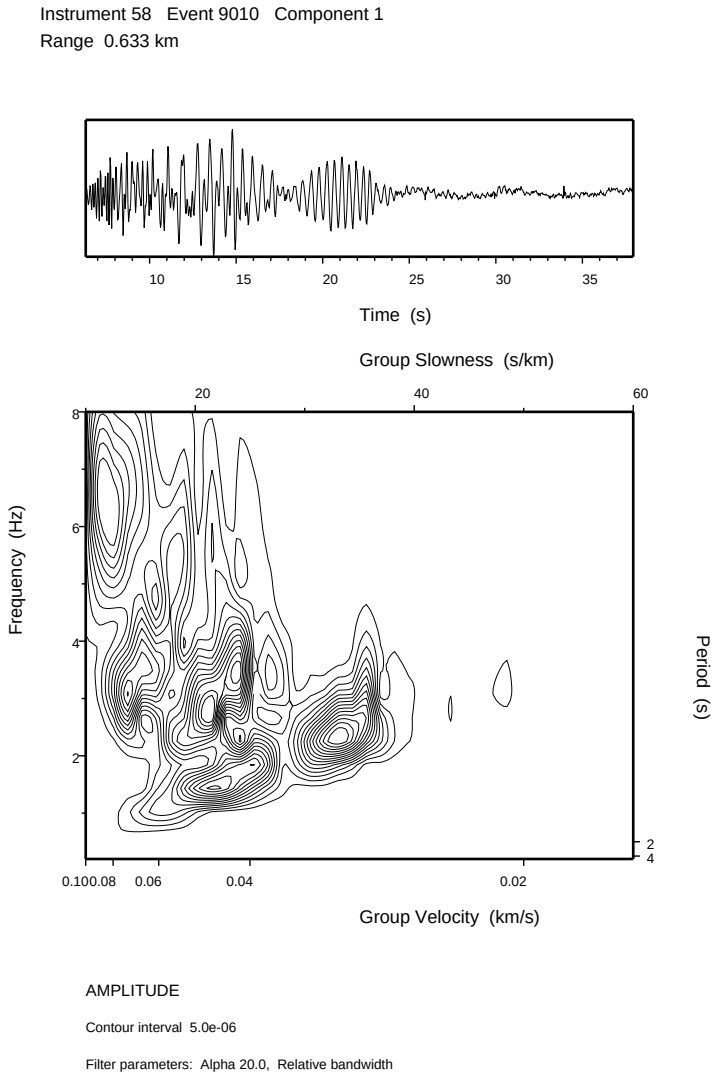

Figure 2: This is a seismogram showing more comples structure.

Dorman, L. M. (2015). Propagation of Scholte Waves in deep water in a seafloor with power-law shear velocity depth dependence. *AGU Fall Meeting 2015*, paper 69289

Neal Driscoll
Professor of Geology & Geophysics
Email address: ndriscoll@ucsd.edu
Phone: 858-822-5026
***Research Interests**:* Landscape and seascape evolution in response to tectonic deformation, sea-level fluctuations, and climate; neotectonics and geohazards

My lab employs and arsenal of geophysical equipment and approaches to understand better potential geohazards. In this annual report, I will focus on the application of LiDAR data to define slip rates and fault architecture along the southern San Andreas (Figure 1) and Incline Village (Figure 2) faults.

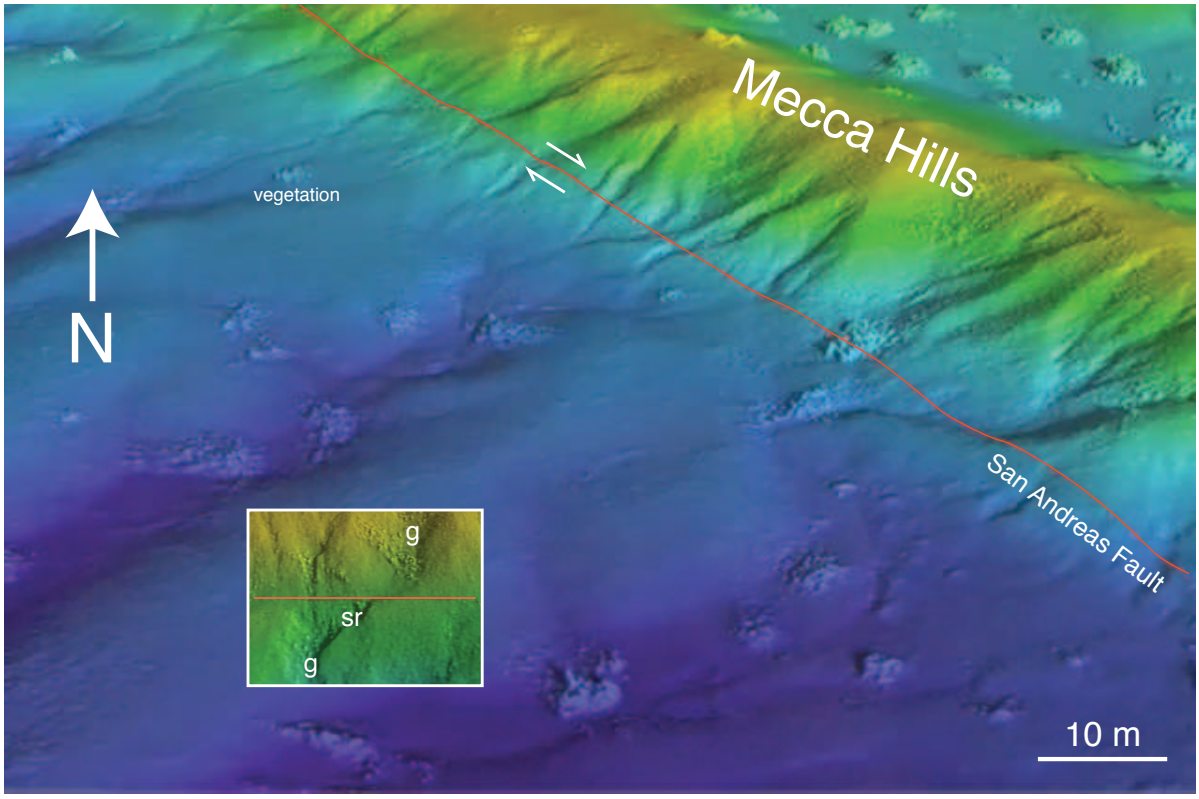

Figure 1. *Terrestrial LiDAR data from the Mecca Hills acquired across the southern San Andreas Fault. Gullies (g) are offset by right lateral slip across the fault with shudder ridges (sr) forming between the gullies.*

Terrestrial laser scanner data acquired from Mecca Hills, California provide constraints on fault offsets and estimates of paleoearthquake magnitudes for the southern San Andreas Fault. The analysis revealed four gully offsets at 1.4, 5.1, 7.2, and 7.8 m. Based on our interpretation, the first peak at 1.35 m records aseismic creep since the most recent event (MRE). If correct, then the 3.7 m interval between the first and second peak records coseismic slip during the ~1690 A.D. MRE. If a relationship exists between quiescence period and rupture magnitude as purported by the slip-predictable earthquake model, then the ~3.7 m offset for the most recent

event, together with the long modern ~325 yr quiescent period compared with the average recurrence interval (~180 yrs), implies a future rupture would exhibit a range of coseismic rupture between 5.3 – 7.0 m of displacement at the surface. Long-term slip rates derived from the offset of coarse boulders and existing radiocarbon dates on desert varnish suggest a Holocene slip rate of 14 – 20 mm/yr. This long-term rate is consistent with the slip rate of 16 - 21 mm/yr calculated for the closed interval between the MRE and the penultimate event based on measured offset gullies (3.7 m). These rates also are consistent with reported Late Pleistocene slip rate of 15.9 ± 3.4 mm/yr calculated at Biskra Palms.

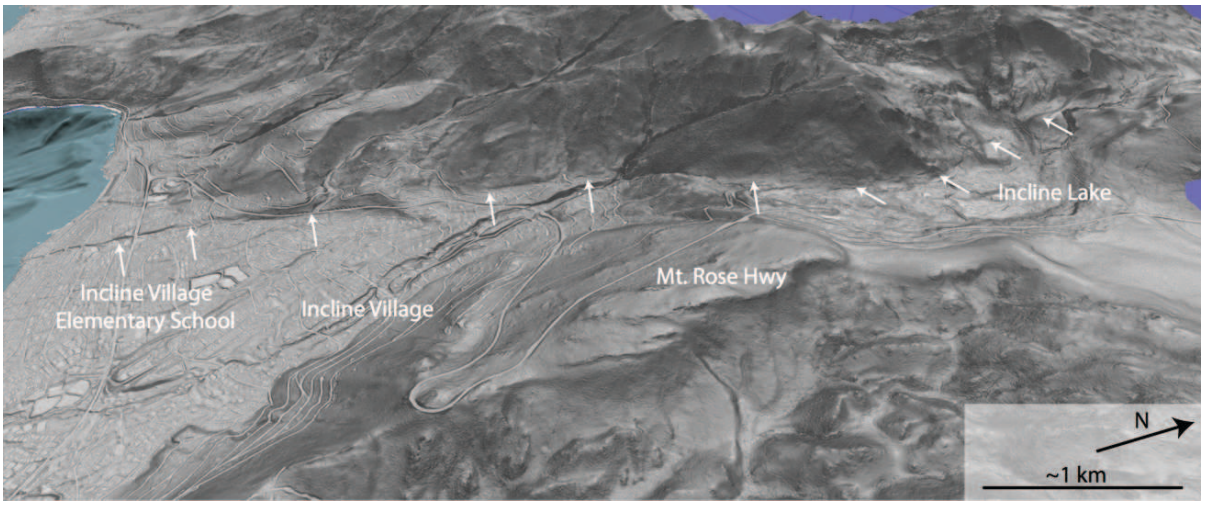

Figure 2. *Airborne LiDAR data acquired across the Incline Village Fault (white arrows) in the Tahoe Basin.*

Complementary onshore and offshore paleoseismic investigations of the Incline Village fault reveal that strain release is accomplished by large magnitude earthquakes in the M_w 6.8 to 7.1 range as evidenced by large vertical displacements ranging from 3.3 to 4 m. The Lake Tahoe basin architecture is predominantly controlled by three north-south trending normal faults with down to the east displacement. These faults are aligned in an en echelon pattern that progressively steps eastward toward the north. High-resolution seismic CHIRP profiles constrain the location of the Incline Village fault in the nearshore and project where it emerges onshore as a laterally continuous scarp. High resolution LiDAR was used to characterize the onshore fault geomorphology. A cross-fault excavation exposed stacked scarp-derived colluvial wedge deposits and provide evidence for 3 events. Radiocarbon dating of detrital charcoal places the most recent event (MRE) near 1375 AD (630 B.P.), with the penultimate event at approximately 32 ka, and evidence for at least one or two additional events post 69 ka based on Tahoe-age boulders. These large displacements events, relative to the fault's minimal length of 15-20 km, suggest that ruptures may include adjacent faults such as the Stateline–North Tahoe fault or Little Valley/Mt. Rose fault system. The observed displacements and their timing are consistent with established long-term slip rate estimates of approximately 0.2 mm/yr estimated offshore. Thus, our combined approach yields a more comprehensive fault characterization and an improved assessment of seismic hazard parameters.

See http://scrippsscholars.ucsd.edu/ndriscoll for publications as well as teaching and research interests.

Matthew Dzieciuch Project Scientist

mdzieciuch@ucsd.edu

Phone: 534-7986

Research Interests*:* Acoustical Oceanography, signal processing for ocean acoustics.

My research has been on using the acoustical properties of sound transmission in the ocean to infer properties of the ocean. An example of this is recent work that I have been doing in the Fram Strait with Peter Worcester at IGPP and with colleagues in the Nansen Center in Bergen, Norway. The Fram Strait is the only deep-water connection between the Arctic and the rest of the world's oceans. It is a narrow channel, about 150 km across located between Greenland and Spitsbergen. There is a current along the eastern side of the strait that carries warm, salty water from the Atlantic into the Arctic. There is also a cold fresh current along the western side of the strait. These two currents exchange heat and mass between the basins.

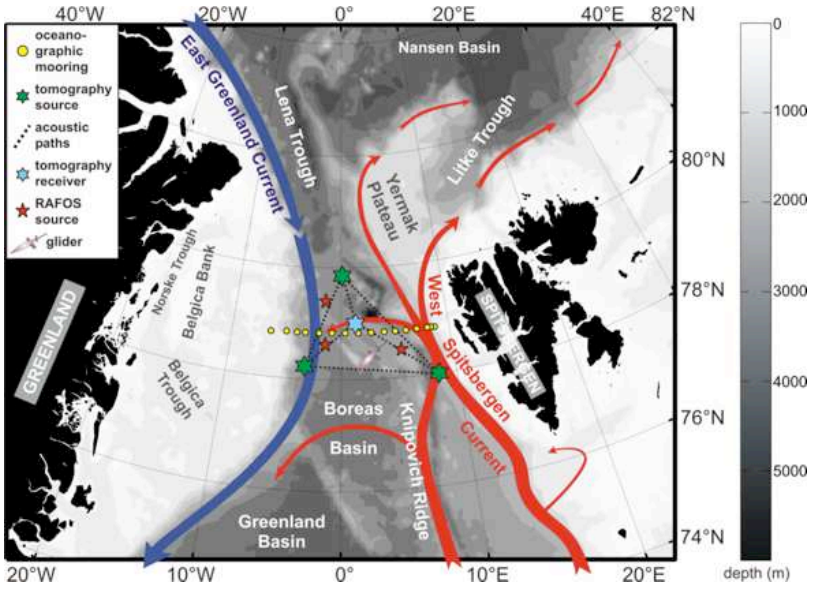

A map of the Fram Strait is shown in the first figure. Since 1997 there have been measurements of the flow through the strait by a line of current meter moorings. These moorings have also measured temperature and salinity. Since 2010 there has also been an acoustic array in the strait that has measured the travel-time of sound propagating across it. This measurement is integral in its nature and thus captures small-scale variability that is invisible to the point measurements. The travel-time is a strong function of temperature due to the dependence of sound-speed on temperature. Reciprocal transmissions measure flow.

Learning how to interpret the acoustic measurements has not been straightforward. There are multiple propagation paths between each source-receiver pair and the receptions are highly variable. Nonetheless, accounting for the natural scattering results in stable, resolvable, and identifiable arrivals. An example of the acoustic arrival pattern is shown in the bottom panel of the second figure. Peaks in the pattern correspond to separate acoustic paths. We have recently learned that a standard interpretation of the sound propagation path as a ray path is not always appropriate.

The top panels of the second figure show the full-wave interpretation of the travel-time sensitivity of the arrival peaks to sound-speed changes in the ocean. The upper left panel shows an arrival (#1) that one interprets in the standard way, with a ray path. The ray path is shown in black and overlaid with the full-wave sensitivity. The upper right panel shows a full-wave sensitivity for an arrival (#2) that is markedly different than the ray path. There are areas of positive as well as negative sensitivity. Also the sensitivity is not confined to the first Fresnel zone. A two year time series of travel-time measurements is now being analyzed using these methods.

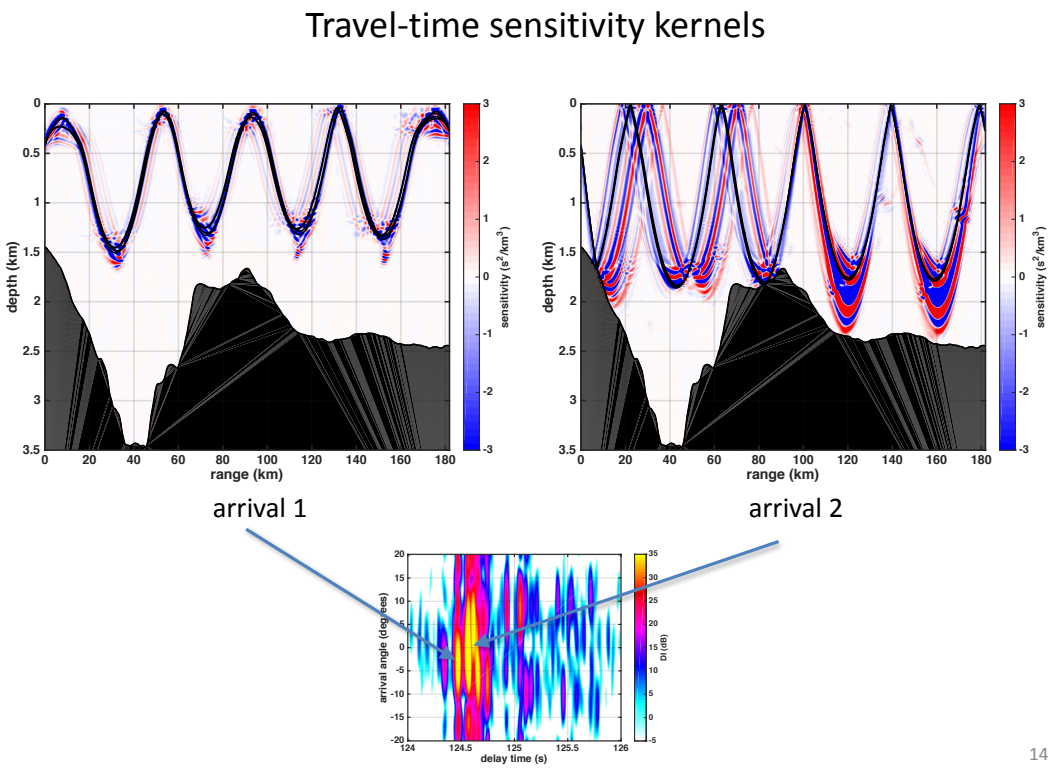

Recent Publications

Dzieciuch, M.A., Cornuelle, B.D. and Skarsoulis, E.K., "Structure and stability of wave-theoretic kernels in the ocean", J. Acoust. Soc. Am., 134, 3318-3331 (2013).

Dzieciuch, M.A, "Signal processing and tracking of arrivals in ocean acoustic tomography", J. Acoust. Soc. Am., 136, 2512-2522 (2014).

Yuri Fialko
Professor
Email: yfialko@ucsd.edu
Phone: x2-5028

Research interests: earthquake physics, crustal deformation, space geodesy, volcanology

Professor Fialko's research is focused on understanding the mechanics of seismogenic faults and magma migration in the Earth's crust, through application of principles of continuum and fracture mechanics to earthquakes and volcanic phenomena. Prof. Fialko is using observations from space-borne radar satellites and the Global Positioning System (GPS) to investigate the response of the Earth's crust to seismic and magmatic loading.

One of the particular interests is finite slip models of large earthquake ruptures from inversions of dense space geodetic data. Prof. Fialko and graduate student Kang Wang used data from the ALOS-2 satellite and continuous GPS network to investigate the rupture pattern of the 2015 magnitude 7.8 Gorkha (Nepal) earthquake that occurred in the central Himalaya, on a tectonic boundary resulted from the India-Eurasia collision. The earthquake caused more than 8000 fatalities, and was the largest seismic event in the area over the last 50 years. The data used in the inversion include vector displacements measured at 13 GPS stations and Line-Of-Sight (LOS) displacements derived from Synthetic Aperture Radar (SAR) data from 3 tracks of the ALOS-2 satellite. The fault geometry (in particular, the dip angle) was found as part of the solution using a grid search. The best-fitting model (Figure 1) has a shallow dip angle of 7°. The rupture of the 2015 Gorkha earthquake was dominated by thrust motion that was primarily concentrated in a 150-km long zone 50 to 100 km northward from the surface trace of the Main Frontal Thrust (MFT), with maximum slip of ∼6 m at a depth of ∼8 km. Most of the aftershocks occurred along the eastern half of the fault, around the patches of relatively large coseismic slip, including the M_w 7.3 aftershock on May 12th, 2015 (magenta circle in Figure 1). The slip model shows that the 2015 rupture did not propagate into shallow part of the Main Hymalaian Thrust (MHT). GPS measurements made before the earthquake indicate that the MHT is locked from surface to a distance of approximately 100 km down dip. Recent investigations of the Quaternary geomorphology along the MFT showed that at least two great earthquakes had ruptured to the surface in Nepal in the past 1000 years. Particularly, the 1934 Bihar-Nepal M 8.2 earthquake ruptured a ∼ 150 km-long segment of the MFT between 85.8° E and 87.3° E, immediately to the east of the 2015 rupture (Figure 1). Unless the degree of seismic coupling varies along the fault strike , the lack of shallow slip during the 2015 Gorkha earthquake implies future seismic hazard, in particular because this part of the fault has been brought closer to failure by the 2015 earthquake. Observations of post-seismic deformation (in particular, the occurrence of afterslip on the upper section of the MFT) will provide important constraints on the degree of seismic coupling and seismic hazard on this part of this fault.

Another area of prof. Fialko's interests is observations and modeling of interseismic deformation. One of the main limitations to space geodetic measurements of low-amplitude (sub-centimeter) deformation is the atmospheric variability. In a recent study prof. Fialko and graduate student Katya Tymofyeyeva developed a new method for estimating radar phase delays due to propagation of elactromagnetic waves through the troposphere and the ionosphere. The method takes advantage of the fact that the interferograms that share a common date also share the same propagation delay due to the atmosphere or long-wavelength "ramp" due to imprecise knowledge of spacecraft orbits. The respective signals can be estimated by averaging of radar interferograms that share a common scene. Estimated atmospheric contributions are then subtracted from the radar interferograms to improve measurements of surface deformation. Inversions using synthetic data demonstrate

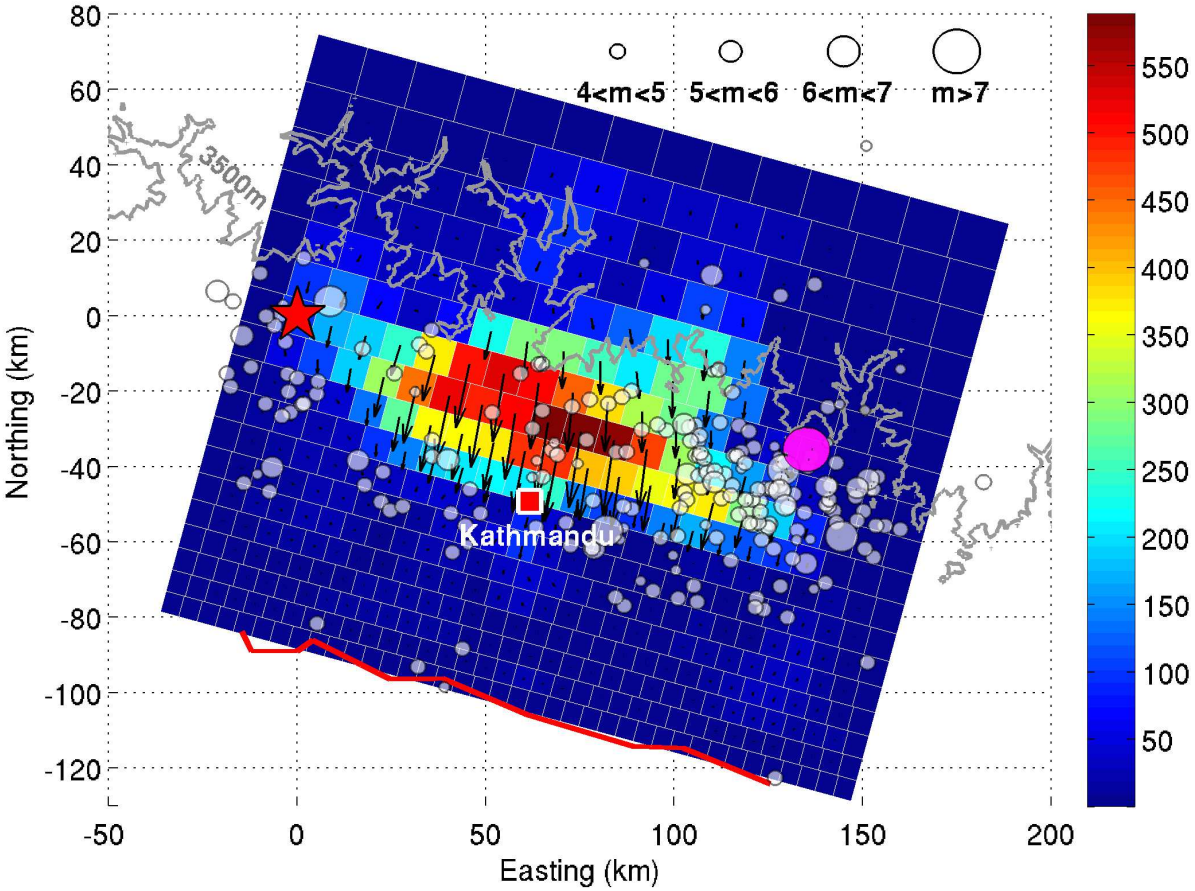

Figure 1: Surface projection of the coseismic slip model of the 25 April M_w 7.8 Gorkha earthquake. Red line represents the surface trace of MFT used to constrain the strike of the fault plane. Red star denotes the epicenter of the M_w 7.8 mainshock. Gray dots denote the aftershocks of $m > 4$ from 25 April to 31 May, 2015. The M_w 7.3 aftershock of May 12th, 2015 is shown by a magenta circle. Color shows the slip magnitude in cm, and arrows correspond to the slip directions. The gray line represents the surface elevation of 3500m. Red square denotes the city of Kathmandu. The origin corresponds to the epicenter of the mainshock (84.731°E, 28.230° N). From Kang and Fialko [2015].

that this procedure is able to recover up to 95% of the atmospheric signal, and considerably reduce scatter in the timeseries of the line-of-sight displacements. Feasibility of the method was demonstrated by comparing the Interferometric Synthetic Aperture Radar (InSAR) time series derived from ERS-1/2 and ENVISAT data to continuous Global Positioning System (GPS) data from Eastern California.

Recent publications:

Wang, K. and Y. Fialko, Slip model of the 2015 M_w7.8 Gorkha (Nepal) earthquake from inversions of ALOS-2 and GPS data, *Geophys. Res. Lett., 42*, 7452-7458, 2015.

Tymofyeyeva, E. and Y. Fialko, Mitigation of atmospheric phase delays in InSAR data, with application to the Eastern California Shear Zone, *J. Geophys. Res., 120*, 5952-5963, 2015.

Mitchell, E., Y. Fialko, and K. Brown, Frictional properties of gabbro at conditions corresponding to slow slip events in subduction zones, *G-cubed*, in press.

Helen Amanda Fricker, Professor, John Dove Isaacs Chair

Email address: hafricker@ucsd.edu Phone extension: 46145

Research Topics: cryosphere, Antarctic ice sheet, subglacial lakes, ice shelves, satellite remote sensing

My research focuses on the Earth's cryosphere, and specifically on understanding the processes driving changes on the Antarctic ice sheet. The Scripps Glaciology Group now has 3 postdocs, 1 Staff Researcher and 2 graduate students. Two of my postdocs were former graduate students Fernando Paolo and Matthew Siegfried who defended their PhDs in September and October 2015 respectively.

One of the primary questions in Antarctica is whether its mass is changing due to climate change, and its potential impact on sea-level rise. Due to its vast size, and the long time periods over which it can change, satellite data are crucial for routine monitoring of Antarctica, in particular data from radar and laser altimetry, and also imagery. My group specializes in monitoring the Antarctic Ice Sheet, focussing on two key dynamic components of the ice-sheet system: (i) active subglacial lakes and (ii) the floating ice shelves. We primarily uses satellite altimetry, either satellite radar altimetry from ERS-1/ERS-2 and Envisat which provides a long record (1994-2012) or NASA's Ice, Cloud & land Elevation Satellite (ICESat), which provides accurate elevation data for ice sheet change detection for the period 2003-2009. I describe these two major projects below:

Subglacial lakes The Antarctic Ice Sheet is on average 2.2 km thick and rests on top of bedrock; the insulation, high pressures, and geothermal heat flux at the ice-bed interface leads to melting of the basal ice layers on the order of mm/year (*Joughin et al.*, 2003). When averaged over the entire ice sheet, this produces high volumes of subglacial water (an amount of 65 Gt/yr was estimated by *Pattyn et al.*, 2010), much of which is stored in subglacial lakes (*Siegert et al.*, 2005) and subglacial aquifers (*Christoffersen et al.*, 2014). In 2006 I discovered active subglacial water systems under the fast-flowing ice streams of Antarctica using ICESat data. This was inferred from observations of large height changes (up to 10m in some places) in repeat-track ICESat data, which corresponded to draining and filling of subglacial lakes beneath 1-2 km of ice. We continue to monitor active lakes, and we have found 124 in total throughout Antarctica. In the decade since the discovery of active Antarctic subglacial water systems, much progress has been made in our understanding of these dynamic systems. My former graduate student (now postdoc) Matthew Siegfried extended the record of volume change for all lakes under the CryoSat-2 mask up to 2015.

I was a PI on a large, interdisciplinary 6-year NSF project (Whillans Ice Stream Subglacial Access Research Drilling (WISSARD)) to drill into one of the subglacial lakes that I discovered – Subglacial Lake Whillans (SLW) on Whillans Ice Stream (WIS; Figure 1) – and the region of the grounding line across which the subglacial water flows and enters the ocean. The final field season was 2015-2016 and my graduate student Matthew Siegfried led the GPS survey, which was centred on the lakes themselves, and the grounding line downstream.

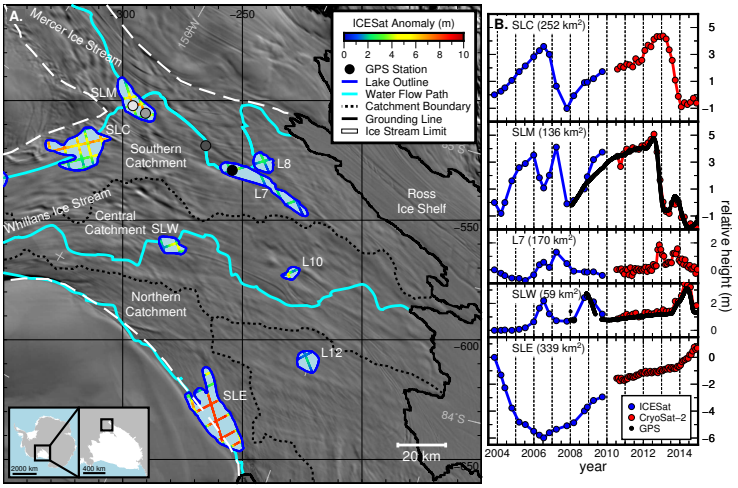

Figure 1. *Subglacial water system of the Whillans/Mercer ice streams, West Antarctica. A. Map of the subglacial lakes in the system (blue outlines) annotated with ICESat track segments used to detect them (colour-coded by surface height change). The lakes are contained within three separate hydrologic systems, and the hydrologic flowpaths and catchment boundaries are shown. B. Time series of average height change over the four largest lakes from ICESat, CryoSat-2 and GPS.*

Ice shelves The Antarctic Ice Sheet is surrounded by floating ice shelves that are several hundred metres thick. Since ice shelves have already displaced their weight in water, their melting does not contribute directly to sea level. However, ice shelves provide mechanical support to 'buttress' seaward flow of grounded ice, so that ice-shelf thinning and retreat result in enhanced ice discharge to the ocean (*Scambos et al.*, 2005; *Rignot et al.,* 2005). We used satellite radar altimeter data from a series of three ESA satellites to obtain estimates of ice-shelf surface height since the early 1990s. These data revealed accelerated losses in total Antarctic ice-shelf volume from 1994 to 2012 (*Paolo et al., 2015*; Figure 2).

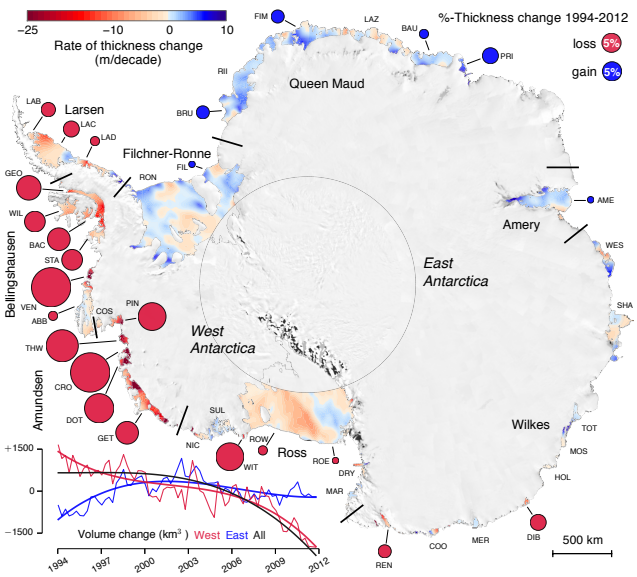

Figure 2. *Eighteen years of change in thickness and volume of Antarctic ice shelves. Rates of thickness change (m/decade) are color-coded from -25 (thinning) to +10 (thickening). Circles represent percentage of thickness lost (red) or gained (blue) in 18 years. Lower left corner shows time series and polynomial fit of average volume change (km^3) from 1994 to 2012 for the West (in red) and East (in blue) Antarctic ice shelves. Black curve is polynomial fit for All Antarctic ice shelves.*

Changes in mass for East and West Antarctic ice shelves were not synchronous. In East Antarctica the first half of the record showed a mass increase, believe to be a result of increased accumulation. In West Antarctica, and in particular its Bellingshausen and Amundsen Sea regions, ice shelves lost mass throughout the record although with changes in rates on multi-year time scales. Ice-shelf thinning in these regions was substantial: some ice shelves thinned by up to 18% in 18 years. This thinning raises concerns about future loss of grounded ice and resulting sea level.

Publications 2015

1. **FRICKER, H. A.**, M. R. Siegfried, S. P. Carter, T. A. Scambos (2015) A decade of progress in observing and modelling Antarctic subglacial water systems, Philospohical Transactions of the Royal Society, in press.
2. BOUGAMONT, M., P. CHRISTOFFERSEN, S. PRICE, **H. A. FRICKER**, S. TULACZYK, S.P. CARTER (2015) Reactivation of Kamb Ice Stream tributaries triggers century-scale reorganization of Siple Coast ice flow. *Geophysical Research Letters*, in press.
3. CARTER, S. P., **H. A. FRICKER**, M. R. SIEGFRIED (2015) Active lakes in Antarctica survive on a sedimentary substrate--Part I: Theory, *The Cryosphere Discussions*, 9, 2053-2099,doi:10.5194/tcd-9-2053-2015.
4. HOLLAND, P. R., A. BRISBOURNE, H.F.J. CORR, D. MCGRATH, K. PURDON, J. PADEN, **H. A. FRICKER**, F. S. PAOLO, A.H. FLEMING (2015). Oceanic and atmospheric forcing of Larsen C Ice-Shelf thinning. *The Cryosphere*, *9*(3), 1005-1024.
5. PAOLO, F. S., **H.A. FRICKER**, AND L. PADMAN (2015). Volume loss from Antarctic ice shelves is accelerating. *Science*, *348*(6232), 327-331.
6. WALKER, C. C., J.N. BASSIS, **H.A. FRICKER** AND R.J. CZERWINSKI (2015). Observations of interannual and spatial variability in rift propagation in the Amery Ice Shelf, Antarctica, 2002–14. *Journal of Glaciology*, *61*(226), 243.
7. MASSOM, R. A., A.B. GILES, R. C. WARNER, **H.A. FRICKER**, B. LEGRÉSY, G. HYLAND, AND N. YOUNG (2015). External influences on the Mertz Glacier Tongue (East Antarctica) in the decade leading up to its calving in 2010. *Journal of Geophysical Research: Earth Surface*, *120*(3), 490-506.

Alistair Harding
Research Geophysicist
Email: aharding@ucsd.edu
Phone: 534-4301
Research Interests: *Marine seismology, mid-ocean ridges, continental rifting, tectonic hazards in California*

Axial Seamount is a large submarine volcano situated on the spreading axis of the Juan de Fuca Ridge offshore of Washington and Oregon. It has a history of frequent volcanic activity with the latest eruption occurring in April 2015. Due to its activity and proximity to shore, Axial Seamount is the most extensively studied seafloor volcano on earth and has been the object of numerous scientific expeditions over the last three decades covering geology, geochemistry, geophysics and biology. It is now home to a permanent seafloor observatory with nearly 40 instruments on its summit and east flank connected to shore and sending back real time data. Despite this interest, relatively little has been known about the subsurface structure of the seamount, with the primary information coming from a 3D seismic tomography experiment that used six Ocean Bottom Seismographs (*West et al.*, 2001). Better knowledge of the subsurface structure can help to better constrain the response to magmatic intrusions, better locate earthquakes, and improve understanding of the tectonic history.

We have analyzed a grid of 12 multichannel seismic (MCS) profiles covering Axial Seamount in conjunction with travel times from the earlier OBS experiment. The individual MCS profiles have been downward continued and used for both travel time tomography and waveform inversion, producing high resolution velocity models of the upper 1+ km of the crust (*Arnulf et al.*, 2014a). These models and MCS travel times have in turn be used for prestack depth migration and for a 3D tomographic inversion in combination with the earlier OBS travel times. The upper crustal velocity models capture the largest subsurface velocity variations and gradients outside of any magma chambers, facilitating much better imaging of deeper structure by both the migration and 3D tomography. The improved knowledge of upper crustal structure allows the travel time delays associated with long ray paths beneath the seamount to partitioned between an upper crustal delay due to the summit caldera and one associated with the deeper magma chamber structure, while the earlier image smeared the two together (*West et al.,* 2001).

The depth migrated images reveal a very large primary magma chamber approximately 14 km long, 3 km wide and up to 1 km thick centered ~1.5-2.5 km beneath the large horseshoe shaped caldera at the summit of the seamount (Figure 1; *Arnulf et al.*, 2014b). The magma chamber width is similar to that of the caldera, but lengthwise it extends beyond the northwest and southeast limits of the caldera. The imaging also reveals a secondary, smaller magma chamber to the Northwest at approximately the same depth as the main chamber and a possible connection between the two. Extrusive volcanics within the caldera appear to thicken rapidly towards the northwest end of the caldera where the boundary scarp is the highest, suggesting that caldera subsidence has persistently been greater at this end of the caldera. The magma chamber is shallowest at the southeast end of the caldera and this is the site of both the 2011 eruption and known hydrothermal vents. This region of the chamber also appears to have the highest melt concentration based on variations in reflection amplitude in the migrated images, which indicates the magma chamber is zoned between melt and mush rich regions. The 3D tomography results indicate that the deeper travel time delays can be explained by a ~1-2 km/s velocity reduction within the main magma chamber and a slightly smaller reduction associated with the secondary chamber without the need for an additional reservoir.

Arnulf, A. F., A. J. Harding, S. C. Singh, G. M. Kent, and W. C. Crawford (2014a), Nature of upper crust beneath the Lucky Strike volcano using elastic full waveform inversion of streamer data, *Geophys. J. Int.*, 196(3), 1471–1491, doi:10.1093/gji/ggt461.

Arnulf, A. F., A. J. Harding, G. M. Kent, S. M. Carbotte, J. P. Canales, and M. Nedimović (2014b), Anatomy of an active submarine volcano, *Geology*, 42, 655–658, doi:10.1130/G35629.

West, M., W. Menke, M. Tolstoy, S. Webb, and R. Sohn (2001), Magma storage beneath Axial volcano on the Juan de Fuca mid-ocean ridge, *Nature*, 413, 833–836, doi:10.1038/35101581.

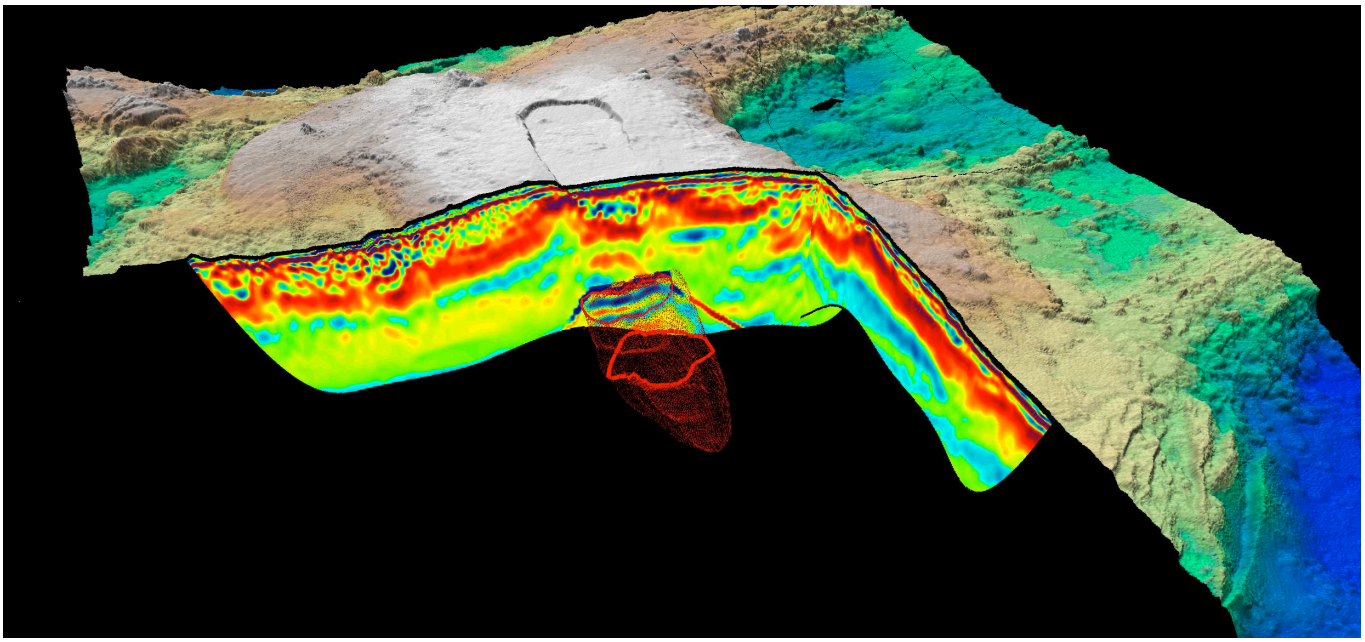

Figure 1. Cross-sectional view of Axial Seamount looking approximately northwest, showing the velocity gradient structure for two intersecting MCS profiles and the outline of the main magma chamber as a wire mesh as inferred from multiple profiles. Warmer colors in the velocity gradient images indicate higher gradients. The continuous band orange-red colors, which extends ~ 1 km below the seafloor at its deepest on the left side of the figure, represents the transition from more porous extrusive to less porous intrusive volcanics. The rim of the caldera is underlain by a ring of high velocity material causing the shallowing of the gradient with lava flows ponding within the caldera and flowing to the Southwest creating the thick extrusive carapace.

James Hawkins **Research Professor**
jhawkins@ucsd.edu
Phone: 534-2161

I am continuing work on a major synthesis of 220 million years history of the region around the Mariana Trench in the western Pacific Ocean Basin. This is based largely on my own work done on SIO expeditions, drilling on ODP Leg 135 (on which I was co-chief scientist), and dives with ALVIN and Japanese submersible SHINKAI.

References

Tian, L., P. Castillo, D. Hilton, J. Hawkins, B. Hanan, and A. Pietruszka (2011). Major and trace element and Sr-Nd isotope signatures of the northern Lau Basin lavas: Implications for the composition and dynamics of the back-arc basin mantle, *J. Geophys. Res.*, **116**, http://dx.doi.org/10.1029/2011JB008791

Michael A.H. Hedlin

Research Geophysicist

Email address: hedlin@ucsd.edu

Phone extension: 48773

Research Interests: Study of large atmospheric phenomena, study of long-range propagation of subaudible sound in the atmosphere, seismo-acoustics

Infrasound: The study of subaudible sound, or infrasound, has emerged as a new frontier in geophysics and acoustics. We have known of infrasound since 1883 with the eruption of Krakatoa, as signals from that event registered on barometers around the globe. Initially a scientific curiosity, the field briefly rose to prominence during the 1950's and 1960's during the age of atmospheric nuclear testing. With the recent Comprehensive Test-Ban Treaty, which bans nuclear tests of all yields in all environments, we have seen renewed interest in infrasound. A worldwide network of infrasound arrays, being constructed for nuclear monitoring, is fueling basic research into man-made and natural sources of infrasound, how sound propagates through our dynamic atmosphere and how best to detect infrasonic signals amid noise due to atmospheric circulation. This network has been supplemented with deployments, such as the 400-station seismo-acoustic USArray Transportable Array (TA), for basic research and enhanced monitoring of regions of great interest.

Research at L2A: The Laboratory for Atmospheric Acoustics (L2A) is the home of research in this field at IGPP. Several faculty, post-docs and PhD students work full or part time in L2A, supported by engineers and technicians in the lab and the field. More information about this lab can be found at l2a.ucsd.edu. Presently we study a broad suite of problems related to both natural and man-made sources.

Dense network studies: The global infrasound network is unprecedented in scale however it is still very sparse, with ~ 100 stations operating worldwide. To increase the density of sampling of the infrasonic wavefield we have used acoustic–to-seismic coupled signals recorded by dense networks, such as the 400-station USArray Transportable Array (TA) and various PASSCAL deployments. We have used the original (seismic-only) TA network to create a catalog of atmospheric events in the western United States similar to commonly used seismic event catalogs. The acoustic catalog is used in part to find sources of interest for further study and to use the recorded signals to study long-range infrasound propagation. Recorded signals from instantaneous sources are commonly dispersed in time to several 10's of seconds. Modeling indicates that this is due to interaction of the sound waves with fine-scale structure in the atmosphere due to gravity waves. We are currently using infrasound to constrain the statistics of this time-varying structure.

The National Science Foundation funded our group to upgrade the entire TA with infrasound microphones and barometers. Our sensor package is sensitive to air pressure variations from D.C. to 20 Hz, at the lower end of the audible range. The upgrade converted the TA into the first-ever semi-continental-scale seismo-acoustic network. The network has moved east across the US as stations are redeployed. Figure 1 (left panel) shows station locations from January 1, 2010 through the end of September, 2014. We have divided this collection of stations into 3,600 elemental arrays (triads) to study

atmospheric gravity waves. An early result is shown in the right panel of figure 1. This map shows a histogram of gravity waves in the 2-6 hour pass-band weighted by the amplitude of each detected wave. As expected, large gravity waves are common to the west of the Great Lakes due largely to convective activity. Other structure apparent in the image, such as the low along the Appalachian mountain trend, with the string of hotspots to the east, is actively being studied.

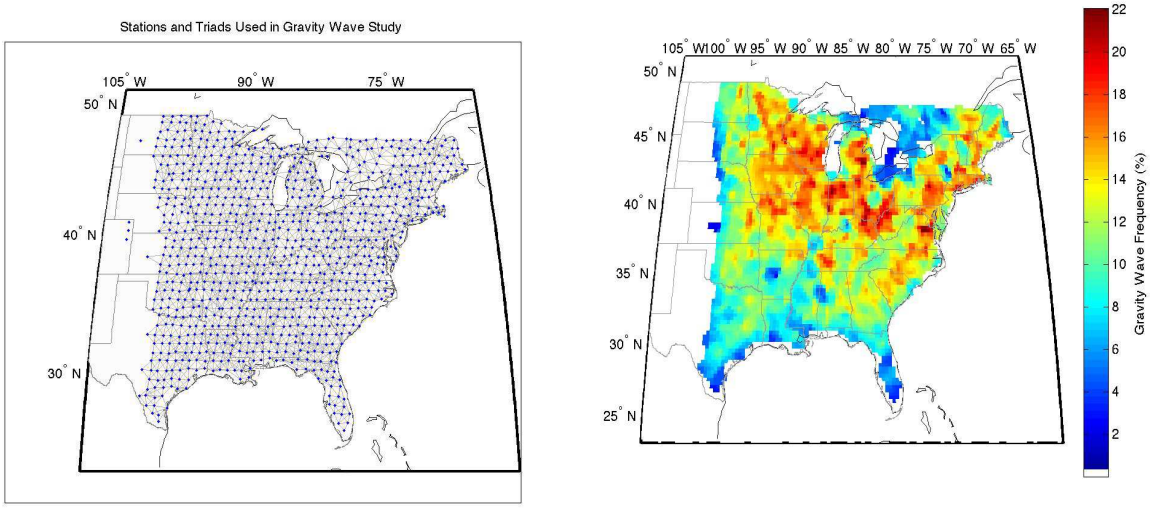

Figure 1. left) sites occupied by stations in the TA from January 1, 2010 through Sept 30, 2014. These stations have been grouped into 3-element arrays (triads) for the study of long-period atmospheric gravity waves. The panel on the right shows the frequency of gravity waves in this time period with the count weighted by the amplitude of each detected wave. The most vigorous activity occurs to the west of the Great Lakes, as expected from satellite studies.

Field operations: Our group has built infrasound arrays for nuclear monitoring in the US and Africa. We operate research arrays located near San Diego.

Recent Publications

Brown, P., Assink, J., Astiz, L.,Blaauw, R., Boslough, M., Borovicka, J., Brachet, N., Brown, D., Campbell-Brown, M., Ceranna, L., Cooke, W., de Groot-Hedlin, C., Drob, D., Edwards, W. Evers, L., Garces, M., Gill, J., Hedlin, M.A.H., Kingery, A., Laske, G., Le Pichon, A., Mialle, P., Moser, D., Saffer, A., Silber, E., Smets, P., Spalding, R., Spurny, P., Tagliaferri, E., Uren, D., Weryk, R., Whitaker, R., Krzeminski, Z., 2013, The Chelyabinsk airburst: Implications for the Impact Hazard, *Nature*, DOI: 10.1038/nature12741.

de Groot-Hedlin, C.D. and Hedlin, M.A.H., 2015, A method for detecting and locating geophysical events using groups of arrays, *Geophys. J. Int.*, v203, 960-971, doi: 10.1093/gji/ggv345

de Groot-Hedlin, C.D., Hedlin, M.A.H. and Walker, K.T., 2013, Detection of gravity waves across the USArray: A case study, in press with *Earth and Planetary Sciences Letters*, DOI: 10.1016/j.epsl.2013.06.042

de Groot-Hedlin, C.D. and Hedlin, M.A.H., 2014, Infrasound detection of the Chelyabinsk Meteor at the USArray, *Earth and Planetary Sciences Letters* http://dx.doi.org/10.1016/j.epsl.2014.01.031

Edwards, W.N., de Groot-Hedlin, C.D. and Hedlin, M.A.H., 2014, Transportable Array Acoustic capabilities confirm apparent meteor sighting, in press with Seismological Research Letters.

Hedlin, M.A.H. and Drob, D.P., 2014, Statistical characterization of atmospheric gravity waves by seismoacoustic observations, *J. Geophys. Res. Atmos.*, doi: 10.1002/2013JD021304

David R. Hilton

Professor of Geochemistry

Email address: drhilton@ucsd.edu

Phone extension: 2-0639

Research Interests: Noble gas and major volatile isotope geochemistry of subduction zones, mantle hotspots, groundwaters and geothermal systems.

We continue to engage in a variety of studies involving volatiles – noble gases and major volatiles (such as CO_2 and N_2) – from different tectonic environments. New publications this year include work on peridotite xenoliths from the continental lithosphere, earthquake prone areas, and subduction zones.

The publication by Barry et al. (2015) measured helium in minerals from two kimberlite pipes from the Siberian craton: the 360 Ma Udachnaya and 160 Ma Obnazhennaya pipes which bracket the eruption of the Siberian Flood Basalts at 250 Ma. We found radiogenic He isotope values characterize the Udachnaya peridotites whereas Obnazhennaya xenoliths had higher (mantle) values, allowing us to differentiate between the different types of metasomatic fluids (crustal versus basalt-derived) involved in modifying the Siberian craton through time. Day et al. (2015) produced a wide-ranging study of Archean peridotites from various regions worldwide together with helium and trace elements for pyroxenites and eclogites from a host of other localities. These latter xenoliths are considered to be derived from ancient oceanic crust recycled into the mantle. Collectively, the results of this study were used to argue that the flux of 3He for the continental lithospheric mantle is likely much smaller than previously thought due to a sampling bias in previous studies towards non-cratonic areas in spite of ~50% of the continents being composed of ancient (Archean or Proterozoic) stable cratons.

On a different theme, Aydin et al., (2015) reported helium and carbon isotope (3He/4He, δ13C) and relative abundance (CO2/3He) characteristics of hydrothermal gases from eastern Anatolia sampled ~1 month after the October 23, 2011 Van earthquake (Mw: 7.2, focal depth: 19 km). Sampling localities were divided into three groups: Group I were sited along the Caldiran Fault about 58-66 km from the earthquake epicenter. Group II were located north of the fault, about 93-113 km away, and Group III were further afield again, about 110-126 from the epicenter. Significantly, all sites were sampled in 2009 facilitating a direct comparison between pre- and post-seismic values. Group I samples showed a consistent post-earthquake increase in 3He/4He whereas Group II localities decreased in 3He/4He. No change was recorded for the Group III localities. For Group I sites, which showed an increase in the mantle He contribution, we hypothesize that the enhanced mantle He signal is derived from asthenospheric melts intruded into the crust, with seismic perturbations responsible for bubble formation and growth leading to overpressure and gas loss. The strike–slip Çaldıran Fault Zone provides the permeable pathway for the liberated volatiles to reach hydrothermal systems at shallow levels in the crust. Release of crustal He dominates the He mass balance of Group II samples as locations are further from the earthquake epicenter and ground shaking is the main process. No obvious permeable pathways to the surface at present in this region. Group III samples are even further away from the earthquake and show no perturbations in He isotopes. The results emphasize the sensitivity of He isotopes to seismic perturbations in the crust and illustrate how location of sampling sites – on permeable segments of faults and close to seismic events, influence resulting changes.

Finally, we continue our studies of subduction-related geothermal systems and report He isotope evidence of mantle fluid contributions to a modern flat-slab subduction setting – the Cordillera Blanca, Peru (Newell et al., 2015). The Cordillera Blanca represents an unusual tectonic setting of low angle downgoing slab with an absence of active arc magmatism. However, the region is still characterized by relatively high 3He/4He values indicating an origin for the mantle He from either continental mantle lithosphere or from asthenospheric mantle via a tear in the Peruvian flab slab. The publication by Fischer et al. (2015) reports the gas chemistry complementary to the isotope data reported previously (Hilton et al., Geochemical Journal, 2010) for Poas volcano in Costa Rica.

New Publications

Barry, P.H., **Hilton, D.R**., Day, J.M.D., Pernet-Fisher, J.F., Howarth, G.H., Agashev, A.M., Magna, T., Agashev, A.M., Pokhilenko, N.P., Pokhilenko, L.N. and Taylor, L.A. (2015) Helium isotopic evidence for modification of the cratonic lithosphere during the Permo-Triassic Siberian flood basalt event. Lithos 216-217, pp 73-80.

Day, J.M.D., Barry, P.H., **Hilton, D.R**., Burgess, R. and Pearson, D.G. (2015) The helium flux from the continents and ubiquity of low-^{3}He/^{4}He recycled crust and lithosphere. Geochim. Cosmochim. Acta, 153, pp 116-133.

Fischer, T.P., Ramirez, C., Mora Amador, R. A., **Hilton, D.R.**, Barnes, J.D., Sharp, Z.D., Le Brun, M. de Moor, J.M., Barry, P.H., Furi, E. and Shaw, A.M. (2015) Temporal variations in fumarole gas chemistry at Poas volcano, Costa Rica. J. Volcanol. Geotherm. Res., 294, pp 56-70.

Aydin, H., **Hilton, D.R.**, Gulec, N. and Mutlu, H. (2015) Post-earthquake anomalies in He-CO_2 isotope and relative abundance systematics of thermal waters: The case of the 2011 Van earthquake, eastern Anatolia, Turkey. Chem. Geol. 411, pp 1-11.

Newell, D.L., Jessup, M.J., **Hilton, D.R**., Shaw, C. and Hughes, C. (2015) Mantle-derived helium in hot springs of the Cordillera Blanca, Peru: evidence for slab-derived fluid transfer in a flat slab subduction setting. Chem. Geol., 417, pp 200-209.

Miriam Kastner Distinguished Professor

mkastner@ucsd.edu

Phone: 534-2065

Research Interests*:* The role and fluxes of fluids and solutes in subduction zones and ridge-crests; Marine gas hydrates and implications for the C cycle and global change; Chemical paleoceanography; The geochemistry and diagenesis of marine sediments and the implications for paleoceanographic interpretations.

Fluid Origins, Thermal Regimes, and Fluid and Solute Fluxes in the Forearc of Subduction Zones

Evidence of large-scale fluid flow is manifested by widespread seafloor venting, associated biological communities, extensive authigenic carbonate formation, chemical and isotopic anomalies in pore-fluid depth-profiles, and thermal anomalies. An in-depth analysis and synthesis of newly acquired and published data on the chemical and isotopic compositions of forearc fluids, fluid fluxes, and the associated thermal regimes in five well-studied, representative erosional and accretionary subduction zone (SZ) forearcs indicate that the nature of fluid venting seems to differ at the two types of SZs. At both, fluid and gas venting sites are primarily associated with faults. The décollement and underthrust coarser-grained stratigraphic horizons are the main fluid conduits at accretionary SZs, whereas at non-accreting and erosive margins, the fluids from compaction and dehydration reactions are to a great extent partitioned between the décollement and focused conduits through the prism, respectively.

The measured fluid output fluxes at seeps are high, ~15-40 times the amount that can be produced through local steady-state compaction, suggesting that in addition, other fluid sources or non-steady-state fluid flow must be involved. Recirculation of seawater must be an important component of the overall forearc output fluid flux in SZs.

The most significant chemical and isotopic characteristics of the expelled fluids relative to seawater are: Cl dilution, sulfate, Ca and Mg depletions and enrichments in Li, B, Si, Sr, alkalinity, and hydrocarbon concentrations; they often have distinctive $\delta^{18}O$, δD, $\delta^{7}Li$ $\delta^{11}B$, and $\delta^{37}Cl$ values, and variable Sr isotope ratios. These characteristics provide key insights on the source of the fluid and the temperature at the source. Based on the fluid chemistry, the most often reported source temperatures reported are 120-150 °C.

Considering an ocean volume of 1340×10^{6} km^3 and the average composition of end-member fluids across the five representative SZs, the return fluxes of the solutes and isotope ratios from subduction zone forearcs to the ocean were recently estimated (Kastner et al., 2014). The results show that a residence time of the global ocean in SZs of ~100 million years, is about 5 times faster than the previous estimate, is similar to the residence time of ~90 million years for fluids in the global ridge crest estimate by Elderfield and Schultz (1996), and ~3 times longer than the 20-36 million years estimate by German and von Damm (2004). Based on this extrapolated fluid reflux to the global ocean, SZs are an important, mostly overlooked, source and sink for several elements and isotopic ratios, in particular an important sink for seawater Mg and SO_4, and an important source of Li and B. For example, the SZs estimated Mg output flux is up to 27% of the output flux estimated for hydrothermal circulation at mid-ocean ridges and accounts for 8% of the input flux from rivers; at SZs the sink of seawater SO_4 accounts for 10% of the river flux and up

to 44% of the hydrothermal flux. The results also show that the output flux of Ca at SZs is high enough to completely consume the input of Ca from hydrothermal circulation. The flux of B from SZs is ~13-100% of the flux from hydrothermal circulation, and the Li input flux is ~10-30% of the input flux from hydrothermal circulation. As yet the data-base for Li and B isotopic compositions of SZ fluids is too sparse for flux estimates, thus for impact on seawater chemistry calculations.

Recent Publications:

Rose, K.K., Johnson, J.E., Torres, M.E., Hong, W., Giosan, L., Solomon, E.A., Kastner, M., Cawthern, T., Long, P.E., and Schaef, T.H., (2014). Anomalous porosity preservation and preferential accumulation of gas hydrate in the Andaman Accretionary Wedge, NGHP-01 Site 17A. Marine Petrol. Geol. Spec. Publication. DOI: 10.1016/j.marpetgeo.2014.04.009.

Solomon, E.A,, Spivack, A.J., Kastner,M., Torres, M.E., and Robertson, G., (2014). Gas hydrate and carbon sequestration through coupled microbial methanogenesis and silicate weathering in the Krishna-Godavari basin, offshore India. Marine and Petrol. Geol. 58, 233-253.

Kastner, M., Solomon, E.A., and Harris, R.N., and Torres, M.E. (2014). Fluid origins, thermal regimes, and fluid and solute fluxes in the forearc of subduction zones. In Developments in Marine Geology, V. 7, "Earth and Life Processes Discovered from Subseafloor Environments, A Decade of Science Achieved by the Integrated Ocean Drilling Program", Stein, R., Blackman, D.K., Inagaki, F. and Larsen, H.-C., Eds. ,Elsevier B.V, .p. 671-733, ISBN: 978-0-444-62617-2.

Martinez-Ruiz, F., Kastner, M., Gallego-Torres, D., Rodrigo-Gámiz, M., Nieto-Moreno, V., Ortega-Huertas, M., (2015). Paleoclimate and Paleoceanography Over the Past 20,000 yr in the Mediterranean Sea Basins as Indicated by Sediment Elemental Proxies. Quaternary Science Reviews, 107, 1, 25-46.

Kerry Key
Associate Professor
kkey@ucsd.edu
http://marineemlab.ucsd.edu/kkey
858 822-2975

Research Interests*:* Marine electromagnetic exploration, subduction zones, mid-ocean ridges, continental margins, hydrocarbon exploration, finite element methods, parallel computing, geophysical inversion.

My research uses electromagnetic geophysical methods to study the geologic structure and fluids of the oceanic crust and upper mantle. Along with Steven Constable, I manage the Seafloor Electromagnetic Methods Consortium at Scripps, an industry funded program that brings in support for the PhD students and postdocs working in our group.

This year my graduate student Samer Naif completed his PhD thesis (Naif, 2015), which focused on the Serpentinite, Extension and Regional Porosity Experiment across the Nicaraguan Trench (SERPENT). We collected this data set several years ago, but as is often the case with new research endeavors, it takes some time to develop the tools required by the unique aspects of each data set. We think the results have been worth the wait. Figure 1 shows the complete electrical conductivity model derived from non-linear 2D inversion of the controlled-source electromagnetic data. We decided that trying to publish the complete story in one paper was going to be too much material, so we've split this image at the trench and first published the incoming plate story (Naif et al., 2015), which describes how bending faults that form in the trench outer rise are high porosity channels that increase the bulk water content of the subducting plate by about a factor of two. We are currently working on a manuscript describing the results from the right side of the image, where the subducting plate carries down fluid rich sediments beneath the forearc margin.

The other papers published this year are associated with our work with the offshore exploration industry. Myer et al. (2015), Constable et al. (2015) and Hoversten et al. (2015) look at controlled-source EM data collected for imaging geologic structures at oil and gas fields offshore Australia, the Gulf of Mexico and near the Faroe and Shetland Islands, respectively. Wheelock et al. (2015) looks at a particular aspect of EM data analysis with the unexpected result that scaling the data into the logarithm domain offers a better chance for robust interpretation.

We also had a string of luck this year with funding from the National Science Foundation. The MOCHA magnetotelluric survey described in last year's annual report received funding for the data interpretation phase. Early in the year we also found out that two field surveys were going to be funded and that both had accelerated schedules with cruises on the books for the summer. The first of these was an amphibious survey of Okmok volcano in the Aleutian islands of Alaska that involved collecting seafloor magnetotelluric data across the volcanic arc and a three week onshore campaign of magnetotelluric data collection and broadband seismometer installation inside and around Okmok caldera, done in collaboration with colleagues at UW Madison, the USGS and Alaska Volcano Observatory. I will include results from this project in next year's report, but in the mean time you can check out photos and videos of the field work on our blog at http://okmok.ucsd.edu. The second field survey this summer involved collecting controlled-source EM data to map offshore groundwater on the continental shelf off New Jersey and Martha's Vineyard, with a successful cruise in early September.

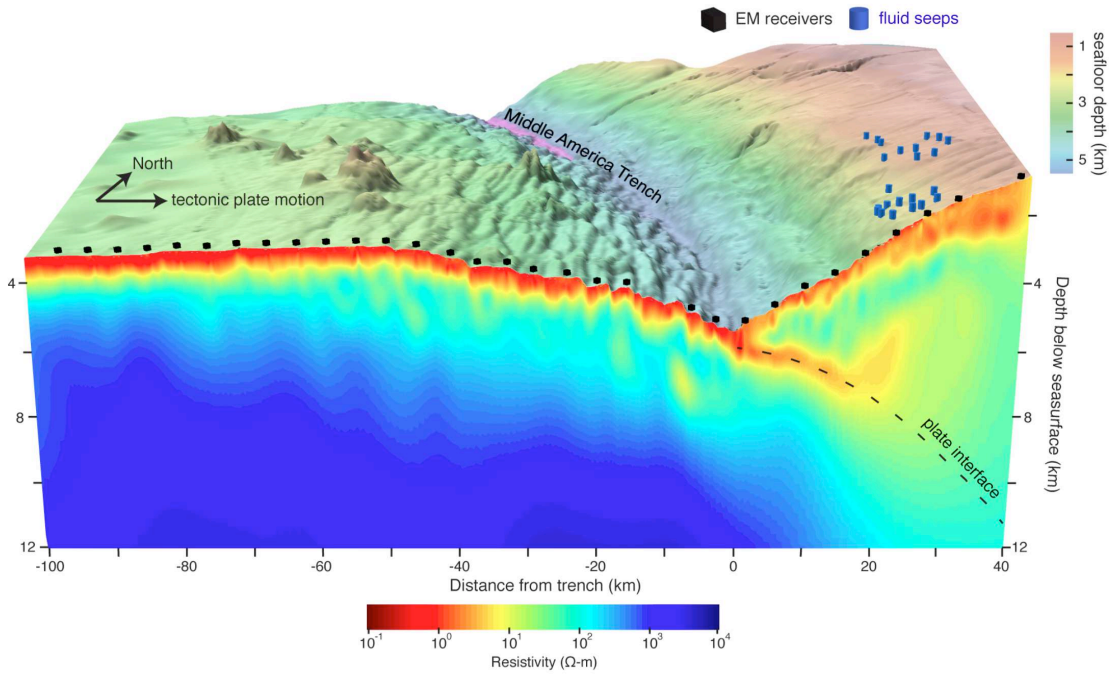

Figure 1: The electrical structure of the Middle American subduction zone offshore Nicaragua obtained from nonlinear inversion of deep-towed CSEM data. The vertical cross-section shows the sub-seafloor electrical resistivity structure and the stitched upper panel shows seafloor bathymetry. The dark blue cubes show the location of EM receivers. The region of the seafloor marked by steeply dipping relief correlates with sub-vertical conductive channels, which we interpret as evidence for the migration of seawater along bending faults. From Naif (2015).

Recent Publications

Naif, S., K. Key, S. Constable, and R. L. Evans (2015), Water-rich bending faults at the Middle America Trench, *Geochemistry, Geophysics, Geosystems*, 16(8), 2582–2597, doi:10.1002/2015GC005927.

Naif, S. N. (2015), Marine electromagnetic experiment across the Nicaragua Trench: Imaging water-rich faults and melt-rich asthenosphere, *PhD thesis*, University of California, San Diego.

Constable, S., A. Orange, and K. Key (2015), And the geophysicist replied: "Which model do you want?," *Geophysics*, 80(3), E197–E212, doi:10.1190/geo2014-0381.1.

Hoversten, G. M., D. Myer, K. Key, D. Alumbaugh, O. Hermann, and R. Hobbet (2015), Field test of sub-basalt hydrocarbon exploration with marine controlled source electromagnetic and magnetotelluric data, *Geophysical Prospecting*, 63, 1284–1310, doi:10.1111/1365-2478.12278.

Wheelock, B., S. Constable, and K. Key (2015), The advantages of logarithmically scaled data for electromagnetic inversion, *Geophysical Journal International*, 201(3), 1765–1780, doi:10.1093/gji/ggv107.

Myer, D., K. Key, and S. Constable (2015), Marine CSEM of the Scarborough gas field, Part 2: 2D inversion, *Geophysics*, 80(3), E187–E196, doi:10.1190/geo2014-0438.1.

Deborah Lyman Kilb
Project Scientist
Email address: dkilb@ucsd.edu
Phone extension: 2-4607

Research Interests: Crustal seismology, earthquake triggering, earthquake source physics.

Research Interests: Deborah Kilb's current research areas include crustal seismology and earthquake and icequake source physics, with an emphasis on understanding how one quake can influence another.

Exploring Remote Earthquake Triggering Potential using Frequency Domain Array Visualization [Linville et al., 2014]. To better understand earthquake source processes involved in dynamically triggering remote aftershocks, we use data from the EarthScope Transportable Array (TA), an array of over 400 seismic stations deployed in a grid pattern in the continental US. These stations provide uniform station sampling, similar recording capabilities, large spatial coverage, and in many cases, repeat sampling at each site. To avoid spurious detections, which are an inevitable part of automated time-domain amplitude threshold detection methods, we developed a frequency domain earthquake detection algorithm that identifies coherent signal patterns through array visualization (Figure 1). This method is tractable for large datasets, ensures robust catalogs, and delivers higher resolution observations than what are available in current catalogs. We explore to what extent there is an increase or decrease in small earthquake activity (i.e., seismicity rate changes) local to the TA stations following 18 global mainshocks (M≥7) that generate median peak dynamic stress amplitudes of 0.001- 0.028 MPa across the array. For these 18 mainshocks, we find no evidence of prolific or widespread remote dynamic triggering in the continental U.S. within the mainshock's wavetrain or within the next 2 days following the mainshock stress transients. There is, however, limited evidence of seismicity rate increases in localized source regions. These results suggest that for these data, prolific, remote earthquake triggering is a rare phenomenon. We further conclude that within the lower range of previously reported triggering thresholds, surface wave amplitude does not correlate well with observed cases of dynamic triggering. Therefore, other characteristics of the triggering wavefield, in addition to specific site conditions, must contribute to triggering at these amplitudes.

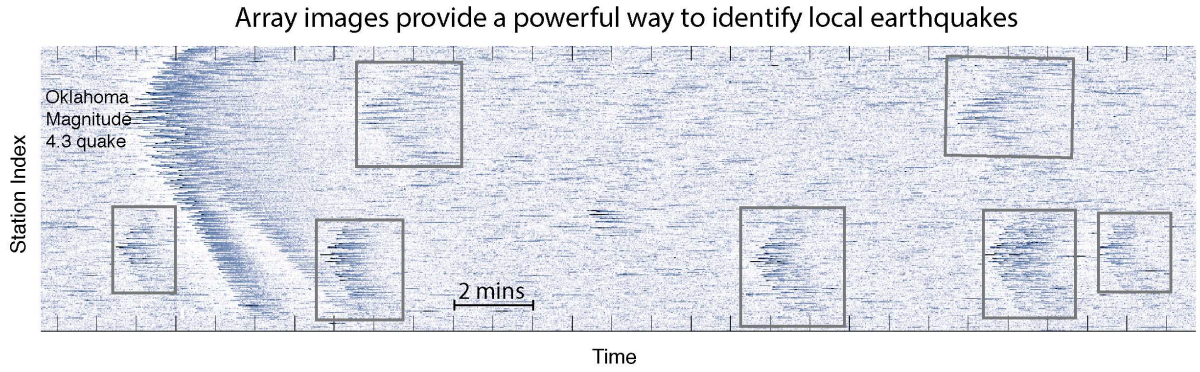

Figure 1: Data from the 02/27/2010 Chile M8.8 mainshock recorded by 415 USArray stations. In these "array images" we assign each pixel element a hue that represents amplitude intensity (higher amplitudes in darker hues). We use these array images to identify local and remote earthquakes based on amplitude variations in combination with appropriate seismic move-out. For example, a magnitude 4.3 earthquake in Oklahoma is visible across the entire array (upper left of the image, unboxed). We examine these high-frequency signals to identify those that are likely local (black boxes) or regional earthquakes.

Humming Icequakes [Heeszel et al., 2014]: Mountain glaciers represent one of the largest repositories of fresh water in alpine regions globally. However, little is known about the processes by which water moves through these systems. Gornersee is a lake that forms each spring at the confluence of two glaciers in the Swiss Alps. This lake drains during most summers, sometimes suddenly. Because glacial lake drainage events can occur with little or no warning, there is the potential for damaging floods in valleys below the glacier. We use seismic recordings collected near the lake to look for signs of water moving through fractures near the glacier bed. We see tremor, signals that are stronger at specific frequencies, in both single icequakes and over long periods. These observations suggest there is a complex network of fluid induced fracture processes at the glacier base. Modeling changes in the observed harmonic frequencies indicates that seismic data's spectral characteristics can provide important information about hydraulic fracture geometry and fluid pressure at depth. Similar to industrial fracking, this hydraulic fracturing at the base of a glacier can provide a mechanism to track fluid flow within glaciers in near real-time.

Glacier Ambient Noise Study [Walter et al., 2015]: We use seismic ambient noise data from the Greenland Ice Sheet and a Swiss Alpine glacier. Using the direct and scattered wave fields from the vast numbers of icequake records (tens of thousands per month), we can measure small changes in englacial (within the glacier) velocities, and in turn monitor bedrock depth and structural changes within the ice. In this way, seismic networks can be used to monitor a glacier's subsurface structure at sub daily time scales over months or longer. This constitutes a clear advantage over active source techniques that require considerable manpower for data acquisition.

See http://eqinfo.ucsd.edu/~dkilb/current.html for an expanded description of these projects.

Recent Publications

Heeszel, D., F. Walter and **D.L. Kilb** [2014]. "Humming Glaciers", *Geology,* 1099-1102, doi: 10.1130/G35994.1

Kilb, D, D Rohrlick, A Yang, Y Choo, L Ma, and R Ruzic [2014]. "The Game of Curiosity: Using Videogames to Cultivate Future Scientists", *Seis. Res. Lett.,* 85, 923-929, doi: 10.1785/0220130182.

Lawrence, JF, ES Cochran, A Chung, A Kaiser, CM Christensen, R Allen, JW Baker, B Fry, T Heaton, **D Kilb,** MD Kohler and M Taufer [2014]. "Rapid earthquake characterization using MEMS accelerometers and volunteer hosts following the M 7.2 Darfield, New Zealand, Earthquake", *Bull. Seism. Soc. Am.*, 104:184-192. doi: 10.1785/0120120196.

Linville L., K. Pankow, **D. Kilb** and A. Velasco [2014]. "Exploring Remote Earthquake Triggering Potential Across Earthscopes' Transportable Array through Frequency Domain Array Visualization", *J. of Geoph. Res.*. doi: 10.1002/2014JB011529. Dynamic Content: interactive visualization of a high-resolution array image http://siogames.ucsd.edu/Zoom/linville_etal_2014

Walter, F., P. Roux, C. Roeoesli, A. Lecointre, **DL Kilb,** P-F. Roux [2015]. "Using glacier seismicity for phase velocity measurements and Green's function retrieval", *Geophysical Journal International*, 201: 1722-1737, doi: 10.1093/gji/ggv069.

Gabi Laske
Professor in Residence
Email: glaske@ucsd.edu
Phone: 4-8774

Research interests: regional and global seismology; surface waves and free oscillations; seismology on the ocean floor; observation and causes of seismic noise; natural disasters and the environment

Gabi Laske's main research area is the analysis of seismic surface waves and free oscillations, and the assembly of global and regional seismic models. She has gone to sea to collect seismic data on the ocean floor. Laske's global surface wave database has provided key upper mantle information in the quest to define whole mantle structure. Graduate students Christine Houser and Zhitu Ma as well as students from other universities have used her data to compile improved mantle models.

Global reference models: Laske has collaborated with Guy Masters, graduate student Zhitu Ma and Michael Pasyanos at LLNL to compile a new lithosphere model, LITHO1.0. A 1-degree crustal model, CRUST1.0 was released in 2013 for initial testing. Applications relying on CRUST1.0 are found across multiple disciplines in academia and industry, and sometimes reach into quite unexpected fields such as the search for Geoneutrinos. Laske has continued to compile community feedback and provides updates to the distribution website and links to related research outside of IGPP.

The PLUME project: For the past decade or so, Laske has been focusing on waveforms collected on ocean bottom seismometers (OBSs). She was the lead-PI of the Hawaiian PLUME project (Plume–Lithosphere–Undersea–Mantle Experiment) to study the plumbing system of the Hawaiian hotspot. Results from both body wave and surface wave tomography were published. During the last two years, Laske has collaborated with Kate Rychert to identified two upper-mantle boundaries that align with anomalies found in the surface wave study. The published images suggest a restite root beneath the Island of Hawaii around which ascending plume material has to flow, providing a possible cause for the low-velocity anomaly to the west of Hawaii. Laske has worked with Christine Thomas at Münster University, Germany to search for new and **previously unmapped D" precursors** in the PLUME database. The good quality of vertical-component records allowed the team to detect PdP waves for some areas and found convincing null-results for other areas. This is the first study of its kind using OBS data.

We are continuing the analysis of frequency-dependent Rayleigh-wave **azimuthal anisotropy**. While shear-wave splitting results appear to be sensitive only to the fossil spreading direction "frozen" into the lithosphere, Laske found a clear signal in the long-period data that suggests a plume-related flow in the asthenosphere beneath Hawaii. This served served as project for IRIS intern Rachel Marzen who presented an AGU poster at the 2013 Fall meeting.

PhD student Adrian Doran continues the analysis of PLUME **seafloor compliance as well as ambient-noise** Green's functions. The combined analysis will help constrain elastic parameters in the shallow sediments and crustal layers that were not resolved by the surface wave study.

The ADDOSS project: For the ADDOSS (Autonomously Deployed Deep-ocean Seismic System) Laske collaborates with Jon Berger, John Orcutt and Jeff Babcock and Liquid Robotics Inc. to develop an untethered OBS system that is capable of providing near-real time data collected on the ocean floor. A wave glider towing an acoustic modem in a tow

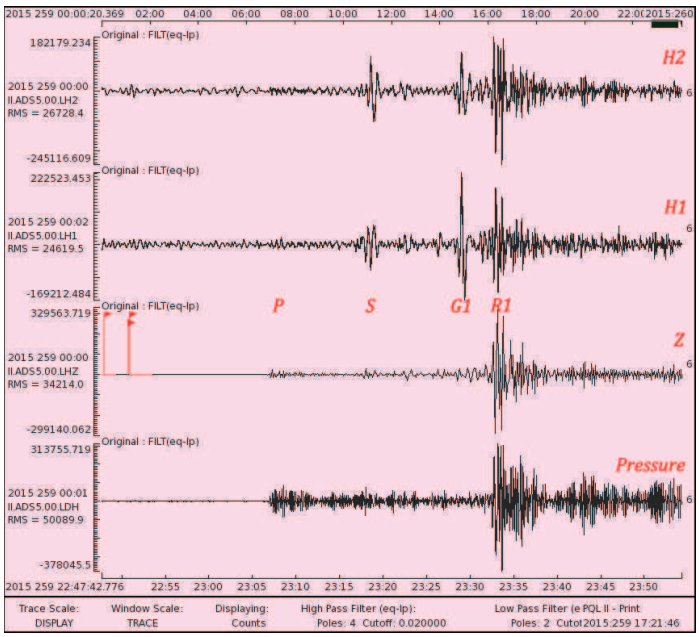

Figure 1: Near-real-time four-component OBS time series of the of the great tsunamigenic Sep 16, 2015 Illapel, Chile earthquake. Top three traces are the two horizontal and the vertical component of a Nanometrics Trillium T-240 seismometer. The bottom record is from a differential pressure gauge (DPG) developed at SIO. The traces are bandpass filtered to emphasize long-period seismic waves. Laske and Programmer Analyst David Chavez witnessed how the waveform arrived on IGPP computer screens in near-real time.

body maintains a communications link to the OBS, where the glider then sends data to shore via satellite. The group has performed several tests in shallow (1000 m) and deep (3800 m) water. During a 3-month deep-water test about 300 km west of La Jolla in the winter of 2013 provided crucial new seismicity data. The group has identified several magnitude 2 seismic events that remained undetected by shore-based seismic monitoring networks that include island stations in the Inner California Borderland. In addition, a pair of seismometers picked up numerous micro earthquakes, for which the location determination is still ongoing. Doran and Laske successfully competed for UC ship funds and smaller UC grants for a follow-up deployment near the 2013 site, and ADDOSS joined as a piggy-back experiment. Due to needed repairs, the wave glider was sent from shore later. It successfully established communication after a 10-day ride. On Sep 16, 2015, the group witnessed how the waveforms of the great Illapel, Chile earthquake arrived in near-real time. The instrument also successfully recorded the tsunami that arrived some 12 hours later. A nearby DART buoy was not operational at the time.

Recent publications:

Ma., Z., Masters, G., Laske, G. and Pasyanos, M., A comprehensive dispersion model of surface wave phase and group velocity for the globe, *Geophys. J. Int.*, 199, 113-135, DOI: 10.1093/gji/ggu246, 2014

Thomas, C. and Laske, G., D" observations in the Pacific from PLUME Ocean Bottom Seismometer recordings. *Geophysical Journal International*, 200, 851–862, doi:10.1093/gji/ggu441, 2015.

Laske, G., Berger, J., Orcutt, J. and Babcock, J., ADDOSS: Autonomously Deployed Deep-ocean Seismic System - Communications Gateway for Ocean Observatories, *Proceedings of the IUGG eGeneral Assembly*, Prague, Czech Republic, July 2015.

Berger, J., Laske, G., Babcock, J. and Orcutt, J., An Ocean Bottom Seismic Observatory with Real-time Telemetry. *Earth and Space Science*, in revision, 2015.

Jean Bernard Minster Distinguished Professor of Geophysics
jbminster@ucsd.edu
Phone: 858-945-0693
Research Interests*:* Seismology, Geodesy, Data Science and Policy

After chairing the ICSU World Data System (ICSU-WDS) Scientific Committee (SC) since 2008, I have rotated off that position in July, 2015, and the new chair is Professor Sandy Harrison of the University of Reading.

Of the six years of my tenure as Chair of the SC, WDS has grown from an idea proposed by the International Council of Science (ICSU) at their 2008 General Assembly in Maputo, Mozambique, to a global system, counting 94 members. These include

- 61 *Regular Members*, organizations that are data stewards and/or data analysis services,
- 10 *Network Members*, umbrella bodies representing groups of data stewardship organizations and/or data analysis services,
- 5 *Partner Members*, organizations that are not data stewards or data analysis services, but that contribute support or funding to ICSU-WDS and/or WDS Members, and
- 18 *Associate Members*, organizations that are interested in the WDS endeavor and participate in our discussions, but that do not contribute direct funding or other material support.

In addition, thanks to the generosity of the Japanese Government, and in particular the National Institute of Information and Communications Technology (NICT), ICSU-WDS enjoys the support of an International Programme Office (WDS-IPO). The agreement between ICSU and NICT to host the IPO has recently been extended until March 31, 2021, thereby providing WDS with a stable home base for the next 5 years, and to live up to its motto *"Trusted Data Services for Global Science."*

The World Data System continues to animate and lead several international working groups to address difficult data science problems. As Chair of the SC, I have participated in their work and continue to do so. These include:

- Data Publishing
- Creation of a Knowledge Network
- Streamlining the Certification of trusted data repositories (in partnership with the Data Seal of Approval (DSA)

In addition, WDS sponsors a series of worldwide webinars on current data community issues.

In the course of this past year, WDS has been engaged in numerous global activities. First and foremost, the First international Scientific Data Conference (SciDataCon-2014) was held in New Delhi, India in collaboration with ICSU Committee on Data for Science and Technology (CODATA). The theme of the conference was *"Data Sharing and Integration for Global Sustainability."* On that occasion, WDS awarded its first two *Data Stewardship Awards* to Dr. Robert Redmon and Dr. Xiaogang Ma for "exceptional contributions to the improvement of scientific data stewardship by early career researchers through their (1) engagement with the community, (2) academic achievements, and (3) innovations."

Recent work of the WDS-SC involved a reworking of its Data Policy, necessitated to accommodate the special requirements of disciplines such as Health Sciences, and Social Sciences. The revised policy us currently being aligned with that of the Group on Earth Observations (GEO). Special attention is being accorded to the rapidly expanding concept of Open Access worlswide. In my report to the 2014 ICSU General Assembly in Auckland I

emphasized the potential blind applications of metrics to evaluate the value of data sets. This caution is now part of the ICSU record.

In the past year, WDS was represented in innumerable scientific meetings and forums. WDS is now a partner with GEO/GEOSS, and a significant participant in the new *Future Earth* ICSU program. I have participated on a number of these, too numerous to list here.

The final meeting of the WDS-SC that I chaired was held, appropriately, at IGPP on February 7-8, 2015 (see picture). The gavel was passed to Sandy Harrison during the September meeting of the SC at ICSU Headquarters in Paris. I leave WDS in good shape and in good hands.

ICSU World Data System Scientific Committee meeting at IGPP, February 8, 2015.

A recent entrant on the international data scene is the *Research Data Alliance* (RDA). I have participated in several of RDA's plenary meetings, notably the one held in San Diego in February, 2015. I am an active participant in several of the innumerable RDA Working Groups and Interest Groups, in particular:

- Repository Audit and Certification DSA–WDS Partnership WG
- Libraries for Research Data IG
- RDA/CODATA Legal Interoperability IG
- RDA/WDS Certification of Digital Repositories IG
- RDA/WDS Publishing Data IG
- Digital Practices in History and Ethnography IG

The Fall 2016 RDA Plenary meeting will be co-located with the SciDataCon-2016 (CODATA ands WDS) to support a new International Data Week in Denver, CO September , 2016.

Finally, I continue my participation in the NASA planning and review activities surrounding two important Low-Earth-Orbit geophysical missions planned for the end of the decade, namely ICESAT-2 and NISAR.

Walter Munk **Research Professor**
wmunk@ucsd.edu
Phone: 534-2877

1. Deep Pressures. According to linear wave theory, surface waves $y = A\cos(kx - \omega t)$ have a pressure signature $\rho g a \exp(-kz)$ that becomes infinitesimal at the depth of a few wavelengths. Longuet-Higgins has explained the deep pressures in terms of some oppositely traveling wave energy (the microseism theory). The theory works well at frequencies of less than 1 Herz, but we have some doubts at high frequencies (100 Hz, say). Continuing work with J. Berger and W. Farrell, we have joined forces with Ken Melville and are developing plans for a 6 month simultanous deployment of bottom sensors and near surface observations, including a vertical hydrophone array, wave gliders and aircraft flights.

2. Wind Drag. For half a century Cox's observation that sea surface slope increases linearly with wind speed has remained unexplained. Nor has the surprisingly large slope perpendicular to the mean wind direction. New insight comes from a reexamination of Lord Kelvin's classical explanation of ship wakes. Looking at much higher wave numbers than usual, and accounting for the effect of surface tension, a wide angular spread in the wave field is obtained. We imagine that pressure pulses from moving turbulent cells in the atmospheric boundary layer constitute a moving source, analogous to Kelvin's ship. The problem is important for the understanding of wind drag.

References

Cox, C. and W. Munk (1956). Slopes of the sea surface deduced from photographs of sun glitter. *Scripps Inst. Oceanogr. Bull.*, **6**(9), 401-488.

Thompson, W. (1887) On the waves produced by a single impulse in water of any depth, *Proc. R. Soc. London, Ser. A.*, **42**, 80-83.

Munk, W. (October 30, 2015) Wind drag and Kelvin's 1877 popular lecture on Ship Waves, in preparation.

Richard D. Norris Paleobiology Professor and Curator, SIO Geological Collections

rnorris@ucsd.edu

Phone: 822-1868

Research Interests*:* Paleobiology, paleoceanography, human impacts on ocean ecosystems, marine biodiversity, extinctions, evolution of pelagic ecosystems, tipping points in reef communities

85 million years of fish and shark evolution in the open ocean.
With Ph.D student, Elizabeth Sibert, I have been using the fossil record of fish teeth in the open ocean to reconstruct fish populations through recent geologic history. Pelagic fish teeth and shark scales (ichthyoliths) are durable, highly resistant to dissolution or breakage, readily identifiable, easily separated from sediments, and ubiquitous in the deep sea. Hence, both their abundance (as a productivity proxy) and their identification (as a measure of ecosystem structure by analogy with living fish distributions and ecologies) makes them useful as direct recorders of environmental information. We have been using this remarkable record to reconstruct the impact of major ecosystem disruptions—the Cretaceous-Paleogene mass extinction, the Paleocene-Eocene thermal Maximum, and the Eocene-Oligocene glaciation—on fish productivity and biodiversity.

A recent result of this work is the finding (in Sibert and Norris. 2015), that there has been a dramatic change in the relative abundance of fish and sharks in the open ocean over the past 85 million years. In the Cretaceous oceans (>66 Ma), the production of shark denticles (mineralized scales) was about equal to that of fish teeth. However, after the Cretaceous-Paleogene mass extinction (66 Ma), fish production doubled over that of sharks, and later doubled again, while sharks remained 'stuck' with Cretaceous-rates of abundance. New, unpublished work further shows that about 20 million years ago, shark production dropped dramatically relative to fish—a situation of low shark abundance that persists to the present day.

We have dubbed these changes in shark and fish abundances, the "Cretaceous Ocean", "Paleogene Ocean" and "Neogene Ocean" (see figure 1) that each reflects different basic roles for sharks and fish in open ocean ecosystems. We speculate that in the Cretaceous, fish and sharks competed extensively against now extinct groups of predators such as the ammonites. The removal of ammonites by mass extinction 'released' fish from predation and allowed them to explode in abundance in the warm 'greenhouse' world of the Paleogene. Later, in the Neogene, the evolutionary diversification of marine mammals, seabirds and large pelagic fish effectively competed with sharks, driving shark abundance down in the pelagic ocean.

Recent Publications

Sibert, EC, Norris RD. 2015. New Age of Fishes initiated by the Cretaceous−Paleogene mass extinction. Proceedings of the National Academy of Sciences. 10.1073/pnas.1504985112

Yamaguchi, T, Norris RD. 2015. No place to retreat: Heavy extinction and delayed recovery on a Pacific guyot during the Paleocene-Eocene Thermal Maximum. Geology. 43:443-446. 10.1130/g36379.1

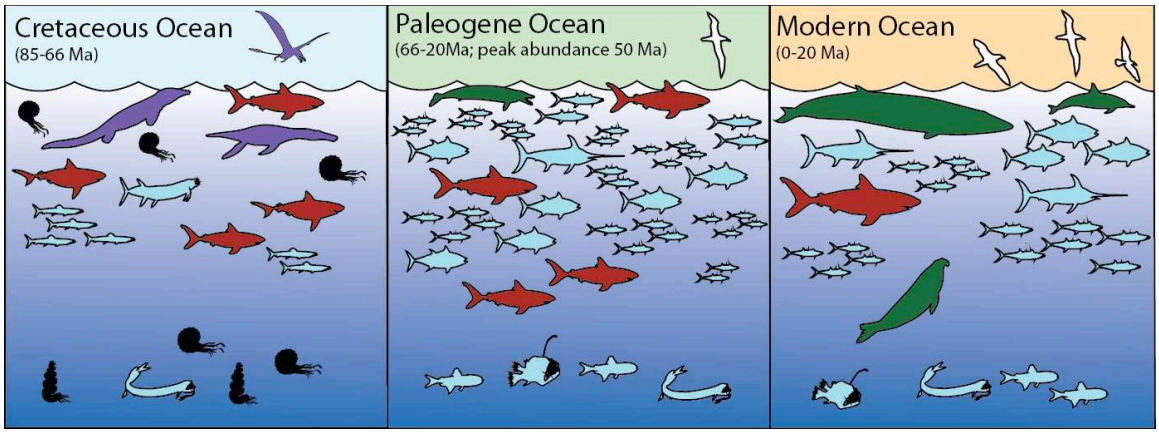

Figure 1 Caption:
Changes in pelagic ecosystems are reflected in the relative abundance of fish teeth and shark dermal denticles over the past 85 million years. Cretaceous oceans had relatively few fish (light blue outlines) relative to more recent times, perhaps because of competition for resources with the now-extinct ammonites (black outlines) and marine reptiles (purple outlines). The Cretaceous-Paleogene mass extinction (66 Ma) appears to have removed fish-competitors, allowing fish to greatly increase in both abundance and diversity. Both fish and sharks (red outlines) were unusually productive during the "greenhouse" climate of the early Eocene (~50 Ma). Finally, the evolutionary diversification of marine mammals (green outlines), seabirds and large pelagic fish (like tuna and swordfish) about 15-25 Ma, drove down shark abundance in the open ocean, even as some of the largest sharks (like *Megalodon*) appeared in coastal waters.

Anne Pommier, Assistant Professor
pommier@ucsd.edu
Phone: 822-5025

Research Interests*:* physics and chemistry of silicate melts; role of magma in planetary interiors, from the scale of volcanic magma reservoirs to planetary-scale magma oceans; evolution of planetary interiors from "deep time" (e.g., planet evolution) to the present.

Ongoing research projects have mainly focused on (i) the experimental investigation of the electrical properties of Earth's upper mantle rocks under pressure, (ii) the experimental investigation of the deep Lunar mantle, and (iii) the time-evolution of the Martian core.

(i) Sheared rocks are thought to explain electrical anomalies in a deformed uppermost mantle as their high electrical conductivity and anisotropy reproduce electromagnetic data. Although melt or water can reproduce asthenospheric electrical anisotropy, the electrical properties of the sheared polycrystalline matrix and its contribution to bulk electrical anisotropy at upper mantle conditions are not fully understood and require further investigation. Under funding from NSF Cooperative Studies Of The Earth's Deep Interior, my collaborators David Kohlstedt, Kurt Leinenweber, Stephen Mackwell, Ed Garnero, Chao Qi, James Tyburczy and I have investigated the effect of melt on the electrical conductivity of deformed materials at upper mantle conditions (Pommier et al., Nature, 2015). Based on electrical anisotropy measurements under pressure on mantle analogues, we observed that electrical conductivity is highest parallel to deformation direction and quantified the effect of shear on conductivity with increasing temperature. Our experimental results and modeling show that field data are best reproduced by an electrically anisotropic asthenosphere overlain by an isotropic, high-conductivity deep lithosphere. The high conductivity could arise from partial melting associated with localized deformation resulting from differential plate velocities relative to the mantle, with upward melt percolation from the asthenosphere. In a second study, we conducted a systematic experimental investigation of the effect of shear deformation on the electrical conductivity of (melt-free) polycrystalline olivine. Starting samples were previously sheared to a strain of up to 7.3 and their electrical conductivity and anisotropy of the samples were then measured at 3GPa in a multi-anvil apparatus. We observe that shear deformation increases electrical conductivity and that conductivity is highest in the direction of shear, with the sample deformed to the highest strain being the most conductive. The role of grain boundaries and dislocations on conduction mechanisms are investigated based on textural analyses and previous electrical and diffusivity studies, in collaboration with Florian Heidelbach, Miki Tasaka, and Lars Hansen. Application of our results to field data indicates that electrical anomalies in the asthenosphere can be solely explained by the electrical properties of the sheared solid matrix.

(ii) The presence of melt at the base of the lower mantle of some terrestrial bodies, such as the Earth and the Moon may indicate a remnant global magma ocean, remained partially molten due to the presence of trapped heat-producing elements. Together with collaborators Kurt Leinenweber and Miki Tasaka and under funding from NSF, I measured the electrical properties of dry and hydrous olivine compacts during melting at 4 and 6 GPa (corresponding to the pressure range for the core-mantle boundary of the Moon) in order to investigate melt transport properties and quantify the effect of partial melting on electrical properties (Pommier et al., EPSL, 2015). At temperature > $T_{solidus}$, we observed a significant increase in conductivity (by a factor ranging from ~30 to 100), consistent with the transition from a tube-dominated network to a structure in which melt films and pools become prominent features (see Figure). It is followed by a plateau at higher temperature, suggesting the sample lacks sensitivity to temperature at an advanced stage of partial melting. Our results can be reproduced satisfactorily by two-phase electrical models and provide a melt conductivity value of > 45 (±5) S/m. Comparison of our

results with electromagnetic sounding data of the deep interior of the Moon supports the hypothesis of the presence of interconnected melt at the base of the lunar mantle. Our results underline that electrical conductivity can be used to investigate *in situ* melt nucleation and migration in the interior of terrestrial planets.

(iii) Though it is accepted that Mars has a sulfur-rich metallic core, its chemical and physical state as well as its time-evolution are still debated. Several lines of evidence indicate that an internal magnetic field was once generated on Mars and that this field decayed around 3.7-4.0 Gyrs ago. The standard model assumes that this field was produced by a thermal (and perhaps chemical) dynamo operating in the Martian core. Former Green Scholar Christopher Davies and I have used this information to construct parameterized models of the Martian dynamo in order to place constraints on the thermochemical evolution of the Martian core, with particular focus on its crystallization regime. Considered compositions are in the FeS system, and other parameters include core radius, density, melting curve and adiabat, core-mantle boundary heat flow and thermal conductivity. Successful models are those that match the dynamo cessation time and fall within the bounds on present-day CMB temperature. Possible crystallization regimes are: growth of a solid inner core starting at the center of the planet; freezing and precipitation of solid iron (Fe-snow) from the core-mantle boundary (CMB); and freezing that begins midway through the core. In parallel, I have conducted experiments in the Fe-S and Fe-S-O systems with collaborators Dan Frost and Vera Laurenz at BGI, Germany, with funding from the Alexander vonHumboldt Foundation. Our results will help place new constraints on the time- and space- evolution of the core of terrestrial bodies, including Mars.

Related publications:
1- Pommier A., K. Leinenweber, and M. Tasaka, Experimental Investigation of the Electrical Behavior of Olivine during Partial Melting under Pressure and Application to the Lunar Mantle, Earth and Planetary Science Letters, 425 242–255, 2015. 2- Pommier A., K. Leinenweber, D. L. Kohlstedt, C. Qi, E. J. Garnero, S. Mackwell, J. Tyburczy, Experimental Constraints on the Electrical Anisotropy of the Lithosphere-Asthenosphere System, Nature, doi: 10.1038/nature14502, 2015.

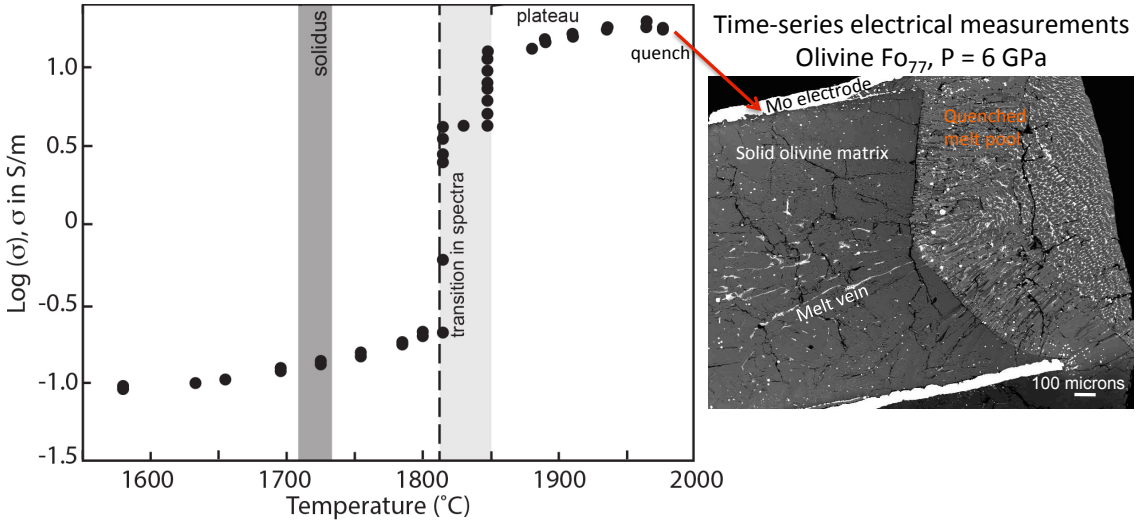

Figure Caption: Electrical conductivity σ during partial melting: example of dry olivine compact at 6 GPa. A slight change in the dependence of σ to temperature is observed after the solidus is crossed, attributed to the nucleation and low interconnectivity of the melt phase. The jump in σ is consistent with a transition from interconnected melt tubes to a completely wetted olivine matrix. At this stage of partial melting, significant changes in olivine chemistry occur caused by the partitioning of iron to the melt phase. Finally, a plateau in σ is reached and corresponds to melt migration and eventual melt pooling. See Pommier et al., EPSL, 2015 for details.

David T. Sandwell
Professor of Geophysics
Email: dsandwell@ucsd.edu
http://topex.ucsd.edu

Research Interests: Geodynamics, global bathymetry, crustal motion modeling, space geodesy

Students and Funding - Research for the 2014-15 academic year was focused on understanding the dynamics of the crust and lithosphere. Our group comprises three graduate students Soli Garcia, Eric Xu, and John Desanto, two postdocs Dan Bassett and Alejandro Gonzalez-Ortega and two lab assistants Rachael Munda and Brenda Mendonca. Our research on improvement in the marine gravity field is co-funded by the National Science Foundation (NSF), the Office of Naval Research, and the National Geospatial Agency. In addition, we are funded by NSF and Google to improve the accuracy and coverage of the global bathymetry. The NSF EarthScope Program as well as the Southern California Earthquake Center funds our research on the strain rate and moment accumulation rate along the San Andreas Fault System from InSAR and GPS.

Global Gravity and Bathymetry – We are improving the accuracy and spatial resolution of the marine gravity field using data from three new satellite radar altimeters (CryoSat-2, Jason-1, and Envisat). This is resulting in a factor of 2-4 improvement in the global marine gravity field. Most of the improvement is in the 12 to 40 km wavelength band, which is of interest for investigation of seafloor structures as small as 6 km (*Garcia et al.,* 2013). The improved marine gravity is important for exploring unknown tectonics in the deep oceans as well as revealing thousands of uncharted seamounts (*Sandwell et al.,* 2014).

Integration of Radar Interferometry and GPS - We are developing methods to combine the high accuracy of point GPS measurements with the high spatial resolution from radar interferometry to measure interseismic velocity along the San Andreas Fault system. We analyzed InSAR observations, initially from ALOS ascending data, spanning from the middle of 2006 to the end of 2010, and totaling more than 1100 interferograms (Tong et al., 2013). These combined GPS/InSAR data are critical for understanding the along-strike variations in stress accumulation rate and associated earthquake hazard (*Tong et al.,* 2015). The InSAR processing was performed with new software called GMTSAR developed at SIO (http://topex.ucsd.edu/gmtsar).

Crustal Motion Modeling – Early 2014, two new InSAR satellites became operational. Sentinel 1A is the first of a series of European Space Agency (ESA) SAR satellites to provide an operational mapping program for crustal deformation along all zones having high tectonic strain. The second new satellite is ALOS-2, launched by JAXA. The L-band radar aboard ALOS-2 operates in a ScanSAR mode having a 350 km wide swath (Figure 1). **These satellites have the measurement cadence and spatial coverage needed to revolutionize our understanding of earthquake cycle processes both globally and along the San Andreas Fault System**.

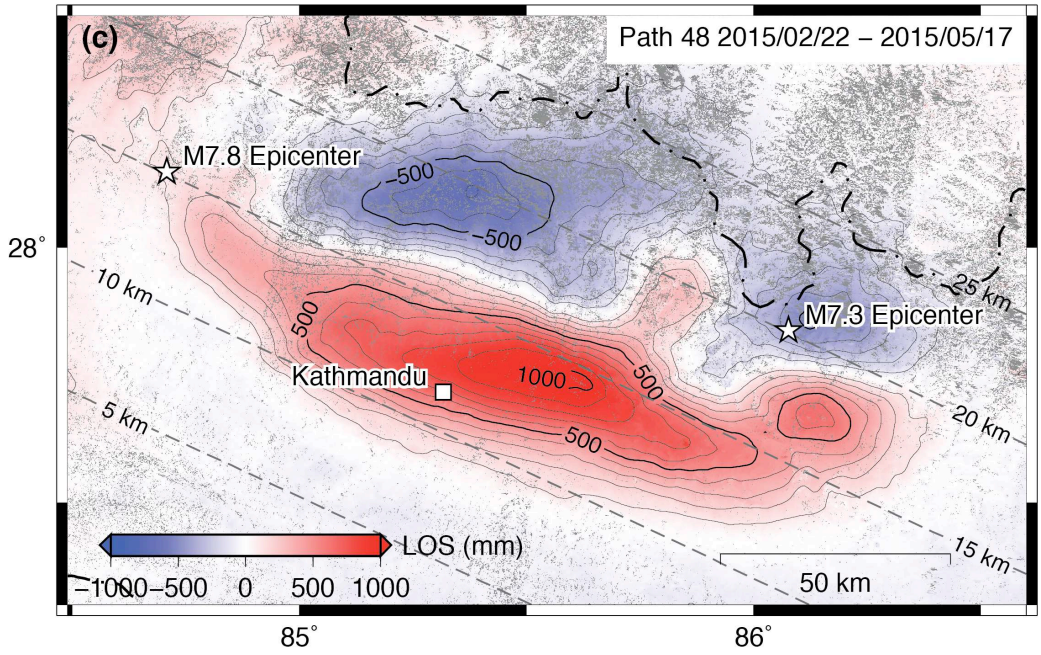

Figure 1. ALOS-2 ScanSAR interferogram of the M7.8 and M7.3 Nepal earthquakes, processed by our lab and publish recently in GRL (*Lindsey et al.,* 2015), highlights the unique and advanced attributes of this InSAR system. The single 350 km-wide interferogram completely captures the extent of the deformation. This region of the Himalayas has the highest topography on Earth with snow-capped peaks, yet it was possible to unwrap and connect the phase of all 5 subswaths.

Relevant Publications

Garcia, E., D. T. Sandwell, W. H. F. Smith. Retracking CryoSat-2, Envisat, and Jason-1 Radar Altimetry Waveforms for Improved Gravity Field Recovery, Geophysical Journal International, doi: 10.1093/gji/ggt469, 2014.

Garcia, E. S., D. T. Sandwell, and K. M. Luttrell, An Iterative Spectral Solution Method for Thin Elastic Plate Flexure with Variable Rigidity, *Geophys. J. Int., 200*, 1012-1028, doi: 10.1093/gji/ggu449, 2014.

Lindsey, E., R. Natsuaki, X. Xu, M. Shimada, H. Hashimoto, D. Melgar, and D. Sandwell, Line of Sight Deformation from ALOS-2 Interferometry: Mw 7.8 Gorkha Earthquake and Mw 7.3 Aftershock, *Geophysical Research Letters, 42*. doi:10.1002/2015GL065385, 2015.

Sandwell, D. T., R. D. Müller, W. H. F. Smith, E. Garcia, R. Francis, New global marine gravity model from CryoSat-2 and Jason-1 reveals buried tectonic structure, Science, Vol. 346, no. 6205, pp. 65-67, doi: 10.1126/science.1258213, 2014.

Tong, X., D. T. Sandwell, and B. Smith-Konter, High-resolution interseismic velocity data along the San Andreas Fault from GPS and InSAR, *J. Geophys. Res.; Solid Earth, 118,* doi:10.1029/2012JB009442, 2013.

Tong, X., D.T. Sandwell, and B. Smith-Konter, An integral method to estimate the moment accumulation rate on the Creeping Section of the San Andreas Fault, Geophys. J. Int., 203, 48-62, doi: 10.1093/gji/gjis140783, 2015.

Annika Sanfilippo-Howard
Specialist, RTAD
Email address: annika@ucsd.edu
Phone: 858-534-2049

Research Interests: Radiolarian taxonomy, evolution, and stratigraphy, correlation of Cenozoic marine sequences to investigate extinction and diversification patterns associated with climate change.

Together with a team of radiolarian colleagues I continue the work stimulated by the World Registry of Marine Species (WoRMS) and the Encyclopedia of Life (EOL) in an ambitious effort to produce an illustrated catalog of all Cenozoic radiolarian genera including type species.

My paleontological research and interest are intimately linked to the geological collections and their proper curation. As the curator for the U.S. West Coast Repository for the DSDP/ODP Micropaleontological References Centers, I continue to inventory new radiolarian slides that are periodically added to the collection. Progress is being made toward revitalization and inventory of unique, retired and/or orphaned paleontological collections acquired by SIO Geological Collections as an important contribution to future paleontologists.

Recent Publications

Lazarus, D., Suzuki, N, Caulet, J.-P., Nigrini, C., Goll, I., Goll, R., Dolven, J.K., Diver, P. and Sanfilippo, S., 2015. An evaluated list of Cenozoic-Recent radiolarian species names (Polycystinea), based on those used in the DSDP, ODP and IODP deep-sea drilling programs. Zootaxa 3999 (3): 301-333, (http://dx.doi.org/10.11646/zootaxa.3999.3.1)

The abstract of the above paper was presented as a poster at the GSA meeting in Vancouver, BC, Oct. 20-24, 2014. (Ref: Abstract No: 247919)

Abstract

D. Lazarus, N. Suzuki, J.-P. Caulet, C. Nigrini, R. Goll, J. K. Dolven, A. Sanfilippo, P. Diver, I. Goll, 2014. A First Comprehensive Evaluated List of Cenozoic Radiolarian Species.
david.lazarus@mfn-berlin.de

Summary
Despite their extensive use in biostratigraphy and paleoceanography, no catalogs exist for Cenozoic radiolarian species names. We present here a first step towards creating a catalog in the form of a list of all species names, with family membership, author, year, and most importantly taxonomic status. Currently there are about 1,200 valid names, plus more than 700 synonyms (including many published misspellings).

Peter Shearer
Distinguished Professor of Geophysics
pshearer@ucsd.edu, 858-534-2260

Research Interests*:* seismology, Earth structure, earthquake physics

My research uses seismology to learn about Earth structure and earthquakes, using data from the global seismic networks and local networks in California, Hawaii, and Japan. My work in crustal seismology has focused on improving earthquake locations using waveform cross-correlation and systematically estimating small-earthquake stress drops from *P*-wave spectra. Recently I collaborated with former IGPP Green Scholar Yoshihiro Kaneko (now at GNS New Zealand) to model simple yet dynamically self-consistent elliptical ruptures and test methods for estimating corner frequency and stress drop from far-field seismic records (*Kaneko and Shearer,* 2015). Our results show that asymmetric rupture models exhibit large variability in corner frequency and scaled energy over the focal sphere and that radiation efficiency estimates derived from seismic spectra alone are not reliable.

Foreshock sequences are important because they are one of the most commonly observed precursors to large earthquakes. Former graduate student Xiaowei Chen (now at the University of Oklahoma) systematically examined 64 California M ≥ 5 earthquakes and found that about half have foreshock sequences (*Chen and Shearer*, 2015). The observed foreshock properties are not easily explained by standard statistical models of earthquake-to-earthquake triggering, favoring models of physical changes in the nucleation zone of large earthquakes.

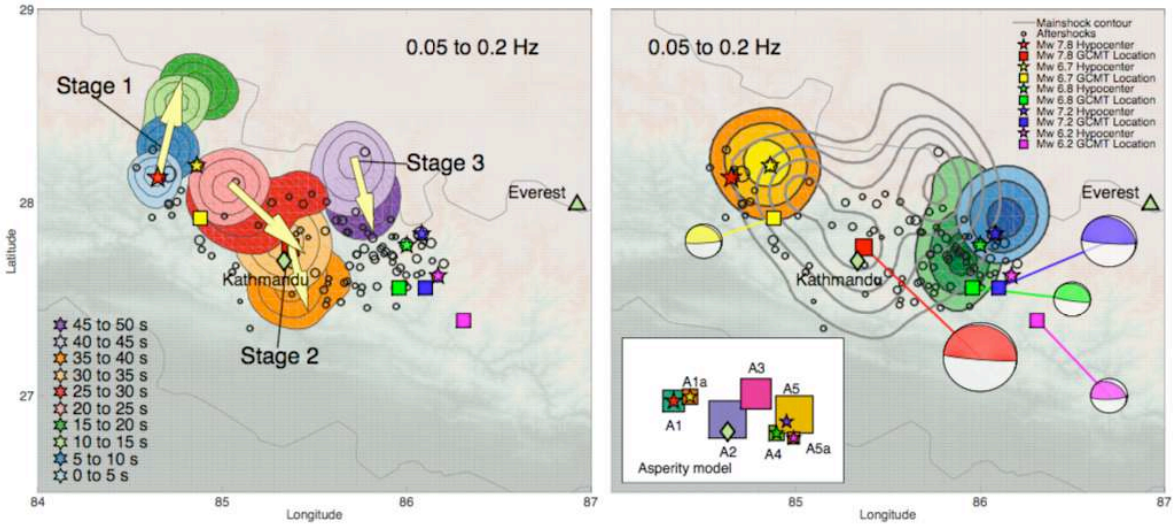

Figure 1. Rupture of the 2015 Nepal earthquake, as seen in time-integrated images of back-projected *P* waves. (left) High-frequency backprojection image over 60 s. (right) Low-frequency backprojection image over 60 s. Figure from *Fan and Shearer* (2013).

The recent Mw 7.8 earthquake in Nepal was the focus of studies by graduate student Wenyuan Fan and Green Scholar postdoc Marine Denolle. *Fan and Shearer* (2015) implemented a global back-projection approach to image the Nepal rupture and identified a complex, frequency-dependent rupture process with three distinct stages (see Fig. 1). There was slow initial downdip rupture, followed by two faster updip ruptures that released most of the radiated energy northeast of Kathmandu. The observed relative lack of high-frequency radiation during the main moment release episode was confirmed by the spectral analysis of *Denolle et al.* (2015), which compared *P*-wave spectra of the mainshock with two large aftershocks. We found that surface reflections (depth

phases) produce interference that severely biases spectral measurements unless corrections are applied. The beginning of the Nepal mainshock likely experienced a dynamic weakening mechanism immediately followed by an abrupt change in fault geometry.

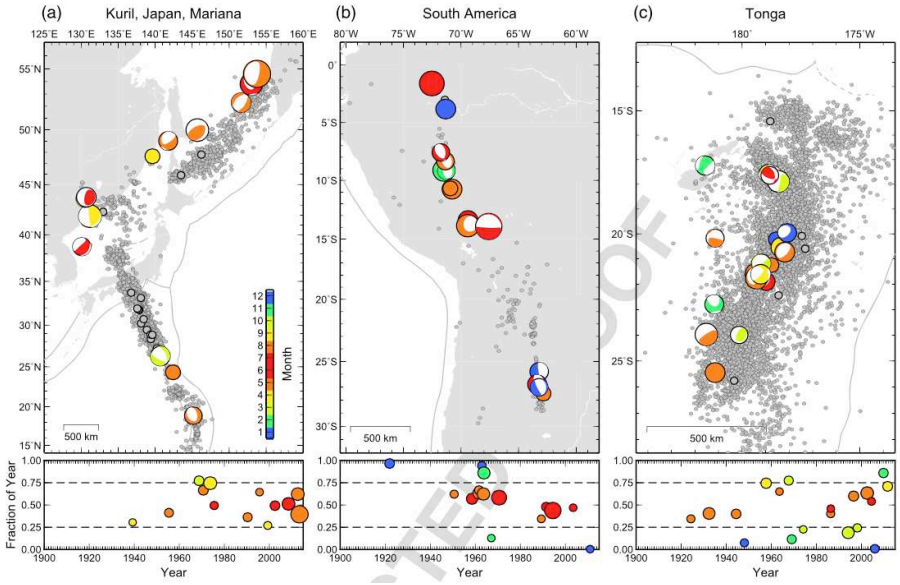

Figure 2. Regional plots of deep-focus earthquakes for the (a) NW Pacific, (b) South American, and (c) Tonga subduction zones. Events larger than M 7 are colored by month. Background seismicity is shown as small grey dots. (bottom row) Event month versus year. Symbol sizes are proportional to magnitude.

Postdoc Zhongwen Zhan (now at Caltech) recently discovered that large deep-focus earthquakes (M > 7, depth > 500 km) have exhibited strong seasonality in their occurrence times for over 100 years (*Zhan and Shearer*, 2015). Of 60 such events from 1900 to the present, 42 have occurred in the middle half of each year. The seasonality appears strongest in the northwest Pacific subduction zones and weakest in the Tonga region (see Fig. 2). This observation has no obvious physical interpretation and is difficult to test statistically, given that the observations have already been made. However, we make a testable prediction of seasonality for future quakes, which, if confirmed, would challenge our current understanding of deep earthquakes.

Stacking of seismic data can sometimes reveal new or unexpected phases. Postdoc Janine Buehler recently stacked high-frequency waveforms from ~5200 earthquakes recorded by the Global Seismic Network and produced clear images of the seismic *T* phase, which propagates as acoustic energy in the ocean (*Buehler and Shearer*, 2015). This observation points the way toward more detailed studies of *T* phase propagation efficiency across major ocean basins.

Selected Recent Publications

Buehler, J. S., and P. M. Shearer, T-phase observations in global seismogram stacks, *Geophys. Res. Lett.*, 42, doi: 10.1002/2015GL064721, 2015.

Chen, X., and P. M. Shearer, Analysis of foreshock sequences in California and implications for earthquake triggering, *Pure Appl. Geophys.*, doi: 10.1007/s00024-015-1103-0, 2015.

Denolle, M. A., W. Fan, and P. M. Shearer, Dynamics of the 2015 M7.8 Nepal earthquake, *Geophys. Res. Lett.*, doi: 10.1002/2015GL065336, 2015.

Fan, W., and P. M. Shearer, Detailed rupture imaging of the 25 April 2015 Nepal earthquake using teleseismic P waves, *Geophys. Res. Lett.*, 42, doi: 10.1002/2015GL064587, 2015.

Kaneko, Y., and P. M. Shearer, Variability of seismic source spectra, estimated stress drop and radiated energy, derived from cohesive-zone models of symmetrical and asymmetrical circular and elliptical ruptures, *J. Geophys. Res.*, **120**, doi: 10.1002/2014JB011642, 2015.

Zhan, Z., and P. M. Shearer, Possible seasonality in large deep-focus earthquakes, *Geophys. Res. Lett.*, doi: 10.1002/2015GL065088, 2015.

Leonard J. Srnka Professor of Practice

lsrnka@ucsd.edu

Phone: 822-1510

Research Interests*:* Land and marine electromagnetic (EM) methods; integrated geophysical data analysis and interpretation; inverse theory; energy outlooks and global change

In the second year of my SIO appointment, I continued my research begun at ExxonMobil on earth-field (~2.2 kHz) nuclear magnetic resonance (NMR) as a technology for detecting contaminates in the shallow subsurface. This technology is particularly well suited for detecting oil under ice and snow, which is a crucial environmental need in the Arctic. The research led to a unique transmit/receiver antenna and signal protocol to detect oils of various properties in the presence of the huge water proton NMR signal. This approach demonstrated for the first time that such detection is feasible. Full-scale prototype testing using a helicopter-slung system has begun.

My research in seafloor electromagnetics turned to re-examining data acquired in the San Diego Trough in 2006 in about 900m water depth, where novel electric field gradient measurements were made using tandem long-wire electric (LEM) receivers pioneered by Professor Steve Constable and his laboratory at SIO. New techniques to suppress magnetotelluric (MT) and natural noises are being studied.

Responding to government and professional society interests in scoping better academic cooperation with the extensive marine industry, I participated in workshops at UC Irvine (NRC/OSB) and at the POGO-16 conference held at Tenerife, Spain, and summarized the opportunities and challenges of increased cooperation. One recommendation from POGO-16 is to form an industry-academic steering committee that would further explore cooperation options. Along the same lines, I began working with NSF on opportunities to use industry seismic vessels to augment or supplant the aging R/V Marcus G. Langseth.

Recent Publications

Chavez, L., Altobelli, S., Fukushima, E., Zhang, T., Nedwed, T., Palandro, D., Srnka, L., and Thomann, H., 2015, Using NMR to detect Arctic oil spills. *Near Surface Geophysics*, **13** (4), 409-416. **DOI:** 10.3997/1873-0604.2015023

Dave Stegman **Associate Professor**
dstegman@ucsd.edu
Phone: 822-0767

Research Interests: Global tectonics, mantle dynamics, planetary geophysics, high-performance computing

Dr. Stegman researches dynamic processes within planetary interiors that shape their geologic, tectonic, magnetic and magmatic evolutions. My research group employs some of the nations fastest supercomputers to simulate these processes with the ultimate goal of developing a dynamical theory that explains how Earth and other planets evolve.

One of the questions I've recently investigated is what were the largest factors driving global sea level variations during Earth's 4.5 Billion year evolution? Earth's oceans have played an important role in the evolution of life and tectonics on Earth, yet our understanding of how long Earth's oceans have persisted, or how deep such oceans may have been, remains limited.

Plate tectonics continuously alters the age-distribution of seafloor in the world's oceans, and seafloor subsides as it gets older, the volume of water that the ocean basins can hold is consequently changing as well. Over the past 140 Myr, global sea level may have varied 200m due to variations in the age-area distribution of oceanic plates as estimated from reconstructions of tectonic plates (Muller et al., 2008). The growth of continents over Earth history also influences the distribution of seafloor age, because as the amount of continent increases there is more opportunity for passive continental margins to develop, allowing ocean basins a stable tectonic environment to age.

Working with PhD student Joyce Sim and collaborator Nicolas Coltice (ENS-Lyon), we used synthetic plate configurations derived from 3D spherical mantle convection models to estimate variations of global sea level under conditions appropriate for early Earth. By varying the amount of continents (0%, 10%, and 30%), we consider the competing effects of continental growth and seafloor age distribution leading to deepening ocean basins within the context of Earth's thermal evolution. The warmer, early Earth, is expected to have faster surface velocities and, on-average, younger seafloor as indicated in the scale bars for the different models (see Figure).

Our main conclusion was that, according to these models, global sea level has remained fairly constant over geologic time, because the effect of continental growth approximately balances the effect of changes in average seafloor-age. As the continents on Earth grew, some of the surface became covered by continents, leading to an increase in global sea level which was nearly offset by the decrease associated with an older mean age of ocean basins.

Some other research activities during the year included working with PhD student Robert Petersen, building upon the models of subduction Petersen et al. (2015) and now considering the effects of damage rheologies in the slabs and effects of slab dehydration on rheology of the mantle wedge. I continued working with Green Scholar Chris Davies on a study related to gravitational coupling of the inner core, following up on our recent publication (Davies, Stegman, and Dumbery, GRL, 2014). Leah Ziegler and I worked with Chris to adapt his entropy-based parameterized inner core solidification model to the situation of a basal magma ocean dynamo, as was proposed by Stegman and Ziegler (2014).

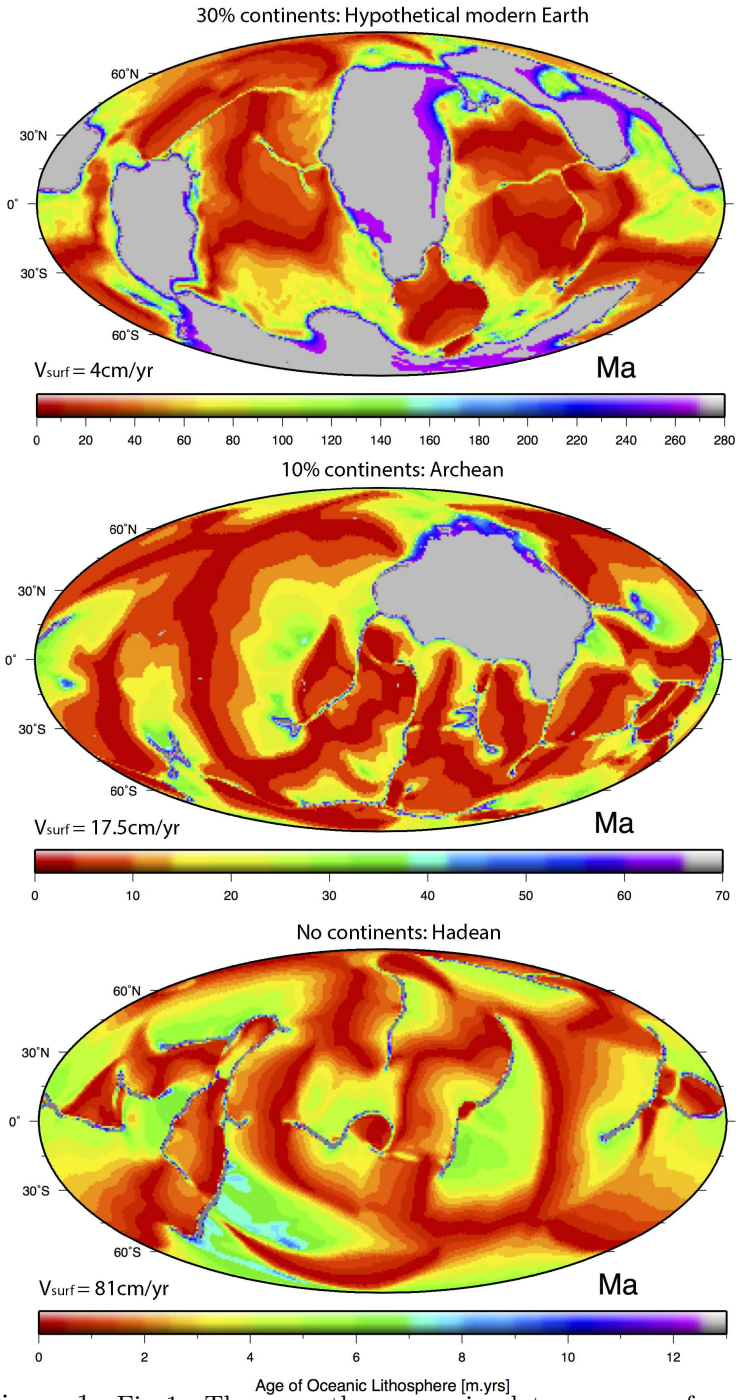

Figure 1: Fig 1. These are three oceanic plate age maps from our mantle convection models showing a representative time step for our 30% (top), 10% (middle) and 0% continents (bottom) models. The color contours shows the ages of the oceanic crust with the ages shown in each colorbar, which are different since each model is scaled to have surface velocity as shown on left bottom corner of each panel to represent the corresponding time period. The grey areas represent continents..

Recent Publications

Petersen, R.I., **D.R. Stegman**, and P.J. Tackley (2015) A Regime Diagram of Mobile lid Convection with Plate-like Behaviour, *Physics of the Earth and Planetary Interiors* **241**, 65-76.

Sim, S., **D.R. Stegman** and N. Coltice (2015) The effect of continental growth on long-term global sea level, *submitted*.

Lisa Tauxe Distinguished Professor

ltauxe@ucsd.edu

Phone: 534-6084

Research Interests: Behavior of the ancient geomagnetic field and applications of paleomagnetic data to geological problems.

This year, we continued to work on ways of improving the methods by which we estimate the strength of the geomagnetic field (Cromwell et al., 2015b, Shaar and Tauxe, 2015). We also generated new data sets for high latitudes (Cromwell et al., 2015a), and archaeomagnetic results from China (Cai et al., 2015) and Cyprus (Shaar et al., 2015). We also investigated how hematite acquires its magnetization when it crystallizes (Jiang et al., 2015) and applied rock magnetic techniques to explore the stability of the East Antarctic Ice Sheet in the Pliocene (Tauxe et al., 2015) and updated the database for paleointensity in the Precambrian (Biggin et al., 2015).

Despite decades of effort, such fundamental properties of the geomagnetic field as its average strength and variation through time, remain hotly debated. One diagnostic feature of an axial geomagnetic dipole is that the field strength should double from the equatorial value to the poles. This behavior is readily apparent in the present field but paleointensity database for the last five million years, reveals no such pattern (Figure 1a).

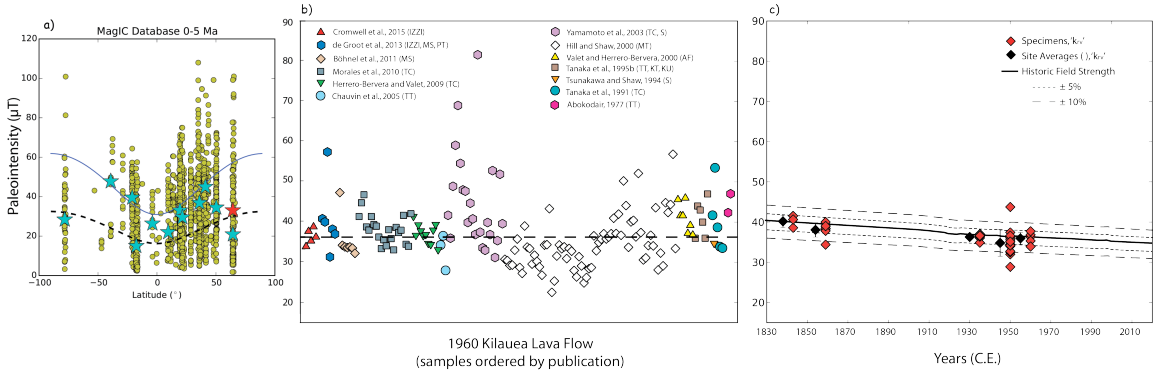

Figure 1: a) Pulished paleointensity data for the last 5 Myr. Data are plotted against latitude and median values for 10° bins are shown as cyan stars. Solid blue line the variation expected for the present field. The red star is the new results from subglacially erupted flows in Iceland of Cromwell et al. (2015a). b) Sample level paleointensity estimates for the 1960 Kilauea flow from the literature. 1960 C.E. IGRF field strength at the location is 36.1 μT. c) Paleointensity from Cromwell et al., (2015a). Expected historic field strength for the locations is plotted as a solid line with 5% and 1% bounds. Hawaiian field strength calculated from D/IGRFs for 1900 to 2000 C.E., prior to 1900 C.E. calculated from ARCH3K.1 (Korte et al., 2009). [Figure modified from Cromwell et al., 2015b.]

One clue about the cause of the missing dipole signal comes from the published data from the 1960 flow on Hawaii (Figure 1b), which display the entire range of intensity values observed on the Earth's surface today, yet they should all have a value of ~36 μT (Figure 1b). Cromwell et al. (2015b) found that better experimental methods, better

sampling targets and better selection criteria go a long way to achieving accurate and precise paleointensity estimates (Figure 1c). We are now applying the approach by Cromwell et al., 2015b to re-analyze paleointensity data from around the world, including Iceland (Cromwell et al., 2015a). These new data (red star in Figure 1a) confirm the low field strengths as high latitude. Preliminary results from the Hawaiian drill core HSDP-2 (unpublished) suggest strongly that the published data from low latitudes are biased high, a topic we are now devoting considerable effort to.

A second topic of research in my lab was the rate at which the geomagnetic field can change locally. By analyzing high resolution records of paleointensity behavior from copper mining slag deposits in Cyprus, which are exceptionally well dated owing to the co-occurrence of abundant charcoal, we were able to document extremely rapid rates of change (Shaar et al., 2015) of over 36% per century.

Publications:

Biggin, A, Piipsa E, Pesonen L, Holme R, Paterson G, Veikkolainen T, Tauxe L. 2015. Palaeomagnetic field intensity variations suggest Mesoproterozoic inner-core nucleation. Nature. 526:245-248. 10.1038/nature15523

Cai, S, Chen W, Tauxe L, Deng C, Qin H, Pan Y, Zhu R. 2015. New constraints on variation of the geomagnetic field during the late Neolithic period: Archaeointensity results from Sichuan, southwestern China. J. Geophys. Res.. 120:2056-2069. 10.1002/2014JB011618.

Cromwell, G, Tauxe L, Halldorsson SA. 2015a. New paleointensity results from rapidly cooled Icelandic lavas: Implications for Arctic geomagnetic field strength. Journal of Geophysical Research-Solid Earth. 120:2913-2934. 10.1002/2014jb011828

Cromwell, G, Tauxe L, Staudigel H, Ron H. 2015b. Paleointensity estimates from historic and modern Hawaiian lava flows using volcanic glass as a primary source material. Phys. Earth Planet. Int.. 241:44-56. 10.1016/j.pepi.2014.12.007

Jiang, Z, Qin H, Liu Q, Dekkers MJ, Tauxe L, Barron V, Torrent J. 2015. Acquisition of chemical remanent magnetization during experimental ferrihydrite-hematite conversion - implications for paleomagnetic studies of red beds,. Earth Planet. Sci. Let. . 428:1-10. 10.1016/j.epsl.2015.07.024

Shaar, R, Tauxe L, Ben-Yosef E, Kassianidou V, Lorentzen B, Feinberg JM, Levy TE. 2015. Decadal-scale variations in geomagnetic field intensity from ancient Cypriot slag mounds. Geochemistry Geophysics Geosystems. 16:195-214. 10.1002/2014gc005455

Shaar, R, and Tauxe L. 2015. Instability of thermoremanence and the problem of estimating the ancient geomagnetic field strength from non-single-domain recorders. Proceedings of the National Academy of Sciences. 112:11187-11192. 10.1073/pnas.1507986112

Tauxe, L, Sugisaki S, Jiménez-Espejo F, Escutia C, Cook CP, van de Flierdt T, Iwai M. 2015. Geology of the Wilkes land sub-basin and stability of the East Antarctic Ice Sheet: Insights from rock magnetism at IODP Site U1361. Earth and Planetary Science Letters. 412:61-69. 10.1016/j.epsl.2014.12.034

Peter Worcester Researcher Emeritus, RTAD

pworcester@ucsd.edu

Phone: 534-4688

Research Interests*:* Acoustical oceanography, ocean acoustic tomography, underwater acoustics.

My research is focused on the application of acoustic remote sensing techniques to the study of large-scale ocean structure and on improving our understanding of the propagation of sound in the ocean, including the effects of scattering from small-scale oceanographic variability.

Acoustic Propagation in the Philippine Sea. During 2009–2011 investigators from a number of oceanographic institutions worked together to conduct a series of experiments to investigate deep-water acoustic propagation and ambient noise in the oceanographically complex and highly dynamic Philippine Sea (Worcester et al., 2013). Two of the key goals were (i) to improve our understanding of the physics of scattering by internal waves and density-compensated temperature and salinity variations (see, e.g., Andrew et al., 2015) and (ii) to determine whether acoustic methods, together with other measurements and ocean modeling, can yield estimates of the time-evolving ocean state useful for making improved acoustic predictions and for understanding the local ocean dynamics.

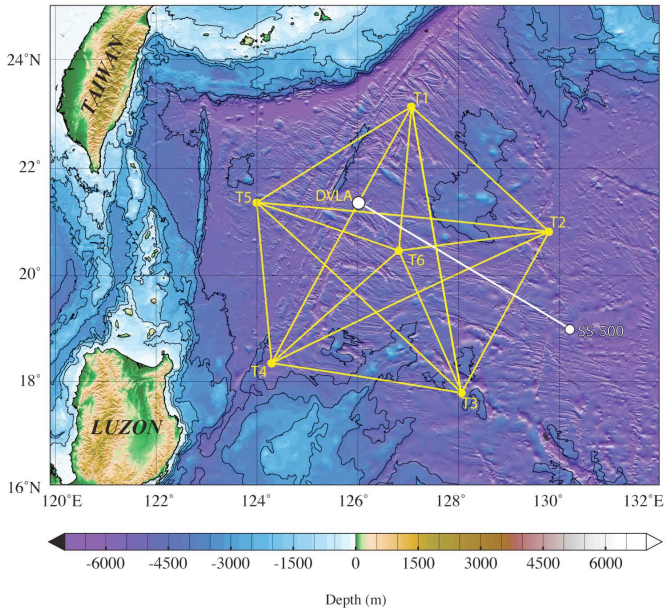

Fig. 1. The 2010–2011 Philippine Sea experiment consisted of six broadband acoustic transceivers (T1, … T6), a Distributed Vertical Line Array (DVLA) receiver, and ship-suspended sources, including one at SS-500.

The measured low-frequency travel-time series between the acoustic transceivers during the 2010–2011 Philippine Sea experiment compare well with time series computed from an ocean state estimate made using a high-resolution regional implementation of the MIT Ocean General Circulation Model (MITgcm) that was constrained by satellite sea surface height data, in situ temperature and salinity data, and other data. Significant (~ 30 ms) differences remained, however, including a bias. Ocean state estimates that incorporate the travel times in addition to

the other data give improved temperature estimates at ~ 500–1500 depth and improved temperature forecasts at depth. The dynamically consistent ocean state estimates provided by the model can be used to quantify processes in a realistic ocean.

Canada Basin Acoustic Propagation Experiment (CANAPE). The Arctic Ocean is undergoing dramatic changes in both the ice cover and ocean structure. Changes in sea ice and the water column affect both acoustic propagation and ambient noise. The implication is that what has been previously learned about Arctic acoustics is now obsolete. Investigators at a number of institutions are working together to conduct a yearlong experiment in the Canada Basin north of Alaska during 2016–2017 to study the effects of changing Arctic conditions on Arctic acoustics. The 2016–2017 experiment was preceded by a pilot study during summer 2015 in which HLF-5 (250 Hz) and J15-3 (75 and 125 Hz) acoustic sources suspended from shipboard transmitted to a moored DVLA receiver at ranges of ~ 50, 100, 200, and 300 km. All of the acoustic paths were covered by a combination of multiyear and first year ice.

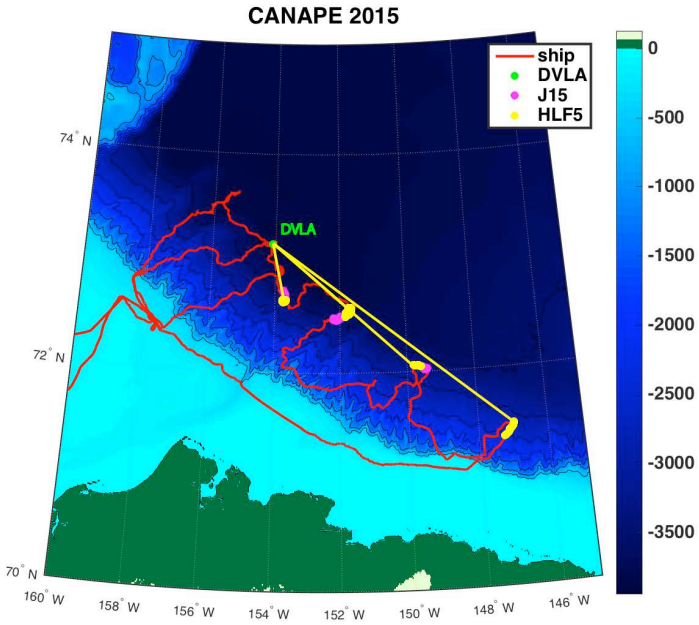

Fig. 2. CANAPE 2015 pilot study geometry showing the DVLA receiver and the acoustic paths.

The hope is that these first steps will lead to a permanent acoustic monitoring, navigation, and communications network in the Arctic Ocean (Mikhalevsky et al., 2015).

Recent Publications

Andrew, R. K., A. W. White, J. A. Mercer, M. A. Dzieciuch, P. F. Worcester, and J. A. Colosi (2015), A test of deep water Rytov theory at 284 Hz and 107 km in the Philippine Sea, *J. Acoust. Soc. Am.*, *138*(4), 2015–2023, http://dx.doi.org/10.1121/1.4929900.

Mikhalevsky, P. N., et al. (2015), Multipurpose acoustic networks in the Integrated Arctic Ocean Observing System, *Arctic*, *68*(5), 11–27, http://dx.doi.org/10.14430/arctic4449.

Worcester, P. F., et al. (2013), The North Pacific Acoustic Laboratory deep-water acoustic propagation experiments in the Philippine Sea, *J. Acoust. Soc. Am.*, *134*(4), 3359–3375, http://dx.doi.org/10.1121/1.4818887.

Mark Zumberge Research Geophysicist

mzumberge@ucsd.edu

Phone: 858-534-3533

Research Interests*:* Measurement of gravity and pressure in the marine and subaerial environments, development of new seismic instrumentation, optical fiber measurements of strain.

A Seafloor Optical Fiber Strainmeter*:* (with Frank Wyatt and William Hatfield)

More than 70% of Earth's surface is underwater. Almost all of the planet's plate boundaries are beneath the oceans, yet we have precious few geodetic observations in the oceans. The tools for seafloor geodesy are limited, and it is important to advance our efforts in this arena. The 2011 Tohoku earthquake is a reminder of the importance of such studies. Risks to US populations along the west coast from offshore earthquakes and tsunami are significant, making inroads into offshore geodesy a high priority.

On land, GPS observations dominate geodetic science. But seafloor positions cannot be tracked directly with GPS because the satellite signals will not penetrate sea water; consequently other techniques are required. One approach is to measure Earth strain.

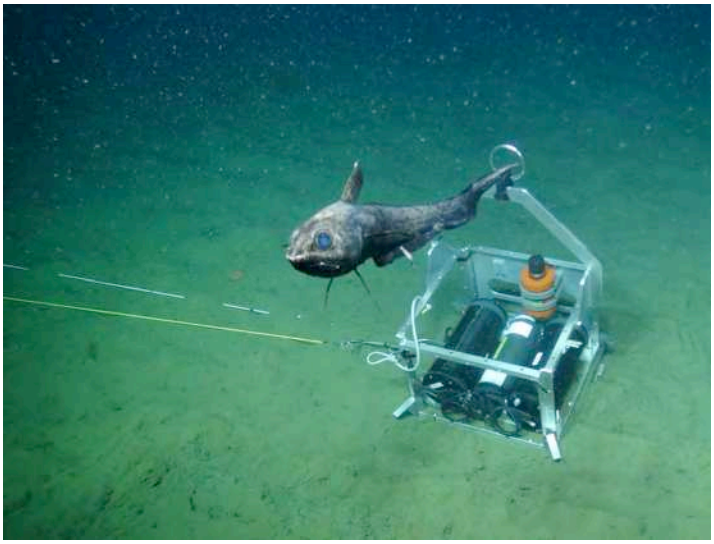

One end of a 200 m long optical fiber strainmeter sited at 1900 m depth in the Pacific Ocean.

In Earth strain measurements, we monitor changes in length Δl over a baseline length l, to give the strain $\varepsilon = \Delta l / l$. For a given displacement-noise in Δl, the longer the instrument length l, the lower the noise in the strain measurement. Optical methods can detect a very small Δl (nanometers) even when l is large (hundreds of meters), making them an excellent technique for strain measurement. Optical fibers allow great flexibility in installation at relatively low cost.

Our collaboration has focused in recent years on using optical fibers to sense Earth strain. An optical fiber is elastically stretched between two anchor points and its length monitored with laser interferometry. We've gotten good results in boreholes and trenches on land. We've been working for years to install a seafloor optical fiber strain sensor – in 2015 we finally succeeded.

Using the ROV Jason, we sited two seafloor anchors 200 m apart in water 1900 m deep, 50 nautical miles west of the Oregon coast near the Cascadia subduction zone trench. We stretched an optical fiber between the two anchors and placed small steel plates on top of it to keep it settled into the seafloor sediment. An infrared diode laser illuminates an interferometer formed by the stretched optical fiber (the strain sensing fiber) and a second fiber of approximately the

same length wound onto a silica mandrel. The nearly equal path Michelson interferometer is less sensitive to small fluctuations in laser wavelength which would otherwise be misinterpreted as Earth strains.

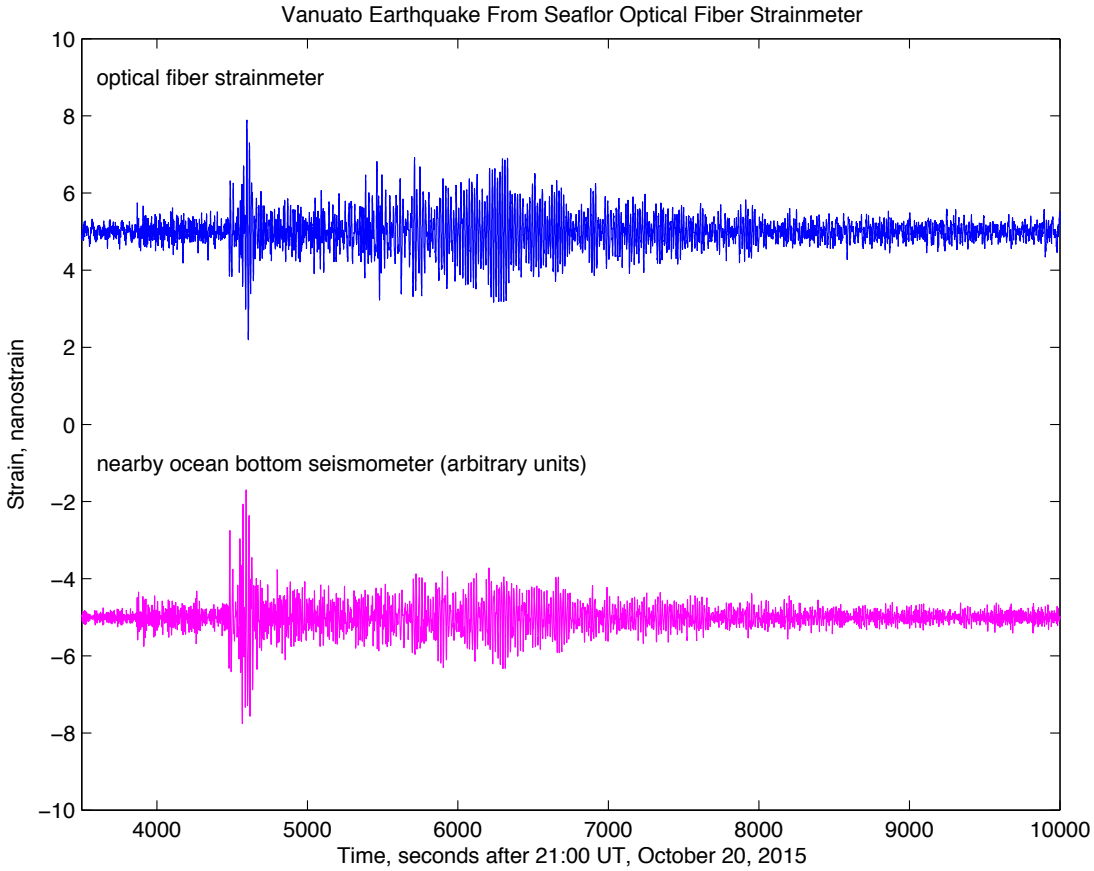

Soon after the installation of the seafloor optical fiber strainmeter, a magnitude 7.1 earthquake occurred 9500 km away. The part per billion (nanostrain) strain signals were clearly observed. A long strain time series awaits recovery of the instrument next year.

One important difficulty with optical fibers in sensing strain is their inherent sensitivity to temperature. A standard fiber's index of refraction varies 10 ppm per °C, yielding a significant apparent strain effect as the temperature along the sensing fiber changes. Even on the seafloor, where daily temperature excursions may be 0.1°C or less, the microstrain effect is significant when nanostrain signals are the ones of interest. To combat this problem, we observe the interferometric length changes of two different types of fiber – one having a different temperature coefficient – in the same sensing cable. This allows us to separate the temperature effect from the strain effect and compensate for thermal signals.

Recent Publications

Zumberge, M.A., DeWolf, S., Wyatt, F.K., Agnew, D.C., Elliott, D., Hatfield, W., Results from a Borehole Optical Fiber Interferometer for Recording Earth Strain, Proc. SPIE 8794, Fifth European Workshop on Optical Fibre Sensors, 87940Q (May 20, 2013); doi:10.1117/12.2025896